E-ISSN: 2636-7688

february 2026
volume 33
issue 4

ANNALS OF MEDICAL RESEARCH

The Official Journal of the Inonu University Faculty of Medicine

Original Articles

İNÖNÜ UNIVERSITY PRESS

ANN MED RES

Ann Med Res

Annals of Medical Research

The Official Journal of Inonu University Faculty of Medicine

Editorial Board | Volume: 33 | Issue: 4 | April 2026

Ann Med Res

Annals of Medical Research

The Official Journal of Inonu University Faculty of Medicine

Editorial Advisory Board | Volume: 33 | Issue: 4 | April 2026

Ann Med Res

Annals of Medical Research

The Official Journal of Inonu University Faculty of Medicine

Table of Contents | Volume: 33 | Issue: 4 | April 2026

Original Articles

Ann Med Res

Current issue list available at Ann Med Res

Annals of Medical Research

journal page: annalsmedres.org

In vitro effects of sertraline and escitalopram on rat uterine smooth muscle

Samet Oksuz[a], ‡,*, Ahmet Ayar[b]

[a]*Karadeniz Technical University, Faculty of Medicine, Department of Psychiatry, Trabzon, Türkiye*
[b]*Karadeniz Technical University, Faculty of Medicine, Department of Physiology, Trabzon, Türkiye*
**Corresponding author: sametoksuz@yahoo.com (Samet Oksuz)*

‡*Samet Oksuz is now at Department of Psychiatry, Recep Tayyip Erdogan University Traning and Research Hospital, Rize, Türkiye.*

MAIN POINTS

- This study examined the efficacy of sertraline and escitalopram on the contractility of rat uterine muscles.
- SSRIs dose-dependently reduce myometrial contraction AUC in vitro.
- Sertraline decreases AUC under oxytocin in nonpregnant and pregnant rats.
- Escitalopram shows no significant pairwise effects after Holm-Bonferroni correction.

Cite this article as: Oksuz S, Ayar A. *In vitro* effects of sertraline and escitalopram on rat uterine smooth muscle. *Ann Med Res*. 2026;33(4):143–150. doi: 10.5455/annalsmedres.2025.07.190.

ABSTRACT

Aim: Depressive disorders affect around 10% of pregnant women. Antidepressant use during pregnancy is important for maternal and fetal health. Although studies link antidepressants to risks of spontaneous abortion, preterm labor, and postpartum hemorrhage, their direct effects on the myometrium remain unclear. This study investigated the effects of sertraline and escitalopram on spontaneous and oxytocin-induced contractions in rat myometrial tissue.

Materials and Methods: 6 pregnant and 14 nonpregnant female Sprague-Dawley rats were used in the study. Myometrial strips measuring 1x0.2x0.2 centimeters were obtained from rats. Female rats were decapitated on day 18-20 of gestation. In oxytocin-induced and spontaneous contractions, sertraline and escitalopram were added cumulatively at concentrations of 1 μM, 3 μM and 10 μM in pregnant and nonpregnant rat groups and AUC (Area Under the Curve), frequency and amplitude values were recorded.

Results: Regression analysis demonstrated a significant dose-dependent decrease in AUC (particularly under oxytocin). Holm-Bonferroni adjusted Wilcoxon tests confirmed that sertraline reduced AUC during oxytocin-induced contractions in both nonpregnant and pregnant strips, while escitalopram showed no significant effects on AUC, amplitude, or frequency.

Conclusion: In vitro, AUC decreased dose-dependently---particularly with sertraline during oxytocin-induced contractions---while the effects of escitalopram were inconsistent. These results may support cautious use of the lowest effective dose in pregnancy and motivate further translational work.

Keywords: Myometrium, Pregnancy complications, Selective serotonin reuptake inhibitors, Uterine contractions

Received: Jul 11, 2025 **Accepted:** Nov 24, 2025 **Available Online:** Apr 24, 2026

INTRODUCTION

Pregnancy is a physiological process accompanied by hormonal, biological, and psychosocial changes. These adaptations may predispose individuals to psychiatric conditions, with depressive disorder being the most prevalent. Affecting approximately 280 million people globally, depressive disorder exhibits a higher incidence in women, particularly during pregnancy and the postpartum period [1]. In low- and middle-income countries, the prevalence of antenatal depression is estimated at 10% [2], while one in ten pregnant women in the United States receives antidepressant therapy during gestation [3,4].

The diagnosis and management of depressive disorder during pregnancy require a specialized approach, because reluctance in the initiation of the treatment may adversely affect maternal and fetal outcomes. While psychotherapy remains the first-line intervention for mild to moderate depression, severe cases necessitate pharmacological treatment [5,6]. Selective serotonin reuptake inhibitors (SSRIs), such as sertraline, citalopram, and escitalopram, are frequently prescribed due to their favorable safety profile in pregnancy [7].

Although antidepressant use during pregnancy has been associated with obstetric complications—including preterm birth, spontaneous abortion, neonatal adaptation syndrome, persistent pulmonary hypertension, cardiac malformations, and postpartum hemorrhage— untreated depression carries comparable risks [8–10]. A systematic review further highlighted that adverse outcomes linked to untreated depression

often mirror those observed in treated populations [11]. Additionally, untreated depressive disorder may exacerbate behaviors detrimental to maternal and fetal health, such as poor self-care, inconsistent prenatal monitoring, nutritional deficiencies, smoking, substance use, and elevated suicide risk [12].

SSRIs are known to exert nonspecific effects beyond their primary mechanism of action, including relaxation of smooth muscle in structures such as blood vessels [13,14], the vas deferens [15], and the ileum [16]. While epidemiological studies suggest a potential association between SSRI use and myometrial dysfunction—manifesting as preterm labor, postpartum hemorrhage, or spontaneous abortion—the precise mechanisms underlying these complications, particularly their impact on uterine contractility, remain poorly understood. Consequently, further investigation into the effects of widely used antidepressants on uterine muscle activity is warranted. This study aims to evaluate the *in vitro* effects of sertraline and escitalopram on spontaneous and oxytocin-induced contractions in rat myometrium, utilizing isolated uterine smooth muscle tissue from both pregnant and nonpregnant rats.

MATERIALS AND METHODS

Experimental procedures

The protocol of this study was reviewed and approved by the Karadeniz Technical University Animal Research Ethics Committee (No: 2021–7; February 8, 2021). All animal experiments were carried out in compliance with the Republic of Türkiye's national legislation and internationally accepted guidelines for the care and use of laboratory animals. In study, 6 pregnant and 14 nonpregnant adult Sprague-Dawley female rats, weighing between 250-300 grams and six months old, obtained from the Surgical Application Research Center of Karadeniz Technical University, were used. The animals were kept in an environment with 65-70% humidity at 22-25°C under a 12-hour light-dark cycle. They were fed with standard pelleted rat food and tap water (ad libitum).

Female rats that were determined to be in the appropriate cycle (in proestrus and estrus phases) were mated with an adult male Sprague-Dawley rat in single cages. Vaginal smear method was applied to determine pregnancy in rats that were allowed to mate.

Rats that were determined to be pregnant were decapitated without anesthesia on days 18-20 of pregnancy, starting from day 0 (because anesthetic drugs may have effects on smooth muscle function). After decapitation, the uteruses of the rats were quickly removed and 4 myometrial strips of 1x0.2x0.2 centimeters were obtained from each pregnant rat and 2 myometrial strips of 1x0.2x0.2 centimeters were obtained from nonpregnant rats. Since spontaneous contractions were not observed in 3 myometrial strips obtained from pregnant rats and 1 myometrial strip obtained from nonpregnant rats, they were excluded from the study.

The obtained myometrial strips were hung vertically in an isolated organ bath containing Krebs solution with a constant temperature of 37°C and a pH of 7.4, continuously gassed with normoxic gas (95% O2 + 5% CO2). One end of the myometrial strips was connected to an isometric force transducer (BIOPAC, FDT 05, MAY, Turkey), while the other end was fixed to the bottom of the organ bath. The myometrial strips were washed with fresh solutions every 15 minutes for 60 minutes and monitored under 1 g resting tension. After regular spontaneous contractions were observed, contractions were recorded for 10 minutes.

Experimental groups were determined using a sealed opaque envelope system to ensure random allocation and minimize selection bias. Sertraline (Catalog no:14839, Cayman, USA) and escitalopram (Catalog no:22405, Cayman, USA) to be used in the study were prepared by dissolving them in distilled water. Sertraline was dissolved in a beaker containing 37°C warm water using a vortex mixer prior to the experiment. In pregnant and nonpregnant rat groups, sertraline and escitalopram were added cumulatively at concentrations of 1 μM, 3 μM and 10 μM, respectively, and 10-minute recordings were taken for each dose. For oxytocin-induced contractions, 0.1 nM oxytocin (Synpitan Forte, Deva, Istanbul) was added to the organ bath and 10-minute recordings were taken. Then, with the cumulative addition of sertraline and escitalopram, 10-minute recordings were taken. Isometric tension and its changes were recorded using a physiological data acquisition and recording system (Biopac MP100, MAY, Turkey) via an isometric force transducer and computer. Measurement of AUC, frequency and amplitude values were made using Acq-Knowledge 4.0 (USA) software (Figure 1).

Sample size

Power analysis (G*Power 3.1) with α=0.05 (two-tailed) and power=0.80 indicated n=6 independent samples per group, sufficient to detect ~20% changes in AUC in paired within-strip comparisons. To adhere to 3R principles, multiple strips were obtained from each uterus so that tissues from 6 pregnant and 14 nonpregnant rats yielded n=6 for each of the eight conditions. This approach aligns with prior *in vitro* myometrial studies using 5–8 strips per condition [17,18].

Statistical analysis

Frequency was analyzed as absolute counts. AUC and amplitude were normalized within strip by setting the baseline (control or oxytocin) to 100% and expressing subsequent responses as % of baseline. Because sample sizes were small (5–7 strips/group) and normality was mixed (Shapiro–Wilk), we used nonparametric tests uniformly. Planned within-strip comparisons of each dose (1, 3, 10 μM sertraline or escitalopram) versus baseline were performed with the Wilcoxon signed-rank test, with Holm–Bonferroni adjustment across the three contrasts. To assess the overall dose–response trend while accounting for repeated measurements within strip, we

https://doi.org/10.5455/annalsmedres.2025.07.190

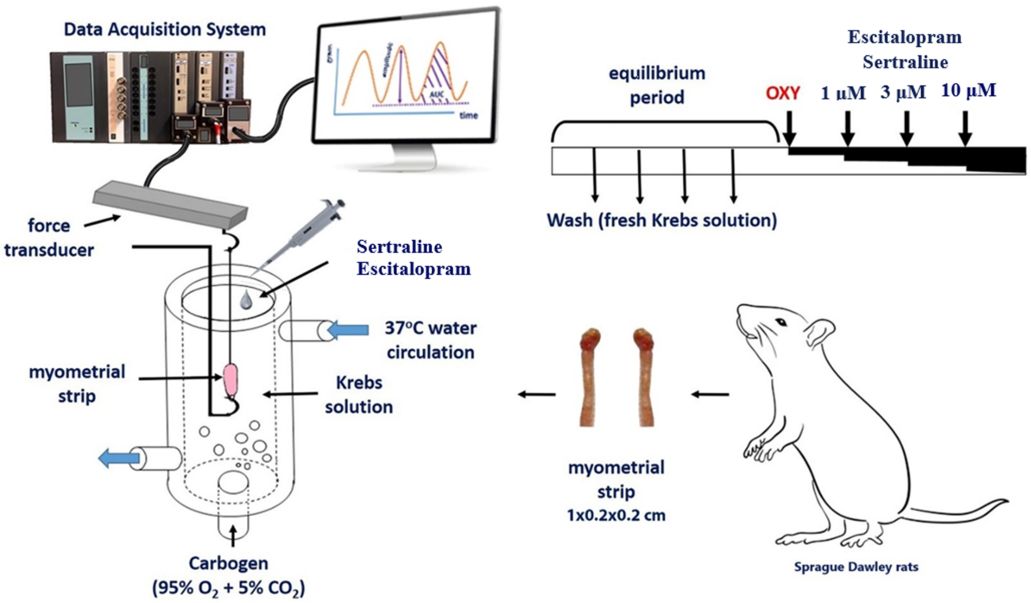

Figure 1. Schematic diagram of the experimental design and protocol. Myometrial strips were mounted in a double-jacketed, temperature-controlled organ bath containing physiological saline solution, continuously gassed with normoxic. Smooth muscle contractile force was recorded using an isometric force transducer and analyzed with computer software. Following a 60-minute equilibration period under resting tension, spontaneous (unstimulated) or oxytocin-induced contractions were elicited. Cumulative concentrations of sertraline and escitalopram were then applied at 10-minute intervals, and contractile responses were evaluated in terms of amplitude, area under the contractility curve, and contraction frequency. OXY = oxytocin.

fitted linear mixed-effects models with a random intercept for strip in IBM SPSS Statistics v25 (MIXED, REML; covariance type: variance components). Dose (µM) was entered as a continuous covariate (baseline coded as 0 µM); for normalized outcomes, the slope (β) is reported as % per µM. Monotonic direction was summarized with Spearman's ρ. Data are presented as median (IQR); two-sided $p<0.05$ was considered statistically significant.

RESULTS

After the tissue samples were subjected to an adaptation process for 60 minutes under 1 g resting tension, spontaneous contractions occurred in 48 of the 52 tissue samples, and 4 tissue strips that did not show regular spontaneous contractions after the adaptation process were excluded from the study.

The effect of sertraline on myometrial contractions

The cumulative effects of sertraline on spontaneous and oxytocin-induced contractions were evaluated in myometrial strips from pregnant and nonpregnant rats and summarized in Table 1.

In myometrial strips from nonpregnant adult female rats (n=6), cumulative effects of sertraline (1, 3, and 10 µM) to the spontaneous contractions were nonspecific as shown by the AUC, amplitude, or frequency after Holm–Bonferroni adjustment (paired Wilcoxon signed-rank test, exact, two-sided) (Table 2).

In myometrial strips from nonpregnant adult female rats (n=7) under oxytocin-induced contractions, cumulative effects of sertraline (1, 3, and 10 µM) were again nonspecific in terms of amplitude after Holm–Bonferroni adjustment (paired Wilcoxon signed-rank test, exact, two-sided), whereas AUC decreased significantly at all doses under oxytocin whereas, the frequency decreased at 10 µM under oxytocin (Table 2).

In myometrial strips from pregnant adult female rats (n=5), cumulative sertraline effects on (1, 3, and 10 µM) spontaneous contractions where nonspecific in terms of AUC, amplitude, or frequency after Holm–Bonferroni adjustment (paired Wilcoxon signed-rank test, exact, two-sided) (Table 2).

In myometrial strips from pregnant adult female rats (n=7) under oxytocin-induced contractions, cumulative sertraline effects (1, 3, and 10 µM) were nonspecific in frequency after Holm–Bonferroni adjustment (paired Wilcoxon signed-rank test, exact, two-sided). AUC decreased significantly only at 10 µM after adjustment, while amplitude showed nominal decreases at 3 and 10 µM that that showed no significant difference after multiplicity correction (Table 2).

The effect of escitalopram on myometrial contractions

The cumulative effects of escitalopram on spontaneous and oxytocin-induced contractions were evaluated in myometrial strips from pregnant and nonpregnant rats and are summarized in Table 3.

In myometrial strips from nonpregnant adult female rats (n=6), cumulative escitalopram (1, 3, and 10 µM) effects on spontaneous contractions were insignificant in terms of AUC, amplitude, or frequency after Holm–Bonferroni ad-

https://doi.org/10.5455/annalsmedres.2025.07.190

Table 1. The effect of sertraline on myometrial contractions.

		Sertraline					
		Nonpregnant			Pregnant		
Contraction Type	Drug Concentration μM	Median (IQR) Frequency	Median (IQR) amplitude %	Median (IQR) AUC %	Median (IQR) Frequency	Median (IQR) amplitude %	Median (IQR) AUC %
Spontaneous	Control	7.5(8-5)	100	100	7(13.5-6.5)	100	100
	1 (μM)	8(9-5)	100.5(102-95.25)	96.5(98-77)	8(13.5-6.5)	127(149-76)	87(125.5-64.5)
	3 (μM)	7.5(8-4)	100(102.75-90.25)	87.5(91-71)	6(12.5-6)	91(180-76,5)	79(132-61.5)
	10 (μM)	7(9-4)	94.5(102-82)	87(91-70)	7(12.5-5.5)	88(162-60)	73(105-57.5)
Oxytocin-Induced	Control	10(11-9)	100	100	11(11-8)	100	100
	0.1 (nM) oxytocin	12(14.5-11.5)	106(116.5-97)	152(213-128)	11(12-9.5)	231(263-130.5)	216(302.5-164.5)
	1 (μM)	13(13.5-11)	109(120.5-97)	138(188.5-120)	11(11-10)	186(205-141)	195(248.5-123.5)
	3 (μM)	11(11-9.5)	106(122-100)	118(152.5-107.5)	10(11-8.5)	198(219.5-110)	142(250-125)
	10 (μM)	8(9-6.5)	94(102.5-93)	108(116-92)	9(9.5-7.5)	148(173-90)	105(196-98.5)

AUC: Area Under the Curve.

Table 2. Dose-dependent comparisons versus baseline.

		Wilcoxon for Sertraline											
		Nonpregnant						Pregnant					
Contraction Type	Drug Concentration μM	AUC		Frequency		Amplitude		AUC		Frequency		Amplitude	
		P (two-sided)	P (adjusted)	P (two-sided)	P (adjusted)	P (two-sided)	P (adjusted)	P (two-sided)	P (adjusted)	P (two-sided)	P (adjusted)	P (two-sided)	P (adjusted)
Spontaneous	1 (μM)	0.03	0.09	1.00	1.00	0.87	1.00	0.62	1.00	1.00	1.00	0.62	1.00
	3 (μM)	0.03	0.09	0.50	1.00	1.00	1.00	0.62	1.00	0.62	1.00	0.81	1.00
	10 (μM)	0.03	0.09	0.81	1.00	0.22	1.00	0.37	1.00	0.75	1.00	1.00	1.00
Oxytocin-Induced	1 (μM)	0.02	**0.048§**	0.62	0.62	0.84	1.00	0.03	0.06	0.75	0.75	0.16	0.16
	3 (μM)	0.02	**0.048§**	0.06	0.13	1.00	1.00	0.047	0.06	0.28	0.56	0.03	0.09
	10 (μM)	0.02	**0.048§**	0.02	**0.048§**	0.03	0.09	0.016	**0.048§**	0.14	0.42	0.03	0.09

AUC: Area Under the Curve, bold and § indicate statistically significant differences compared to control ($p<0.05$. Wilcoxon signed-rank test, Holm–Bonferroni–adjusted).

Table 3. The effect of escitalopram on myometrial contractions.

		Escitalopram					
		Nonpregnant			Pregnant		
Contraction Type	Drug Concentration μM	Median (IQR) Frequency	Median (IQR) amplitude %	Median (IQR) AUC %	Median (IQR) Frequency	Median (IQR) amplitude %	Median (IQR) AUC %
Spontaneous	Control	8.5(9-5)	100	100	8(9-8)	100	100
	1 (μM)	7(9-4)	101.5(103-99)	92.5(94-89)	9(10-8)	119(159-105)	123(145-95)
	3 (μM)	7(8-4)	99(102-98)	88.5(95-88)	9(10-8)	93(103-80)	86(93-78)
	10 (μM)	6.5(8-5)	99(102-88)	84.5(89-79)	9(10-8)	91(98-43)	81(98-51)
Oxytocin-Induced	Control	4.5(5-3)	100	100	8(12-8)	100	100
	0.1 (nM) oxytocin	11(12-9)	133(239-106)	285(315-167)	8.5(12-7)	209.5(318-143.5)	291.5(377.5-227.25)
	1 (μM)	11(12-9)	134(207-112)	265(294-153)	10.5(11-7)	187(425-128,5)	298.5(359.75-205)
	3 (μM)	10(10-9)	137.5(208-113)	251.5(269-133)	10(11-7)	190.5(320.25-121.5)	257.5(325-184)
	10 (μM)	10(10-9)	138(209-115)	236.5(251-125)	9.5(12-7)	172(314.5-112.5)	231.5(297-165.5)

AUC: Area Under the Curve.

justment (paired Wilcoxon signed-rank test, exact, two-sided) (Table 4).

In myometrial strips from nonpregnant adult female rats (n=6) under oxytocin-induced contractions, cumulative ef-

https://doi.org/10.5455/annalsmedres.2025.07.190

Table 4. Dose-dependent comparisons versus baseline.

		Wilcoxon for Escitalopram											
		Nonpregnant						Pregnant					
Contraction Type	Drug Concentration μM	AUC		Frequency		Amplitude		AUC		Frequency		Amplitude	
		P (two-sided)	P (adjusted)	P (two-sided)	P (adjusted)	P (two-sided)	P (adjusted)	P (two-sided)	P (adjusted)	P (two-sided)	P (adjusted)	P (two-sided)	P (adjusted)
Spontaneous	1 (μM)	0.06	0.09	0.31	0.94	0.53	1.00	0.31	0.63	1.00	1.00	0.12	0.37
	3 (μM)	0.03	0.09	0.41	0.94	0.81	1.00	0.12	0.37	0.50	1.00	0.31	0.63
	10 (μM)	0.03	0.09	0.69	0.94	0.50	1.00	0.62	0.63	0.75	1.00	0.62	0.63
Oxytocin-Induced	1 (μM)	0.09	0.09	0.50	0.50	0.84	1.00	0.44	0.44	0.87	1.00	0.62	1.00
	3 (μM)	0.03	0.09	0.06	0.19	0.72	1.00	0.06	0.19	1.00	1.00	0.56	1.00
	10 (μM)	0.03	0.09	0.12	0.25	0.78	1.00	0.06	0.19	0.81	1.00	0.56	1.00

AUC: Area Under the Curve, bold and § indicate statistically significant differences compared to control (p<0.05. Wilcoxon signed-rank test, Holm–Bonferroni–adjusted).

Table 5. Linear Mixed-Effects Model (LMM) analysis of dose-dependent contractility trend.

			Slope β (%/dose code*)	95% CI	p	Spearman ρ
Sertraline	Nonpregnant spon	AUC	−1.43	[−2.28, −0.59]	<0.001	−0.76
		Amplitude	−0.03	[−0.12, 0.05]	0.46	−0.06
		Frequency	−0.88	[−1.65, −0.10]	0.03	−0.18
	Nonpregnant Oxytocin Induced	AUC	−5.96	[−7.95, −3.97]	<0.001	−0.57
		Amplitude	-4.44	[-9.27, 0.39]	0.07	-0.22
		Frequency	−0.48	[-0.64, -0.32]	<0.001	−0.66
	Pregnant spontaneous	AUC	−1.85	[−4.92, 1.22]	0.24	−0.35
		Amplitude	−0.09	[−0.23, 0.06]	0.24	−0.09
		Frequency	−0.12	[−4.59, 4.35]	0.96	−0.14
	Pregnant Oxytocin Induced	AUC	−9.33	[−13.21, −5.44]	<0.001	−0.39
		Amplitude	−0.19	[−0.34, −0.04]	0.01	−0.41
		Frequency	−9.38	[−16.87, −1.88]	0.01	−0.34
Escitalopram	Nonpregnant spontaneous	AUC	−1.52	[−2.17, −0.86]	<0.001	−0.75
		Amplitude	−0.02	[−0.12, 0.07]	0.65	−0.15
		Frequency	−1.00	[−1.93, −0.06]	0.04	−0.14
	Nonpregnant Oxytocin Induced	AUC	−3.66	[−5.38, −1.95]	<0.001	−0.64
		Amplitude	−0.36	[−0.59, −0.14]	0.002	−0.48
		Frequency	−0.29	[−1.25, 0.68]	0.56	0.07
	Pregnant spontaneous	AUC	−2.16	[−3.54, −0.78]	0.005	−0.62
		Amplitude	−0.05	[−0.15, 0.05]	0.34	−0.09
		Frequency	−1.44	[−2.79, −0.09]	0.04	−0.36
	Pregnant Oxytocin Induced	AUC	−6.97	[−10.61, −3.32]	<0.001	−0.45
		Amplitude	0.06	[−0.12, 0.23]	0.53	0.08
		Frequency	−3.40	[−14.28, 7.49]	0.54	−0.16

*Cl: Confidence Interval, AUC: Area Under the Curve, dose code: control, 1 μM, 3 μM, 10 μM.

fects of escitalopram (1, 3, and 10 μM) insignificant in terns of AUC, amplitude, or frequency after Holm–Bonferroni adjustment (paired Wilcoxon signed-rank test; exact, two-sided) (Table 4).

In myometrial strips from pregnant adult female rats (n=5), cumulative effects of escitalopram (1, 3, and 10 μM) during spontaneous contractions were insignificant in terms of in AUC, amplitude, or frequency after Holm–Bonferroni adjustment (paired Wilcoxon signed-rank test, exact, two-sided) (Table 4).

In myometrial strips from pregnant adult female rats (n = 6) under oxytocin-induced contractions, cumulative effects of

https://doi.org/10.5455/annalsmedres.2025.07.190

escitalopram (1, 3, and 10 μM) were insignificant in terms of AUC, amplitude, or frequency after Holm–Bonferroni correction (paired Wilcoxon signed-rank test, exact, two-sided) (Table 4).

Analysis of the dose-response trend

Across datasets, dose–response modeling with a linear mixed-effects model (LMM) framework showed that increasing dose was associated with a reduction in myometrial contraction, most consistently for AUC and often for amplitude, while effects on frequency were smaller or dataset-dependent. Importantly, even in conditions where individual dose vs control comparisons (Wilcoxon) did not reach significance, the mixed-effects slope (β) indicated a negative trend across the given doses, and Spearman's ρ supported the monotonic decrease. Collectively, these findings indicate that higher cumulative doses tend to inhibit the myometrial contraction (Table 5).

DISCUSSION

In our *in vitro* rat model, both SSRIs demonstrated a dose-dependent reduction in total contractile activity (AUC) across spontaneous and oxytocin-induced conditions. This was reflected by a negative dose–response slope ($\beta < 0$) in the linear mixed-effects model (LMM), with the notable exception of sertraline's effect on spontaneous contractions in pregnant strips. The inhibitory trend was most pronounced under oxytocin stimulation. For sertraline, the LMM indicated significant AUC reductions under oxytocin in both (e.g., nonpregnant: $\beta = -5.96$ %/μM, 95% CI −7.95 to −3.97; pregnant: $\beta = -9.33$ %/μM, 95% CI −13.21 to −5.44). Conversely, amplitude and frequency varied by condition and group, failing to form a consistent pattern.

Holm–Bonferroni-adjusted Wilcoxon comparisons confirmed a consistent reduction in AUC only for sertraline under oxytocin stimulation; in contrast, escitalopram showed no statistically significant changes in AUC, amplitude, or frequency after correction for multiple comparisons. Corroborating our findings, previous studies have reported that sertraline exerts a relaxant effect on smooth muscle, particularly at higher concentrations and under induced contractile conditions [13, 19]. Although escitalopram has likewise been shown to induce dose-dependent relaxation in various smooth muscle tissues (20), no significant changes were observed in our study via pairwise comparisons. This discrepancy may stem from the inherent limitations of the Wilcoxon test; particularly with small sample sizes and stringent multi-comparison corrections, it may fail to detect subtle but consistent effects. In contrast, statistical methods that directly model ordinal dose–response relationships, such as the LMM and Spearman's rho coefficient, offer greater statistical power to detect uniform changes distributed across dose levels.

Myometrial contraction depends not only on IP_3-mediated Ca^{2+} release from the sarcoplasmic reticulum (SR) but also on extracellular Ca^{2+} influx through L-type Ca^{2+} channels [21]. Previous reports indicating that sertraline and escitalopram can inhibit Ca^{2+} currents at micromolar concentrations align with the patterns observed here [19, 20]. Under conditions of elevated Ca^{2+} demand (such as oxytocin stimulation), a channel-level "brake" on stimulus-dependent Ca^{2+} entry may reduce total activity (AUC) and lower contraction frequency at higher concentrations without necessarily suppressing amplitude in a uniform manner. Furthermore, escitalopram is known to inhibit not only calcium channels but also voltage-dependent potassium (Kv) channels in vascular smooth muscle [22]. The possibility that these ion channel effects are less pronounced in uterine smooth muscle, or require higher concentrations to manifest, is consistent with the smaller negative dose–response slope observed for escitalopram ($\beta < 0$) and the absence of significant effects in pairwise Wilcoxon comparisons. These findings likely reflect drug-specific pharmacodynamic properties and inherent limitations in statistical power.

If SSRIs attenuate oxytocin-dependent contractility, exposure during pregnancy may contribute to variability in intrapartum uterotonic responsiveness, potentially slowing labor progression or increasing the need for augmentation. Nevertheless, these *in vitro* findings are hypothesis-generating and do not, in isolation, warrant changes in clinical practice. Observational studies have reported a consistent association between SSRI use and postpartum hemorrhage [10, 23, 24], whereas associations with preterm birth [25] and miscarriage [26] remain more heterogeneous. In the clinical context, the dose-dependent inhibition of myometrial contractions observed in our study aligns with the principles of utilizing the lowest effective dose, avoiding polypharmacy, and selecting agents with favorable reproductive safety profiles to maintain a patient-centered risk–benefit balance that safeguards maternal mental health [27, 28].

Limitations

Our study has several limitations. First one is the fact that current study is an ex vivo study. Species differences and the absence of investigations regarding the endocrine, vascular, and inflammatory components of the effects may limit extrapolation of our results to human subjects .

Another limitation is the small number of subjects and the Holm-Bonferroni adjustment reduces sensitivity of pairwise tests; thus, subtle dose-specific effects may be under-detected even when a global trend exists. Furthermore, we did not perform blocking experiments (e.g., nifedipine, SOCE inhibitors) or direct Ca^{2+} imaging/patch-clamp, so ion-channel involvement is inferred from the pattern and prior literature rather than demonstration with our results.

In the present study, we did not assess the probable indirect SSRI effects via uteroplacental or fetoplacental perfusion

https://doi.org/10.5455/annalsmedres.2025.07.190

(e.g., 5-HT–sensitive vasoreactivity); such changes could contribute to clinical outcomes (postpartum hemorrhage, spontaneous abortion, preterm labor) even in the absence of strong direct myometrial effects at therapeutic exposures. We did not test the serotonin–oxytocin crosstalk. Although serotonin can be uterotonic and oxytocin may increase local serotonin availability (e.g., by limiting uptake in mast cells), our setup did not test these interactions explicitly. We did not assess how depression itself (neuroendocrine/inflammatory alterations) might modify uterine contractility; disease-model studies are warranted.

CONCLUSION

Our data demonstrate a negative dose–response slope ($\beta < 0$) for AUC with SSRI treatment—most robustly for sertraline under oxytocin stimulation—while amplitude and frequency exhibit condition-dependent variability. These findings suggest drug-specific, rather than uniform class-wide, effects on myometrial contractility. Such results underscore the need for future research to delineate dosing strategies that minimize obstetric risks while preserving antidepressant efficacy.

Ethics Committee Approval: The protocol of this study was reviewed and approved by the Karadeniz Technical University Animal Research Ethics Committee (No: 2021–7; February 8, 2021).

Peer-review: Externally peer-reviewed.

Conflict of Interest: The authors declare that they have no conflict(s) of interests.

Author Contributions: Concept: A.A., S.Ö.; Design: A.A., S.Ö.; Supervision: A.A.; Fundings: S.Ö., A.A.; Materials: A.A., S.Ö. ; Data Collection and/or Processing: A.A., S.Ö.; Analysis: A.A.,S.Ö.; Literature Review: A.A., S.Ö.; Writing: S.Ö.; Critical Review: A.A.

Financial Disclosure: No financial support was obtained for this study.

Artificial Intelligence Disclosure: During the preparation of this work, the author utilized generative artificial intelligence tools, specifically ChatGPT (OpenAI), primarily for linguistic refinement and translation assistance to ensure clarity and academic rigor, as English is not the author's native language. Additionally, these tools were employed as a supplementary verification mechanism to support the interpretation of selected data points during the analysis phase. All outputs generated by the AI tools were critically reviewed, edited, and validated by the author. The author takes full responsibility for the accuracy, integrity, and originality of the final manuscript.

REFERENCES

1. Stewart D. Depression during pregnancy. *Can Fam Physician.* 2005;51(8):1061–7. PMID: 16121822.
2. Gavin NI, Gaynes BN, Lohr KN, Meltzer-Brody S, Gartlehner G, Swinson T. Perinatal depression: a systematic review of prevalence and incidence. *Obstet Gynecol.* 2005;106(5 Pt 1):1071-83. doi: 10.1097/01.AOG.0000183597.31630.db.
3. Andrade SE, Raebel MA, Brown J, et al. Use of antidepressant medications during pregnancy: a multisite study. *Am J Obstet Gynecol.* 2008;198(2):194.e1-5. doi: 10.1016/j.ajog.2007.07.036.
4. Yonkers KA, Wisner KL, Stewart DE, et al. The management of depression during pregnancy: a report from the American Psychiatric Association and the American College of Obstetricians and Gynecologists. *Gen Hosp Psychiatry.* 2009;31(5):403–13. doi: 10.1016/j.genhosppsych.2009.04.003.
5. Kirby N, Kilsby A, Walker R. Assessing low mood during pregnancy. *BMJ.* 2019;366:l4584. doi: 10.1136/bmj.l4584.
6. Vigod SN, Wilson CA, Howard LM. Depression in pregnancy. *BMJ.* 2016;352:i1547. doi: 10.1136/bmj.i1547.
7. Larsen ER, Damkier P, Pedersen LH, et al. Use of psychotropic drugs during pregnancy and breast-feeding. *Acta Psychiatr Scand Suppl.* 2015:(445):1–28. doi: 10.1111/acps.12479.
8. Lebin LG, Novick AM. Selective Serotonin Reuptake Inhibitors (SSRIs) in Pregnancy: An Updated Review on Risks to Mother, Fetus, and Child. *Curr Psychiatry Rep.* 2022;24(11):687-695. doi: 10.1007/s11920-022-01372-x.
9. Oyebode F, Rastogi A, Berrisford G, Coccia F. Psychotropics in pregnancy: safety and other considerations. *Pharmacol Ther.* 2012;135(1):71–7. doi: 10.1016/j.pharmthera.2012.03.008.
10. Jiang H-Y, Xu L-L, Li Y-C, Deng M, Peng C-T, Ruan B. Antidepressant use during pregnancy and risk of postpartum hemorrhage: A systematic review and meta-analysis. *J Psychiatr Res.* 2016;83:160–7. doi: 10.1016/j.jpsychires.2016.09.001.
11. Jahan N, Went TR, Sultan W, et al. Untreated Depression During Pregnancy and Its Effect on Pregnancy Outcomes: A Systematic Review. *Cureus.* 2021;13(8):e17251. doi: 10.7759/CUREUS.17251.
12. Leung BM, Kaplan BJ. Perinatal depression: prevalence, risks, and the nutrition link–a review of the literature. *J Am Diet Assoc.* 2009;109(9):1566-1575. doi: 10.1016/j.jada.2009.06.368.
13. Van Melle JP, Buikema H, Van Den Berg MP, et al. Sertraline causes strong coronary vasodilation: Possible relevance for cardioprotection by selective serotonin reuptake inhibitors. *Cardiovasc Drugs Ther.* 2004;18(6):441-7. doi: 10.1007/s10557-004-6221-3.
14. Kim HS, Li H, Kim HW, et al. Selective serotonin reuptake inhibitor sertraline inhibits voltage-dependent K+ channels in rabbit coronary arterial smooth muscle cells. *J Biosci.* 2016;41(4):659–66. doi: 10.1007/s12038-016-9645-6.
15. Yaris E, Kesim M, Kadioglu M, Kalyoncu NI, Ulku C, Ozyavuz R. The effects of paroxetine on rat isolated vas deferens. *Pharmacol Res.* 2003;48(4):335–45. doi: 10.1016/s1043-6618(03)00157-9.
16. Pacher P, Ungvari Z, Kecskeméti V, Friedmann T, Furst S. Serotonin reuptake inhibitors fluoxetine and citalopram relax intestinal smooth muscle. *Can J Physiol Pharmacol.* 2001;79(7):580–4. PMID: 11478591.
17. Vedernikov Y, Bolanos S, Bytautiene E, Fulep E, Saade GR, Garfield RE. Effect of fluoxetine on contractile activity of pregnant rat uterine rings. *Am J Obstet Gynecol*. 2000;182(2):296–9. doi: 10.1016/S0002-9378(00)70214-6.
18. Fırat Üniversitesi Sağlık Bilimleri Dergisi n.d. https://tip.fusabil.org/text.php3?id=1223 (accessed October 29, 2025).
19. Medina P, Segarra G, Ballester R, et al. Effects of antidepressants in adrenergic neurotransmission of human vas deferens. *Urology*. 2000;55(4):592–7. doi: 10.1016/S0090-4295(99)00535-X.
20. Engin S, Barut EN, Erac Y, Sari S, Kadioglu M. The inhibitory effect of escitalopram on mouse detrusor contractility: The role of L-type calcium channels. *Toxicol Appl Pharmacol.* 2023;461:116408. doi: 10.1016/J.TAAP.2023.116408.
21. Wray S, Prendergast C, Arrowsmith S. Calcium-Activated Chloride Channels in Myometrial and Vascular Smooth Muscle. *Front Physiol.* 2021;12:751008. doi: 10.3389/FPHYS.2021.751008.
22. Kim HS, Li H, Kim HW, et al. Escitalopram, a selective serotonin reuptake inhibitor, inhibits voltage-dependent K+ channels in coronary arterial smooth muscle cells. *Korean J Physiol Pharmacol.* 2017;21(4):415–21. doi: 10.4196/KJPP.2017.21.4.415.

https://doi.org/10.5455/annalsmedres.2025.07.190

23. Hanley GE, Smolina K, Mintzes B, Oberlander TF, Morgan SG. Postpartum Hemorrhage and Use of Serotonin Reuptake Inhibitor Antidepressants in Pregnancy. *Obstet Gynecol.* 2016;127(3):553–61. doi: 10.1097/AOG.0000000000001200.
24. Grzeskowiak LE, McBain R, Dekker GA, Clifton VL. Antidepressant use in late gestation and risk of postpartum haemorrhage: a retrospective cohort study. *BJOG.* 2016;123(12):1929–36. doi: 10.1111/1471-0528.13612.
25. Huang H, Coleman S, Bridge JA, Yonkers K, Katon W. A meta-analysis of the relationship between antidepressant use in pregnancy and the risk of preterm birth and low birth weight. *Gen Hosp Psychiatry.* 2014;36:13–8. doi: 10.1016/j.genhosppsych.2013.08.002.
26. Andersen JT, Andersen NL, Horwitz H, Poulsen HE, Jimenez-Solem E. Exposure to selective serotonin reuptake inhibitors in early pregnancy and the risk of miscarriage. *Obstet Gynecol.* 2014;124(4):655–61. doi: 10.1097/AOG.0000000000000447.
27. Overview | Antenatal and postnatal mental health: clinical management and service guidance | Guidance | NICE n.d. https://www.nice.org.uk/guidance/cg192?utm_source=chatgpt.com (accessed October 29, 2025).
28. Miller ES, Metz T, Moore Simas TA, Hoffman MC, Byatt N, Roussos-Ross K. Treatment and Management of Mental Health Conditions During Pregnancy and Postpartum: ACOG Clinical Practice Guideline No. 5. *Obstet Gynecol.* 2023;141(6):1262–88. doi: 10.1097/AOG.0000000000005202.

https://doi.org/10.5455/annalsmedres.2025.07.190

Ann Med Res

Current issue list available at Ann Med Res

Annals of Medical Research

journal page: annalsmedres.org

The role of transarterial embolization in the management of hepatic hemangiomas: A retrospective analysis

Huseyin Gokhan Yavas[a,*], Muhammet Sefa Acar[a], Behic Akyuz[b], Furkan Erturk Urfali[b], Mehmet Korkmaz[a]

[a]Kütahya Health Sciences University, Faculty of Medicine, Department of Radiology, Kütahya, Türkiye
[b]Bursa City Hospital, Clinic of Radiology, Bursa, Türkiye
*Corresponding author: huseyingokhanyavas@gmail.com (Huseyin Gokhan Yavas)

MAIN POINTS

- Transarterial embolization with bleomycin–lipiodol emulsion is a safe and effective treatment for giant hepatic hemangiomas.
- Significant volumetric reduction was achieved, with 90% of patients reaching a volume reduction ratio (VRR) ≥50% at 12 months.
- Symptom resolution was observed in 93.5% of patients, with no major complications reported.
- Equal or greater than 75% peripheral contrast filling during embolization predicted higher volumetric response.

Cite this article as: Yavas HG, Acar MS, Akyuz B, Urfali FE, Korkmaz M. The role of transarterial embolization in the management of hepatic hemangiomas: A retrospective analysis. *Ann Med Res*. 2026;33(4):151–158. doi: 10.5455/annalsmedres.2025.09.270.

ABSTRACT

Aim: Hepatic hemangiomas (HHs) are the most common benign liver tumors, and giant lesions may cause symptoms or complications requiring intervention. Surgical resection carries significant morbidity, and minimally invasive alternatives such as transarterial embolization (TAE) have gained importance. This study aimed to evaluate the clinical and radiological outcomes of TAE with bleomycin–lipiodol emulsion for giant HHs and to examine the relationship between peripheral contrast filling and volumetric response.

Materials and Methods: This retrospective, dual-center study included 41 patients who underwent TAE between January 2019 and June 2024. Indications for treatment were symptomatic lesions ≥5 cm, progressive growth of hemangiomas, or all lesions ≥10 cm. Contrast-enhanced MRI or CT was performed at 1, 3, 6, and 12 months post-treatment. Volumetric reduction ratio (VRR) and size reduction were calculated, and angiographic peripheral contrast filling was categorized into four groups (<25%, 25–49%, 50–74%, 75%). Clinical outcomes, technical success, and complications were analyzed.

Results: One patient was identified as a statistical outlier and excluded from the final analysis, which therefore comprised 40 patients (73 HHs). The mean baseline lesion diameter was 8.6±0.5 cm, with a median volume of 178.3 cc (IQR 62.5–376.0). At 12 months, the mean VRR reached 75%, and 90% of patients achieved VRR ≥50%. Patients with ≥75% peripheral contrast filling had significantly greater volume reduction compared with lower filling groups (p<.001). Symptom resolution occurred in 93.5% of symptomatic patients. The overall complication rate was 25%, all of which were minor (SIR Grade A–B), and no major or persistent complications were observed.

Conclusion: TAE with bleomycin–lipiodol emulsion is a safe and effective treatment for giant hepatic hemangiomas, providing substantial volume reduction and symptom relief. The degree of peripheral contrast filling may serve as a predictor of treatment success.

Keywords: Liver hemangioma, Therapeutic embolization, Bleomycin, Treatment outcome, Volume reduction rate

Received: Sep 17, 2025 **Accepted:** Nov 05, 2025 **Available Online:** Apr 24, 2026

INTRODUCTION

Hepatic hemangiomas (HHs) are the most common benign neoplasms of the liver, with a reported prevalence ranging from 0.4% to 20% in population-based studies [1]. Most HHs are detected incidentally; due to their small size and asymptomatic nature, they typically require no intervention [2–4]. However, "giant" hemangiomas—defined by a large diameter, rapid progression, or compression of adjacent structures—may cause symptoms such as abdominal pain, distension, pressure sensation, and early satiety [5–7]. Although rare, spontaneous rupture is also a potential complication [8].

While surgical resection has traditionally been the standard treatment for giant HHs, the associated risks of significant intraoperative bleeding and postoperative morbidity have underscored the need for minimally invasive alternatives [1,9,10]. In this context, transarterial embolization (TAE), particularly using a bleomycin–lipiodol mixture, has emerged

as an effective method for achieving symptom control and lesion size reduction [3,6,7,9].

Recent large series, meta-analyses, and regional case reports demonstrate that bleomycin–lipiodol TAE yields an average volume reduction of approximately 70% to 90% within 6 to 12 months, accompanied by substantial symptomatic improvement [6,7,11]. Furthermore, studies by Zhao et al., Torkian et al., and Akhlaghpoor et al. indicate that, unlike surgery, TAE offers a superior safety profile, shorter recovery time, and the feasibility of repeat sessions [3,6,7]. Cumulative data [4] highlight the emerging role of transarterial approaches as viable alternatives to surgery for giant hepatic hemangiomas. Within this framework, we retrospectively evaluated the clinical and radiologic efficacy of TAE in a two-center cohort and compared our findings with the current literature.

MATERIALS AND METHODS

Study design and ethical approval

This retrospective study included patients with HHs who underwent TAE between January 2019 and June 2024 at two tertiary interventional radiology centers. Ethical approval was obtained from the institutional non-interventional research ethics committee (Kütahya Health Sciences University Non-Interventional Clinical Research Ethics Committee, approval number: 2025/09-23, July 14, 2025). The study was conducted in accordance with the Declaration of Helsinki.

Inclusion and exclusion criteria

Eligible patients met the following criteria: age ≥18 years, at least one hepatic hemangioma diagnosed radiologically by dynamic MRI (or CT in cases of contraindication) [12] (Figure 1), and a minimum lesion diameter of 5 cm. For lesions measuring 5–10 cm, treatment was indicated in symptomatic patients (e.g., abdominal pain, fullness) or in cases showing ≥1 cm growth within one year. For lesions ≥10 cm, treatment was indicated regardless of symptoms or progression status.

Exclusion criteria included known malignancy, active coagulopathy (INR ≥1.5 and platelet count <50,000/mm^3), advanced hepatic or renal dysfunction, iodine contrast allergy, or incomplete clinical and imaging data at baseline or follow-up.

Preprocedural assessment

All patients were reassessed by the interventional radiologist who was to perform the procedure. Pre-existing imaging (MRI or CT) was reviewed, and volumetric as well as triaxial measurements were obtained. Four experienced interventional radiologists (two per center) participated in the study, each responsible for performing the procedure and overseeing follow-up. Pre- and post-procedural lesion dimensions were obtained retrospectively from radiology reports, which had been documented by the interventional radiologist who performed each procedure. Each report included the lesion's

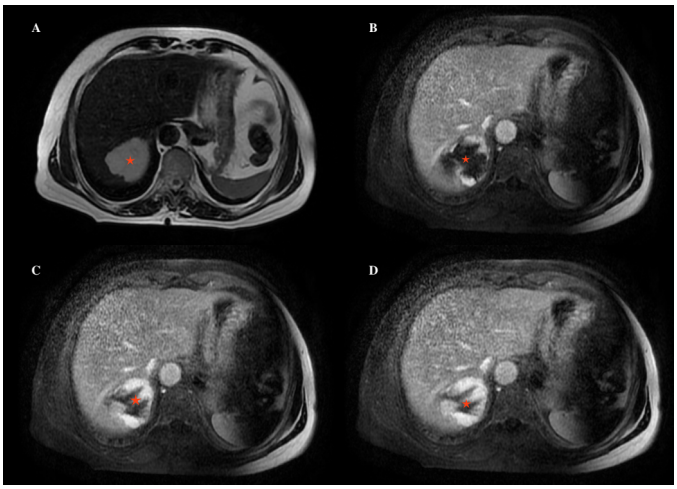

Figure 1. Contrast-enhanced dynamic MRI of the liver in a patient with a right-lobar hepatic hemangioma. A) On the precontrast T2-weighted image, a hyperintense lesion is observed in the right hepatic lobe (marked with a red star). (B–D) Dynamic postcontrast images demonstrate progressive, discontinuous centripetal enhancement, which is characteristic of hepatic hemangioma.

longest diameter and triaxial measurements, from which volumetric data had been calculated using the ellipsoid formula (Volume = 0.52 × length × width × height). These values were verified and recorded from the institutional picture archiving and communication systems (PACS) of both centers.

Embolization procedure

All procedures were performed under local anesthesia without sedation. Vascular access was obtained via the common femoral artery using an 18G needle, followed by placement of a 5–6F vascular sheath with the Seldinger technique. The celiac trunk and/or superior mesenteric artery were catheterized with a Simmons 1 or Cobra 2 catheter over a .035–.038-inch guidewire. Digital subtraction angiography (DSA) was used to evaluate hepatic arterial anatomy. The feeding arteries were catheterized superselectively using a 2.1–2.7F microcatheter and a .014-inch guidewire.

The embolic mixture consisted of 15 mg bleomycin dissolved in 5 mL saline and emulsified with 10 mL lipiodol, yielding a total volume of 15 mL. The solution was prepared by continuous agitation between two syringes connected via a three-way stopcock. It was administered slowly into each feeding artery until reflux was observed (Figure 2). Technical success was defined as full opacification of all feeding arteries and stasis at the end of embolization. No additional embolic materials (particles, coils, or plugs) were used.

Peripheral contrast filling assessment

Angiographic data were retrospectively reviewed from institutional archives. Two interventional radiologists independently evaluated the peripheral distribution of the bleomycin–lipiodol mixture. For standardization, the lesion circumference was divided conceptually into four quad-

https://doi.org/10.5455/annalsmedres.2025.09.270

rants, and peripheral filling was categorized as <25%, 25–49%, 50–74%, or ≥75% (Figure 2). Interobserver agreement was assessed using Cohen's kappa coefficient.

Periprocedural monitoring

All patients were monitored for at least 24 hours post-procedure. Vital parameters and potential periprocedural complications were continuously assessed during and after the embolization. Prophylactic antibiotics were administered when indicated. Analgesics and antiemetics were given as needed. No patients required sedation or general anesthesia.

Both acute and delayed complications were prospectively recorded and retrospectively reviewed in accordance with the Society of Interventional Radiology (SIR) Adverse Event Classification System, which enables standardized grading of procedure-related events.

Follow-up protocol

Follow-up was conducted at 1, 3, 6, and 12 months using dynamic contrast-enhanced MRI (or CT if MRI was contraindicated). At each visit, the longest axis, triaxial measurements, and lesion volume were recorded. Symptomatic patients were also assessed for persistence or resolution of clinical complaints. All patients were followed for at least 12 months after the procedure, and imaging assessments were standardized to the 12-month time point to ensure consistent evaluation across the cohort.

Statistical analysis

No a priori sample size calculation was performed because of the retrospective design. Post-hoc power analysis was conducted using G*Power 3.1 to evaluate the achieved statistical power based on the observed effect size between peripheral filling subgroups.

All statistical analysis was performed using SPSS version 25.0 (IBM Corp., Armonk, NY, USA). The normality of continuous variables was assessed using the Kolmogorov–Smirnov or Shapiro–Wilk tests depending on sample size, complemented by visual inspection of histograms and Q–Q plots. Normally distributed variables were expressed as mean ± standard deviation (SD), whereas non-normally distributed variables were summarized as median [interquartile range (IQR)]. Categorical variables were expressed as counts and percentages.

Temporal changes in lesion VRR and diameter reduction ratio were evaluated using repeated-measures ANOVA, followed by Bonferroni-adjusted pairwise comparisons. The independent-samples t-test was applied to compare 12-month VRR values according to the number of treatment sessions, baseline symptom status, and lesion size categories (5–10 cm vs >10 cm). Comparisons among peripheral filling pattern groups (<25%, 25–50%, 50–75%, >75%) were performed using one-way ANOVA, followed by post-hoc Tukey tests.

For non-normally distributed parameters the Mann–Whitney U test was used. Chi-square testing assessed associations between categorical variables. Correlations between continuous variables were analyzed with Spearman's rank-order and Pearson's correlation coefficient. To further evaluate the predictive role of peripheral contrast filling on 12-month VRR, a simple linear regression analysis was performed. Interobserver agreement between the two radiologists who categorized peripheral filling was assessed using Cohen's kappa ($\varkappa$). Statistical significance was defined as $p<.05$.

RESULTS

A total of 74 HHs were treated in 41 patients included in the inital study cohort; however, one patient was identified as a statistical outlier and excluded from the final analysis. Accordingly, 73 HHs in 40 patients were included in the evaluated dataset. The median age of the patients was 51 years (IQR: 47-56), and the majority were female (32/40; 80%), while 8 patients (20%) were male. The mean pre-procedural longest lesion diameter was 8.57±0.53 cm (range: 5.1–17.0 cm), and the median baseline lesion volume was 178.32 cc (IQR: 62.49–376.02). When evaluated on a per-patient basis, lesion location was right-lobar in 28 patients (70 %), left-lobar in 9 patients (22.5%), and bilateral in 3 patients (7.5%). A single lesion was detected in 24 patients (60.0%), while multiple lesions were present in 16 patients (40.0%) (Table 1).

The mean follow-up duration for the entire cohort was 21.7±10.3 months (range, 12–48 months). For uniformity of analysis, outcomes were primarily evaluated at the 12-month time point, which was completed by all patients. During the available follow-up period, no lesion regrowth or new lesion development was observed. Across all procedures, the mean administered volume of the prepared bleomycin–lipiodol mixture was 15.93 ± 9.71 mL (median: 15 mL; range: 5–41 mL), and the average bleomycin dose per session was calculated as 12.06 mg (Table 2).

A single-session TAE was sufficient in 30 patients (75.%), whereas 10 patients (25%) underwent multiple treatment sessions. Among those requiring more than one session, five had multiple lesions; in three patients, a single lesion could not be fully embolized in one session due to the recommended maximum dose per procedure; and in two patients, additional sessions were performed due to insufficient volume reduction observed during follow-up.

At least one symptom was observed in 31 patients (77.5%). The most commonly reported symptom was pain, present in 27 patients (67.5%), followed by a sense of pressure in 15 patients (37.5%), abdominal distension in 10 patients (25%), and early satiety in 5 patients (12.5%) (Table 2). Patients presenting with a sensation of pressure or abdominal distension had significantly larger pre-procedural lesion volumes ($p=.02$ and $p<.01$, respectively). In contrast, lesion volume was not significantly associated with the presence of pain ($p=.18$) or early satiety ($p=.17$). Additionally, pressure sensation ($p<.01$), distension ($p<.01$), and early satiety ($p=.04$)

https://doi.org/10.5455/annalsmedres.2025.09.270

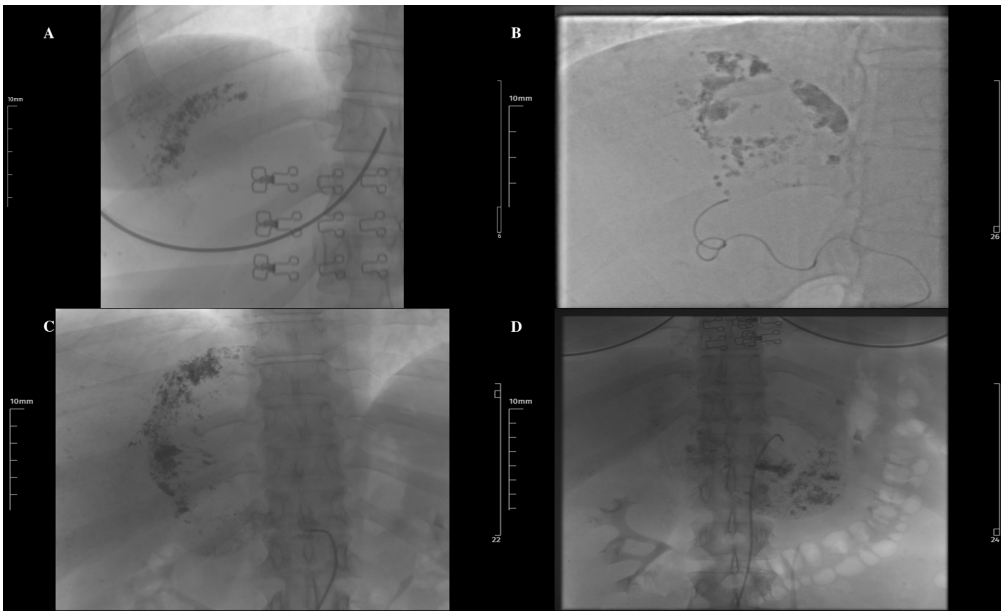

Figure 2. Angiographic images demonstrating variations in peripheral enhancement patterns of hepatic hemangiomas treated with bleomycin–lipiodol embolization. (A) In a patient with a lobulated hemangioma located in the right hepatic lobe, peripheral enhancement was assessed as 50–74%. (B) In another patient, the lesion demonstrated peripheral enhancement greater than 75%. (C–D) Images from a patient who underwent embolization in two separate sessions for a hemangioma supplied by branches of both the right and left hepatic arteries. Peripheral enhancement ranged between 25% and 49% on different angiographic projections.

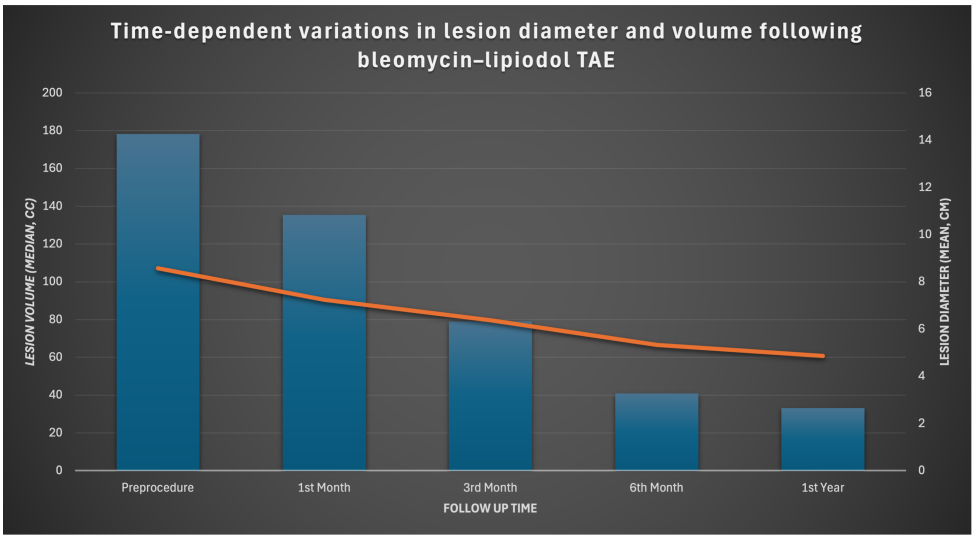

Figure 3. Temporal changes in median lesion volume and maximum diameter following transarterial embolization. The chart depicts median lesion volume (left Y-axis, blue bars) and mean maximum diameter (right Y-axis, orange line) at five time points: baseline (pre-procedure), and 1st, 3rd, 6th, and 12th months post-embolization. Both parameters demonstrated a gradual and consistent decline throughout the follow-up period, indicating a sustained volumetric and morphologic response to embolization.

were more frequently observed in patients with large lesions located in the left hepatic lobe. At the 12-month follow-up, complete symptomatic resolution was achieved in 29 of 31 symptomatic patients (93.5%), while partial improvement was observed in 2 patients.

The mean VRR values at 1, 3, 6, and 12 months were calculated as .32 ± .22, .53 ± .23, .69 ± .19, and .75 ± .16, respectively (Table 3). Repeated-measures ANOVA showed a statistically significant increase in VRR over time ($F[3,120] = 144.29$, $p<0.001$, $\eta^2 = 0.79$). Pairwise comparisons revealed significant improvement between each consecutive time point ($p<0.001$ for all). In parallel, mean diameter reduction ratios were recorded as .17 ± .13, .27 ± .14, .39 ± .16, and .44 ± .15 at the same follow-up intervals, showing a similarly significant trend over time ($F[3,120] = 86.19$, $p<0.001$, $\eta^2 = 0.69$). At the one-year follow-up, the mean long-axis diameter of the lesions was approximately 4.86 ± 2.27 cm, and the median lesion volume was calculated as 33.14 cc (IQR 8.87-102.76) (Figure 3 and 4). The number of cases with a VRR ≥50% was 36 (90%) at 12 months, 32 (80.0%) at 6 months, 22

https://doi.org/10.5455/annalsmedres.2025.09.270

Table 1. Patient demographics and baseline lesion characteristics.

Variable	Value
Total number of patients	40
Total number of lesions	73
Age (years)	51 [47–56]
Gender (F/M)	32 / 8
Presence of symptoms (at least one)	31 (77.5%)
Pain	27 (67.5%)
Sense of compression	15 (37.5%)
Distention	10 (25%)
Early satiety	5 (12.5%)
Preprocedural maximum lesion diameter (cm)	8.57 ± 0.53 (range: 5.1–17.0)
Preprocedural lesion volume (cc)	178.32 [62.49–376.02]
Lesion location (Right/Left/Bilateral)	28 / 9 / 3
Number of lesions (Single/Multiple)	24 / 16

Table 2. Procedural protocol, technical parameters, peripheral distribution pattern, and complication analysis.

Parameter	Details
Embolic agent	Bleomycin–lipiodol emulsion
Total bleomycin amount (mg)	15.93 ± 9.71 (range: 5–41)
Average bleomycin dose per session (mg)	12.06
Number of sessions (Single / Multiple)	30 / 10
Technical success	100%
Postprocedural monitoring	Average 24-hour hospitalization
Prophylactic medication	Antibiotics ± analgesics / antiemetics
Peripheral enhancement pattern (%)	
25–49%	7 patients (17.5%), mean VRR: .61
50–74%	12 patients (30%), mean VRR: .66
≥75%	18 patients (45%), mean VRR: .85
Complications	Pain (15%), PES (10%), total: 25%; no long-term events

PES = Postembolizasyon sendromu; VRR = Volume Reduction Ratio.

Table 3. Volumetric reduction ratio, diameter reduction rate, and time-series analysis.

Follow-up Time Point	Diameter (cm, mean±SD)	Volume (cc, median [IQR])	Diameter Reduction Rate (mean±SD)	Mean VRR (mean ±SD)	Patients with VRR ≥50% (n, %)
1st month	7.24 ± 3.19 (2.7–14.0)	135.46 [34.32-287.07]	.17 ± .14	.32 ± .24	8 (20.0%)
3rd month	6.37 ± 2.83 (2.2–12.5)	79.05 [19.03-200.24]	.27 ± .14	.53 ± .23	22 (55.0%)
6th month	5.32 ± 2.53 (1.5–11.5)	40.87 [11.73-131.04]	.39 ± .16	.69 ± .19	32 (80.0%)
12th month	4.86 ± 2.27 (1.3–11.5)	33.14 [8.87-102.76]	.44 ± .15	.75 ± .16	36 (90.0%)

(55%) at 3 months, and 8 (20%) at 1 month.

Twelve-month VRR outcomes did not differ significantly according to the number of TAE sessions performed (single vs. multiple, p=0.92) or the categorized lesion sizes (5–10 cm vs. >10 cm, p = 0.46). When patients were stratified by baseline symptom status, those who presented with clinical symptoms tended to show higher volumetric reduction ratios at 12 months compared with asymptomatic individuals; however, this difference did not reach statistical significance (p=0.06).

A statistically significant difference was observed in 12-month VRR values across peripheral filling pattern groups (one-way ANOVA, p<.01). Accordingly, the mean VRR was calculated as .85 in patients with 75% peripheral filling, .66 in the 50–74% group, and .61 in the 25–49% group. Subgroup analysis revealed that patients with ≥75% peripheral filling exhibited significantly greater VRR values than those in the 50–74% and 25–49% groups (p<.001) (Figure 5). A strong positive correlation was observed between VRR and the degree of peripheral contrast filling (r=0.64, p<0.001). Linear regression analysis further confirmed that the extent of peripheral contrast filling was a significant predictor of 12-month VRR (β=0.627, p<0.001). The overall regression model was statistically significant (F[1,38] = 24.67, p<0.001), explaining approximately 39% of the variance in volumetric response (R^2=0.39). Interobserver agreement between the two radiologists who performed the peripheral filling pattern classification was very high, with a Cohen's kappa coefficient of .875 (p<.01). Post-hoc power analysis for the comparison

https://doi.org/10.5455/annalsmedres.2025.09.270

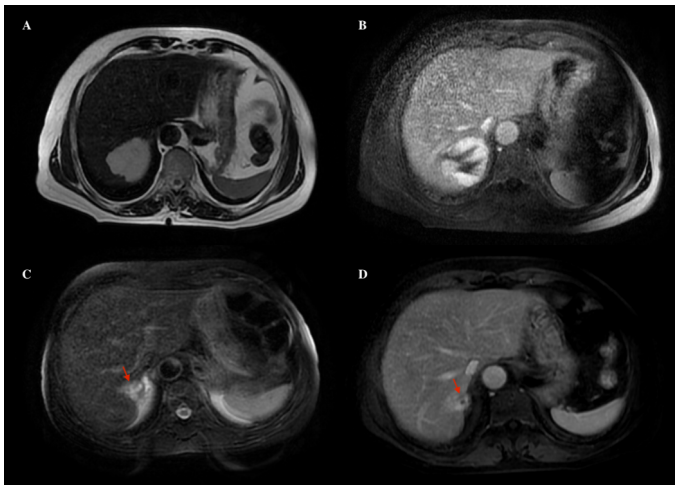

Figure 4. MRI follow-up of the same patient shown in Figure 1, demonstrating treatment response after TAE with a bleomycin–lipiodol emulsion. (A, B) Pre-procedural MRI reveals a lobulated, hyperintense hemangioma in the right hepatic lobe on axial T2-weighted imaging (A) and typical peripheral nodular enhancement on post-contrast T1-weighted imaging (B). (C, D) Corresponding 12-month follow-up images show marked volumetric regression, with near-complete resolution of the lesion on both T2-weighted (C) and post-contrast T1-weighted (D) sequences, consistent with a favorable therapeutic response.

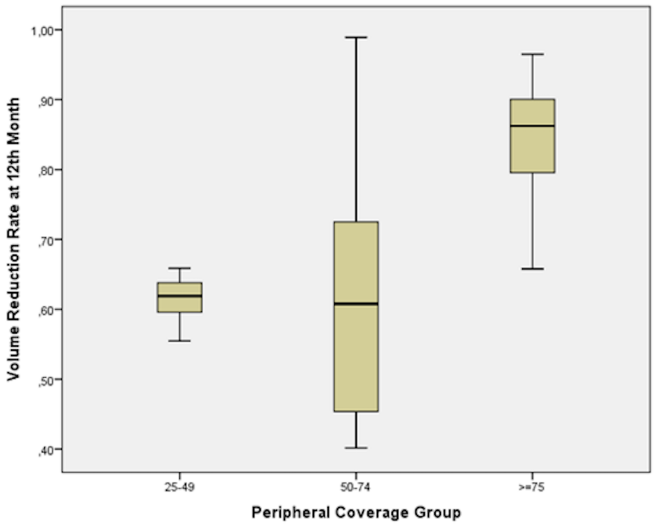

Figure 5. Box plot of 12-month volume reduction ratio (VRR) according to peripheral Lipiodol--bleomycin coverage. Significantly higher VRR was observed in patients with ≥75% peripheral coverage compared to lower coverage groups (p<.01).

of ≥75% and <75% peripheral filling groups demonstrated a large effect size (Cohen's d=1.54) and an achieved power of 0.999 at α=0.05 (two-tailed).

The most common acute complications observed in the post-procedural period were postprocedural pain (n = 6; 15%) and postembolization syndrome (n = 4; 10%), while no acute complications were noted in 30 patients (75%). There was no statistically significant difference in 12-month VRR values between patients with and without acute complications (t test, p=.52). Symptomatic management for patients with complications included paracetamol or NSAIDs, with opioid analgesics and antiemetics added as needed. Complete clinical recovery was achieved in all patients within 24–48 hours, and no long-term complications, including bleomycin-related pulmonary toxicity, were reported during follow-up. All complications were classified as minor (Grade A–B) according to the SIR Adverse Event Classification System, and no major adverse events were encountered.

DISCUSSION

This two-center retrospective study demonstrated that TAE with a bleomycin–lipiodol emulsion is a safe and effective treatment for giant HHs. At the 12-month follow-up, the mean volumetric reduction ratio (VRR) reached 75%, with nearly 90% of patients achieving a VRR ≥50%, accompanied by complete resolution of symptoms in 93.5% of symptomatic patients. Importantly, a significant correlation was found between the extent of peripheral contrast filling and VRR, suggesting that this angiographic parameter may predict treatment response.

The findings of this study are consistent with previous reports in the literature. The study population had a median age of 51 years, and females represented 80% of the enrolled cases. This demographic distribution is consistent with previously reported data in the literature [3,5,6,10,11,13]. The mean pre-procedural long-axis diameter of the lesions was 8.6 cm (range: 5.1–17.0 cm), and the median volume was 178 cc, both of which are comparable to findings reported in similar studies [3,5,14].

Among the 40 patients who underwent bleomycin–lipiodol–based TAE, the proportion of cases achieving ≥50% volume reduction at 12 months was calculated as 90%. This rate is in line with previous studies in the literature, which have reported similar outcomes ranging between 70% and 90% [3,5,6,10,11,14–16]. In a meta-analysis by Torkian et al. [7], the proportion of cases achieving >50% volumetric response within 6–12 months of follow-up was reported to range between 70% and 92%. These findings indicate that the 90% response rate observed in the present series is consistent with large Asian and Western cohorts, as well as with regional case series.

Evaluation of the sequential follow-up data in the present study demonstrated a gradual increase in mean VRR values, measured as 32% at 1 month, 53% at 3 months, 69% at 6 months, and 75% at 12 months, with the difference found to be statistically significant. Similarly, Zhao et al. [6] reported VRR values of 28%, 50%, 70%, and 78% at the corresponding follow-up intervals. In the series by Pehlivan et al. [11], mean VRRs were reported as 65% at 6 months and 74.6% at 12 months. The study by Yuan et al. [16] further supports this gradual trend in early volume reduction, with VRRs of 53% and 69% reported at 3 and 6 months, respectively. This sequential pattern of volume reduction suggests that the bleomycin–lipiodol TAE protocol may provide

https://doi.org/10.5455/annalsmedres.2025.09.270

a time-dependent and sustained volumetric response in the treatment of giant HHs. However, additional long-term data beyond 12 months, supported by larger case series, are warranted to more accurately evaluate the durability of treatment efficacy and the potential risk of lesion regrowth.

A recent study by Kutlu et al. [17] reported that significant volume reduction may also occur in nontarget hemangiomas following bleomycin–ethiodized oil embolization, suggesting a possible systemic or microcirculatory effect of the agent. Although our analysis focused on embolized target lesions, some patients in our cohort had multiple hemangiomas, and retrospective volumetric data of untreated lesions were not systematically collected. Future studies designed to evaluate both target and nontarget lesion responses could further clarify the broader therapeutic impact of this technique.

In the present series, at least one symptom was present in 77.5% of patients prior to the procedure. The most frequently reported complaint was pain (67.5%), followed by a sense of pressure (37.5%), abdominal distension (25%), and early satiety (12.5%). This symptom distribution is consistent with the clinical profiles reported in the series by Zhao et al. and Akhlaghpoor et al., in which pain and a sense of pressure were among the most common symptoms, whereas distension and early satiety were observed less frequently [3,6].

In this study, the finding that patients experiencing a sense of pressure and abdominal distension had significantly higher mean lesion volumes is consistent with previous reports by Akhlaghpoor et al. and Kacała et al., which suggest that mechanical compression in large-volume giant hepatic hemangiomas may play a key role in the development of symptoms [3,5]. Additionally, symptoms such as a sense of pressure, distension, and early satiety were more frequently observed in patients with large lesions located in the left hepatic lobe compared to those with right-lobe involvement. This observation is in line with the interpretation provided by Kacała et al. [5], which emphasized a potential association between lesion location and symptomatology.

The rate of symptomatic improvement following treatment was 93.5%, which aligns with many previous studies reporting rates above 90% [3,6,11,13–15]. Recent literature also highlights that the majority of symptoms resolve after TAE, and any remaining minor complaints are typically manageable with conservative treatment approaches [2,5,18]. Although not statistically significant, symptomatic patients showed a trend toward greater volumetric reduction compared with asymptomatic individuals. Previous studies have not analyzed volumetric outcomes in relation to symptom status, and our findings provide preliminary data on this relationship.

In recent years, technical factors have been increasingly emphasized as critical determinants of volumetric treatment success. In this study, the extent of bleomycin–lipiodol distribution around the lesion was evaluated based on a visually assessed peripheral filling score. The proportion of cases demonstrating ≥75% peripheral distribution was 55%, and this group showed significantly higher 12-month VRR values compared to the 50–74% and 25–49% groups (p<.001). Similarly, in the study by Akhlaghpoor et al., complete circumferential distribution of the lipiodol–bleomycin emulsion was achieved in 37.9% of cases, and this subgroup demonstrated significantly higher rates of volume reduction than other distribution pattern groups (p=.04) [3]. In the series by Kacała et al., extensive (>75%) peripheral distribution of the bleomycin–lipiodol mixture was reported in 77.5% of cases, and this was emphasized as a potential determinant of technical success [5]. The findings of the present study are consistent with these reports and further support them with quantitative subgroup analyses.

Consistent with these reports, the findings of the present study further support the role of peripheral contrast filling as a potential determinant of volumetric response. In our analysis, the degree of peripheral contrast filling showed a significant positive correlation with 12-month VRR (r = 0.64, p<0.001). Linear regression analysis also indicated that peripheral filling was significantly associated with VRR, accounting for approximately 39% of the observed variance (R^2=0.39, β = 0.63, p<0.001). These results suggest that a more extensive peripheral distribution of the bleomycin–lipiodol emulsion during embolization may contribute to greater volume reduction, although additional studies with larger cohorts are needed to confirm this relationship.

The overall postprocedural complication rate was 25%, with the most common adverse events being postprocedural pain (15%) and postembolization syndrome (10%). In the literature, complication rates have been reported to range between 18% and 25% [3,6,11,13]. All complications in this series were managed conservatively, and no long-term persistent complications were observed. Although systemic bleomycin exposure is theoretically associated with pulmonary toxicity, the intraarterial route and low total dose used in embolization procedures substantially minimize this risk. Previous series have also reported no cases of pulmonary fibrosis or systemic toxicity after bleomycin–lipiodol embolotherapy [3,6,13]. Consistent with these findings, no respiratory complications or laboratory abnormalities suggestive of bleomycin toxicity occurred in our study population.

Limitations

The primary limitations of this study stem from its retrospective nature, the inherent subjectivity of symptom evaluation, and the operator-dependent interpretation of peripheral contrast distribution. Although all patients completed at least 12 months of clinical and imaging follow-up, long-term outcomes beyond this period were not systematically assessed; therefore, potential late regrowth could not be fully evaluated. Volumetric measurements were derived from manual calculations obtained from radiology reports, and automated or semi-automated segmentation software was not em-

https://doi.org/10.5455/annalsmedres.2025.09.270

ployed, which may have introduced minor variability in measurement reproducibility. Furthermore, in patients with multiple lesions, the potential volumetric response of nontarget hemangiomas could not be assessed, as quantitative data were available only for embolized target lesions. Despite these limitations, the relatively large sample size, consistent volumetric follow-up, a high rate of VRR success exceeding 50%, and the strong concordance with published literature support the contribution of this series to the existing body of evidence on bleomycin–lipiodol–based TAE protocols. Future prospective, multicenter studies with extended follow-up are warranted.

CONCLUSION

Our findings demonstrate that TAE with a bleomycin–lipiodol emulsion is an effective non-surgical treatment option for giant hepatic hemangiomas, achieving substantial volume reduction (≥50%), marked symptomatic improvement, and a favorable safety profile.

Ethics Committee Approval: The study was approved by Kütahya Health Sciences University Non-Interventional Clinical Research Ethics Committee (Decision number: 2025/09-23, July 14, 2025).

Informed Consent: This was a retrospective study based on anonymized medical records. Therefore, informed consent was not required.

Peer-review: Externally peer-reviewed.

Conflict of Interest: The authors declare that they have no conflict of interest.

Author Contributions: Conception: H.G.Y, M.K; Design: H.G.Y, M.K; Supervision: H.G.Y, F.E.U, M.K; Materials: H.G.Y, B.A, F.E.U, M.K; Data collection and proccessing: H.G.Y, M.S.A, B.A; Analysis and interpretion: H.G.Y, M.K; Literature review: H.G.Y, M.S.A; Writing: H.G.Y, B.A; Critical Review: F.E.U, M.K.

Financial Disclosure: The authors declared that this study received no financial support.

Artificial Intelligence Disclosure: The authors declare that an artificial intelligence–based tool (ChatGPT, GPT-4) was used solely for language editing and improving the clarity and readability of the manuscript. The AI tool did not contribute to the study design, data analysis, interpretation of results, or scientific conclusions. All content was critically reviewed and approved by the authors, who take full responsibility for the manuscript.

REFERENCES

1. Oldhafer KJ, Habbel V, Horling K, Makridis G, Wagner KC. Benign liver tumors. *Visc Med.* 2020;36(4):292-303. doi: 10.1159/000509145.
2. Mikos E, Szmygin M, Kidziński R, Lesiuk P, Czeczelewski M, Pyra K. Unusual outcome following transarterial chemoembolization of giant hepatic hemangioma using bleomycin and lipiodol. *Pol Arch Intern Med.* 2024;134(9):16803. doi: 10.20452/pamw.16803.
3. Akhlaghpoor S, Torkian P, Golzarian J. Transarterial bleomycin-lipiodol embolization (B/LE) for symptomatic giant hepatic hemangioma. *Cardiovasc Intervent Radiol.* 2018;41(11):1674-1682. doi: 10.1007/s00270-018-2010-4.
4. European Association for the Study of the Liver (EASL). EASL clinical practice guidelines on the management of benign liver tumours. *J Hepatol.* 2016;65(2):386-398. doi: 10.1016/j.jhep.2016.04.001.
5. Kacała A, Dorochowicz M, Patrzałek D, Janczak D, Guziński M. Safety and feasibility of transarterial bleomycin-lipiodol embolization in patients with giant hepatic hemangiomas. *Medicina (Kaunas).* 2023;59(8):1358. doi: 10.3390/medicina59081358.
6. Zhao D, Xie L, Makamure J, Liu Z, Zhang L, et al. Transcatheter arterial embolization with bleomycin-lipiodol of hepatic hemangiomas: safety, efficacy and predictors of response. *Cardiovasc Intervent Radiol.* 2024;47(7):931-942. doi: 10.1007/s00270-024-03690-4.
7. Torkian P, Li J, Kaufman JA, Jahangiri Y. Effectiveness of transarterial embolization in treatment of symptomatic hepatic hemangiomas: systematic review and meta-analysis. *Cardiovasc Intervent Radiol.* 2021;44(1):80-91. doi: 10.1007/s00270-020-02611-5.
8. Yamamoto T, Kawarada Y, Yano T, Noguchi T, Mizumoto R. Spontaneous rupture of hemangioma of the liver: treatment with transcatheter hepatic arterial embolization. *Am J Gastroenterol.* 1991;86(11):1645-1649. PMID: 1951244.
9. Kacała A, Dorochowicz M, Matus I, Puła M, Korbecki A, et al. Hepatic hemangioma: review of imaging and therapeutic strategies. *Medicina (Kaunas).* 2024;60(3):449. doi: 10.3390/medicina60030449.
10. Özden İ, Poyanlı A, Önal Y, Demir AA, Hoş G, Acunaş B. Superselective transarterial chemoembolization as an alternative to surgery in symptomatic/enlarging liver hemangiomas. *World J Surg.* 2017;41(11):2796-2803. doi: 10.1007/s00268-017-4069-5.
11. Pehlivan UA, Şen Y, Dağlıoğlu Y, Kara B, Aydın C, et al. Karaciğer dev hemanjiyomlarının tedavisinde bleomisin ve lipiodol karışımı ile kemoembolizasyonun güvenilirliği ve etkinliği (in Turkish). *Cukurova Med J.* 2022;47(1):310-321. doi: 10.17826/cumj.1035544.
12. Caseiro-Alves F, Brito J, Araujo AE, Belo-Soares P, Rodrigues H, et al. Liver haemangioma: common and uncommon findings and how to improve the differential diagnosis. *Eur Radiol.* 2007;17(6):1544-1554. doi: 10.1007/s00330-006-0503-z.
13. Bozkaya H, Cinar C, Besir FH, Parıldar M, Oran I. Minimally invasive treatment of giant haemangiomas of the liver: embolisation with bleomycin. *Cardiovasc Intervent Radiol.* 2014;37(1):101-107. doi: 10.1007/s00270-013-0618-y.
14. Furumaya A, van Rosmalen BV, Takkenberg RB, van Delden OM, Dejong CHC, et al. Transarterial (chemo-)embolization and lipiodolization for hepatic haemangioma. *Cardiovasc Intervent Radiol.* 2019;42(6):800-811. doi: 10.1007/s00270-019-02169-x.
15. Kirnap M, Boyvat F, Boyacioglu S, Hilmioglu F, Moray G, Haberal M. The effect of bleomycin embolization on symptomatic improvement and hemangioma size among patients with giant liver hemangiomas. *Open J Gastroenterol.* 2018;8(4):130-139. doi: 10.4236/ojgas.2018.84014.
16. Yuan B, Zhang JL, Duan F, Wang MQ. Medium and long-term outcome of superselective transcatheter arterial embolization with lipiodol-bleomycin emulsion for giant hepatic hemangiomas: results in 241 patients. *J Clin Med.* 2022;11(16):4762. doi: 10.3390/jcm11164762.
17. Kutlu R, Dag N, Saparbekov E, Yagin FH. Nontarget hemangioma size reduction after bleomycin-ethiodized oil embolization of primary hepatic hemangioma. *J Vasc Interv Radiol.* 2025;36(5):787-794. doi: 10.1016/j.jvir.2025.01.042.
18. Kurniawan J, Teressa M, Budiman RA, Matondang SBRE. Transarterial embolization with bleomycin-lipiodol emulsion: a successful minimal invasive approach for giant liver hemangioma. *Clin J Gastroenterol.* 2024;17(3):511-514. doi: 10.1007/s12328-024-01948-5.

Ann Med Res

Current issue list available at Ann Med Res

Annals of Medical Research

journal page: annalsmedres.org

Assessment of potentially pathogenic bacteria isolated from mobile phones of preclinical and hospital-based medical students and healthcare workers

Sibel Altunisik Toplu [a,*], Elif Seren Tanriverdi [b], Ahmet Furkan Curgatay [c], Emine Nalan Parmaksiz [d]

[a] Inonu University, Faculty of Medicine, Department of Infectious Diseases and Clinical Microbiology, Malatya, Türkiye
[b] Inonu University, Faculty of Medicine, Department of Medical Microbiology, Malatya, Türkiye
[c] Inonu University, Faculty of Medicine, Malatya, Türkiye
[d] Turgut Ozal Medical Center, Infection Control Committee, Malatya, Türkiye
*Corresponding author: saltuntoplu@gmail.com (Sibel Altunisik Toplu)

MAIN POINTS

- Mobile phones used in hospital settings showed a significantly higher contamination rate (65.9%) compared to those of preclinical students (25.7%).
- Potentially pathogenic bacteria, including Staphylococcus aureus, Pseudomonas spp., and Acinetobacter baumannii, were isolated only from hospital-exposed devices.
- Preclinical students' phones carried only commensal skin flora, emphasizing the role of hospital exposure in pathogen acquisition.
- Infection control measures and compliance with hand hygiene should be emphasized from the early years of medical education, and it must not be overlooked that mobile phones—devices used in every aspect of daily life—can also become contaminated in hospital environments.

Cite this article as: Altunisik Toplu S, Tanriverdi ES, Curgatay AF, Parmaksiz EN. Assessment of potentially pathogenic bacteria isolated from mobile phones of preclinical and hospital-based medical students and healthcare workers. *Ann Med Res*. 2026;33(4):159--162. doi: 10.5455/annalsmedres.2025.09.254.

ABSTRACT

Aim: Healthcare-associated infections (HAIs) remain a major global problem, and contaminated personal devices may act as unnoticed vectors. This study aimed to evaluate the bacterial contamination of mobile phones among medical students and healthcare workers in hospital and non-hospital settings.

Materials and Methods: A cross-sectional study was conducted between February and March 2024. A total of 203 mobile phones were sampled: 94 from hospital-exposed participants (clinical students and healthcare workers) and 109 from non-hospital-exposed preclinical students. Surface swabs were inoculated into Mueller-Hinton broth, cultured, and isolates were identified using standard microbiological techniques.

Results: Among hospital-exposed participants, bacteria were cultivated from 62/94 phones (65.9%), with potentially pathogenic organisms detected in 13.8%. Among these bacteria were *Staphylococcus aureus* (n=4, none methicillin-resistant), *Pseudomonas spp.* (n=2), *Acinetobacter baumannii* (n=2), *Enterococcus faecalis* (n=1), *Stenotrophomonas maltophilia* (n=1), and *Bacillus spp.* (n=3). Commensals such as *Staphylococcus epidermidis* (n=36) and *Staphylococcus haemolyticus* (n=7) predominated. In contrast, only 28/109 samples (25.7%) from preclinical students showed growth, limited to skin flora without pathogenic isolates. The contamination rate was significantly higher in the hospital-exposed group ($p<0.001$).

Conclusion: Mobile phones used in hospital settings are more frequently contaminated with potentially pathogenic bacteria compared to those of preclinical students, highlighting their role as overlooked reservoirs of HAIs. Incorporating mobile device hygiene into infection prevention strategies, alongside routine hand hygiene, and reinforcing structured training for students and healthcare professionals are critical measures to reduce cross-contamination risks.

Keywords: Mobile phone contamination, Nosocomial infections, Hand hygiene, Healthcare workers, Medical students, Bacterial colonization

Received: Sep 03, 2025 **Accepted:** Nov 19, 2025 **Available Online:** Apr 24, 2026

INTRODUCTION

Healthcare-associated infections (HAIs) remain a major global health problem, contributing to significant morbidity, mortality, and economic burden. In addition to traditional risk factors, contaminated medical devices and personal items carried by healthcare professionals have been increasingly recognized as potential sources of nosocomial transmission.

Mobile phones are among the most frequently handled personal devices by both healthcare workers and medical students. Their continuous use, close contact with hands and faces, and rare cleaning practices make them ideal reservoirs for microorganisms. Evidence from different regions has highlighted the potential role of these devices in the spread of healthcare-associated pathogens.

In Uganda, Lubwama et al. [1] demonstrated that hands of medical students and mobile phones frequently carried bacteria associated with hospital-acquired infections, underlining their possible role as transmission vehicles. More recently, another study from Türkiye revealed that bacterial contamination was highly prevalent on mobile phones of medical students, especially among those with clinical exposure, with isolates including both commensal and pathogenic organisms [2]. Complementing these findings, a systematic review and meta-analysis from Africa reported a pooled prevalence of contamination exceeding 70% among mobile phones of healthcare workers, confirming that this issue represents a global concern [3].

Taken together, the literature strongly supports the view that mobile phones may serve as important but often overlooked vectors of infection, warranting attention in infection control policies. In our study, we aimed to address this issue by conducting a research project with a group of second-year medical students within the framework of evidence-based medicine practices. We evaluated the mobile phones of our faculty's students both before and after clinical exposure, and additionally included the mobile phones of healthcare workers outside the group of hospital-employed students.

MATERIALS AND METHODS

This cross-sectional study was conducted at İnönü University Faculty of Medicine (Malatya, Türkiye) between February and March 2024. The research was designed and implemented in collaboration with a group of second-year medical students within the framework of evidence-based medicine practices. The study was approved by the Inonu University Health Sciences Scientific Research Ethics Committee (Decision No: 2025/7105, Date: March 11, 2025).

Study population

Participants were divided into two groups:

- Hospital-exposed group (n = 94): clinical medical students in years 4–6 and healthcare workers with direct exposure to hospital wards.
- Non-hospital-exposed group (n = 109): preclinical medical students in years 1–3 without hospital exposure.

Sample vollection and processing

Sterile cotton swabs were used to collect surface samples from participants' mobile phones. Each swab was immediately inoculated into Mueller-Hinton broth and then cultured for bacterial growth.

Identification of isolates

Bacterial isolates were identified using standard microbiological techniques, including colony morphology, Gram staining, and conventional biochemical tests.

Statistical analysis

Descriptive statistics were used to summarize contamination rates and bacterial species distribution. The difference in the proportion of positive cultures between hospital-exposed and non-hospital-exposed participants was evaluated using the chi-square (χ^2) test. Statistical significance was defined as $p < 0.05$. All statistical analyses were performed using IBM SPSS Statistics for Windows, Version 26.0 (IBM Corp., Armonk, NY, USA).

Since no a priori sample-size calculation was performed before data collection, a post-hoc power analysis was conducted based on the observed effect size. Using GPower (version 3.1), with $\alpha = 0.05$ and an effect size (w) of 0.40 obtained from the observed frequencies (62/94 vs. 28/109), the achieved power ($1 - \beta$) was calculated as 0.99, indicating that the sample size (n = 203) was adequate to detect a statistically significant difference between groups.

RESULTS

A total of 203 mobile phone surface swabs were analyzed. Among the hospital-exposed group (n = 94), 62 samples (65.9%) yielded bacterial growth, whereas in the non-hospital-exposed preclinical student group (n = 109), only 28 samples (25.7%) were positive (Table 1). The contamination rate was significantly higher among hospital-exposed participants compared with non-hospital-exposed preclinical students ($\chi^2 = 33.1$, $p<0.001$). The post-hoc power of this comparison was 0.99 ($\alpha = 0.05$, effect size w = 0.40). Pathogenic bacteria were more frequently isolated from hospital-exposed phones compared with non-hospital-exposed phones. Notably, *Staphylococcus aureus*, *Pseudomonas spp*., and *Acinetobacter baumannii* were identified only in the hospital-exposed group. In contrast, isolates from preclinical students' phones were predominantly commensal skin flora such as *Staphylococcus epidermidis* and *Staphylococcus haemolyticus* (Table 2).

DISCUSSION

Our findings demonstrate a significantly higher rate of bacterial contamination on mobile phones belonging to healthcare workers and clinical medical students compared with those of preclinical stages of their studies. Importantly, hospital-associated pathogens such as *Staphylococcus aureus*, *Pseudomonas spp.*, and *Acinetobacter baumannii* were exclusively isolated from the hospital-exposed group, whereas devices from the non-hospital exposed group carried only commensal skin flora. This observation strongly suggests that being in the hospital environment facilitates the acquisition and carriage of nosocomial microorganisms on personal devices.

These results are consistent with prior studies from both low- and high-income countries, which have reported contamination rates of over 70% among healthcare workers' mobile phones [3]. Lubwama et al. showed that final-year medical students in Uganda frequently harbored hospital-acquired bacteria on their phones and hands, highlighting the role of

https://doi.org/10.5455/annalsmedres.2025.09.254

Table 1. Bacterial contamination rates according to study groups.

Group	Total phones (n)	Positive cultures, n (%)
Hospital-exposed (clinical students & HCWs)	94	62 (65.9)
Non-hospital-exposed (preclinical students)	109	28 (25.7)

Table 2. Distribution of bacterial isolates from contaminated mobile phones.

Bacterial species	Number of isolates (n)
Staphylococcus aureus (none MRSA)	4
Pseudomonas spp.	2
Acinetobacter baumannii	2
Enterococcus faecalis	1
Stenotrophomonas maltophilia	1
Bacillus spp.	3
Staphylococcus epidermidis	36
Staphylococcus haemolyticus	7

mobile devices as potential vectors of healthcare-associated infections (HAIs) [1]. Similarly, the systematic review and meta-analysis from Africa confirmed that mobile phone contamination is a widespread issue, with pathogenic species frequently isolated from devices used in clinical environments [3]. In Türkiye, Ünal et al. also reported that bacterial colonization was significantly higher in medical students with hospital exposure compared to their preclinical peers [2].

The absence of pathogenic isolates among preclinical students in our study further emphasizes the influence of hospital exposure on the microbial profile of mobile phones. This supports the notion that mobile phones act as reservoirs in the infection chain, enabling indirect transmission of hospital pathogens between patients, healthcare workers, and the community. Although hand hygiene remains the cornerstone of infection prevention, the continuous handling of contaminated devices can compromise infection control efforts if mobile phone hygiene is neglected.

From a public health perspective, this highlights the importance of not only strict adherence to hand hygiene protocols but also the integration of mobile phone decontamination into standard infection control policies. Regular cleaning of devices with approved disinfectants, coupled with educational interventions for both healthcare workers and students, is essential to minimize cross-contamination risks. Furthermore, reinforcing awareness of device hygiene during medical training may help reduce the silent spread of HAIs and protect both patients and healthcare providers. A study conducted in Southern Ethiopia found that health professionals whose mobile phones were cleaned after each use or at least once daily were significantly less likely to have contaminated devices. Conversely, lapses in handwashing before patient contact dramatically increased contamination risk—those who did not wash hands were nearly 13 times more prone to having contaminated phones [4].

Similarly, environmental contamination within hospitals is not restricted to mobile devices. In a study evaluating hospital public toilets, Altunışık Toplu et al. reported that 26% of 85 samples grew Gram-negative bacteria, although no carbapenem resistance was detected. Notably, 31% of individuals did not wash their hands at all after toilet use, and 27% practiced improper handwashing [5]. These findings emphasize that shared hospital environments, such as toilets, may also serve as reservoirs for nosocomial microorganisms if hand hygiene is neglected. Together with our results, this underscores the dual importance of both personal device hygiene and strict adherence to hand hygiene practices in mitigating the risk of cross-contamination and the spread of healthcare-associated infections.

Our findings highlight that mobile phones used in hospital settings are more likely to harbor potentially pathogenic microorganisms compared with those of preclinical students, supporting their role as overlooked reservoirs in the infection chain. This reinforces the importance of considering personal devices within infection prevention strategies.

It is important to implement infection control measures; however, broader reviews and evidence mappings have emphasized that despite the well-recognized potential of mobile phones to act as vectors of nosocomial pathogens, these devices are frequently overlooked in routine disinfection protocols. This gap in practice highlights the need for formal guidance and educational strategies to ensure mobile device cleanliness in clinical care areas [6].

Taken together, these findings underscore the necessity of integrating mobile phone decontamination into infection control policies, alongside strict hand hygiene compliance. Regular cleaning with approved disinfectants and educational interventions targeting both healthcare workers and students can substantially reduce cross-contamination risks. Practical recommendations include routine cleaning of mobile devices with 70% ethanol-based disinfectants or the use of UV sterilizers, both of which have been shown to effectively reduce mi-

https://doi.org/10.5455/annalsmedres.2025.09.254

crobial contamination [7, 8]. Reinforcing awareness of device hygiene during medical training may further help prevent the silent spread of HAIs and protect both patients and healthcare providers.

Limitations

This study has some limitations. The study did not assess antibiotic susceptibility profiles, viral contamination, or fungal flora, which could provide a more comprehensive overview of the microbial spectrum. Furthermore, detailed data regarding the departments and duration of hospital exposure for participants with nosocomial pathogens were not collected, as the study design prioritized anonymity.

CONCLUSION

Our results indicate that mobile phones used in hospital environments serve as reservoirs for potentially pathogenic microorganisms and may contribute to the transmission of healthcare-associated infections. The absence of such pathogens among preclinical students emphasizes the role of hospital exposure in shaping device. Regular disinfection of mobile phones, strict compliance with hand hygiene, and the incorporation of device hygiene education into medical training are essential strategies to minimize cross-contamination risks and strengthen infection prevention efforts.

Acknowledgment: The authors would like to thank the Evidence-Based Medicine (EBM) student group of İnönü University Faculty of Medicine — Ece Çimen, Emirhan Çevik, Enes Çalğan, Enes Burak Çataldere, Hamza Çelik, İlknur Elif Çoban, Mehmet Cömert, Yasemin Çakır, and Zeynep Çaparuşağı — who actively participated in the data collection process. This project was carried out as part of their EBM training, and their enthusiastic involvement and contributions were invaluable to the success of this study.

Ethics Committee Approval: This study was approved by the İnönü University Health Sciences Scientific Research Ethics Committee (Session No: 5, Decision No: 2025/7105, Date: March 11, 2025).

Informed Consent: Not applicable.

Peer-review: Externally peer-reviewed.

Conflict of Interest: The authors declare that they have no conflict of interest.

Author Contributions: SAT: Conceptualization, study design, supervision, manuscript drafting; EST: Laboratory processing, microbiological identification, data interpretation; AFÇ: Data collection, statistical analysis, manuscript editing; ENP: Infection control coordination, methodology support.

Financial Disclosure: Not applicable.

Artificial Intelligence Disclosure: In the preparation of this article, AI-based tools were used only for language editing and improving text comprehensibility. In this context, ChatGPT (OpenAI, version 5.2) was used in some parts of the article for expression editing, sentence structure improvement, and grammar checking. AI tools were not used for study design, data collection, statistical analysis, data interpretation, or scientific content generation. All scientific content, findings, interpretations, and conclusions of the study were created by the authors.

REFERENCES

1. Lubwama M, Kateete DP, Ayazika KT, Nalwanga W, Kagambo DB, Nsubuga MD, et al. Microbiological Contamination of Mobile Phones and Mobile Phone Hygiene of Final-Year Medical Students in Uganda: A Need for Educational Intervention. *Adv Med Educ Pract.* 2021;12:1247-1257. doi: 10.2147/AMEP.S333223.
2. Ünal E, Tahmaz I, Serin GC, Yılmaz A, Or G, Toroslu İH, et al. Effects of various factors on bacteria colonization at the mobile phones and on the hands of medical faculty students. *J Clin Exp Invest.* 2014;5(3):410–4. doi: 10.5799/ahinjs.01.2014.03.0429.
3. Zenbaba D, Sahiledengle B, Beressa G, Desta F, Teferu Z, et al. Bacterial contamination of healthcare workers' mobile phones in Africa: a systematic review and meta-analysis. *Trop Med Health.* 2023;51(1):55. doi: 10.1186/s41182-023-00547-3.
4. Aliyo A, Bekele C, Gemechu T, Dedecha W, Getachew M. Mobile phone bacterial contaminations, associated factors and antimicrobial susceptibility pattern of bacteria isolates from health professionals' working in public health facilities of West Guji zone, Southern Ethiopia. *BMJ Open Qual.* 2025;14(2):e003321. doi: 10.1136/bmjoq-2025-003321.
5. Altunışık Toplu S, Duman Y, Ersoy Y, Parmaksız N. Can public toilets in hospitals contribute to the spread of carbapenem resistant gram-negative microorganisms? Assessment with social handwashing observations. *ADYÜ Sağlık Bilimleri Derg.* 2020;6(3):338-342. doi: 10.30569/adiyamansaglik.813329.
6. Di Mario S, Dionisi S, Di Simone E, Liquori G, Cianfrocca C, Di Muzio M, Giannetta N. Infections and Smartphone Use in Nursing Practice: A Systematic Review. *Florence Nightingale J Nurs.* 2022;30(2):209-216. doi: 10.54614/FNJN.2022.21190.
7. Lieberman MT, Madden CM, Ma EJ, Fox JG. Evaluation of 6 Methods for Aerobic Bacterial Sanitization of Smartphones. *J Am Assoc Lab Anim Sci.* 2018;57(1):24-29. PMID: 29402348.
8. Malhotra S, Wlodarczyk J, Kuo C, Ngo C, Glucoft M, Sumulong I, Smit MA, Bender JM. Shining a light on the pathogenicity of health care providers' mobile phones: Use of a novel ultraviolet-C wave disinfection device. *Am J Infect Control.* 2020;48(11):1370-1374. doi: 10.1016/j.ajic.2020.05.040.

https://doi.org/10.5455/annalsmedres.2025.09.254

Ann Med Res

Current issue list available at Ann Med Res

Annals of Medical Research

journal page: annalsmedres.org

A concerning condition in childhood: Hemoptysis or pseudohemoptysis?

Yasemin Mocan Caglar[a], *, Sinem Can Oksay[a]

[a]Istanbul Medeniyet University, Göztepe Prof. Dr. Süleyman Yalçın City Hospital, Department of Pediatric Pulmonology, Istanbul, Türkiye
*Corresponding author: dryaseminmocan@gmail.com (Yasemin Mocan Caglar)

MAIN POINTS

- Only half of the children who presented with oral bleeding were diagnosed with true hemoptysis.
- Lower respiratory tract infections were the most common causes of hemoptysis, while upper airway infections predominated in pseudohemoptysis.
- Bright red blood with cough and abnormal lung imaging were key indicators of true hemoptysis.
- This study highlights the importance of distinguishing hemoptysis from pseudohemoptysis based on clinical and radiological findings.

Cite this article as: Mocan Caglar Y, Can Oksay S. A concerning condition in childhood: Hemoptysis or pseudohemoptysis?. *Ann Med Res*. 2026;33(4):163–171. doi: 10.5455/annalsmedres.2025.05.130.

ABSTRACT

Aim: Hemoptysis is defined as expectoration of blood from the lower respiratory tract, whereas pseudohemoptysis is defined as bleeding originating from the upper airways or gastrointestinal tract. Distinguishing between these entities in children is essential because of their differing clinical implications. This study aimed to assess the diagnostic value of clinical features in differentiating hemoptysis from pseudohemoptysis in pediatric patients and to analyze the underlying causes and diagnostic approaches.

Materials and Methods: A retrospective review was conducted on 94 pediatric patients who presented with oral bleeding between January 2018 and December 2024. We analyzed data on demographics, bleeding characteristics, clinical findings, diagnostic imaging, and etiologies.

Results: Hemoptysis was diagnosed in 51% (n = 48) and pseudohemoptysis in 49% (n = 46) of the cases. Cough, sputum production, and pink-to-bright red blood cells were significantly associated with hemoptysis ($p<0.05$). In contrast, pseudohemoptysis was more often associated with blood mixed with saliva, which came directly from the mouth. Fever and purulent sputum were more frequent in the hemoptysis group. Abnormal chest X-ray and CT findings were significantly more common in patients with hemoptysis. The leading causes of hemoptysis were parenchymal lung diseases (58.3%) and idiopathic causes (29.2%), whereas pseudohemoptysis was mainly caused by upper respiratory tract conditions, such as adenoid hypertrophy and sinusitis (24.2%), idiopathic etiologies (21.7%), and artificial bleeding (8.8%).

Conclusion: In children, only half of the cases presenting with blood in the mouth are true hemoptysis. The most important diagnostic indicators of hemoptysis are bright red to pink color, accompanying cough, and any suspicious findings on chest radiography. The most common underlying causes of hemoptysis and pseudohemoptysis are lower and upper respiratory tract infections, respectively.

Keywords: Hemoptysis, Pseudohemoptysis, Factitious hemoptysis, Child, Cough

Received: May 26, 2025 **Accepted:** Nov 26, 2025 **Available Online:** Apr 24, 2026

INTRODUCTION

Hemoptysis is defined as the expectoration of blood or blood-tinged sputum originating from the lower respiratory tract, which is below the level of the larynx. Although it is common in adults, it is a rare symptom in children, presenting a diagnostic challenge. Children tend to swallow their sputum; therefore, hemoptysis may go unnoticed unless the bleeding is significant. Consequently, it often becomes a source of considerable concern for the patient, family, and pediatrician. Hemoptysis in children is commonly classified according to the volume of bleeding: mild hemoptysis refers to expectoration of less than 5 mL of blood per day, moderate hemoptysis to 5–200 mL per day, and massive hemoptysis to more than 200 mL per day or greater than 8 mL/kg/day [1]. Pseudohemoptysis refers to bleeding from extrapulmonary sources, such as the upper airway or gastrointestinal tract, but it can be mistakenly attributed to true hemoptysis. Because diagnostic and therapeutic strategies differ significantly, identifying the source of bleeding is crucial.

Determining hemoptysis incidence in the pediatric population is a challenging task. Contributing factors include inconsistencies in case definitions, presentation to different specialties across various health care facilities, and the potential for pseudohemoptysis to be misclassified as true hemoptysis [2]. In a tertiary pediatric pulmonology center in Türkiye, hemoptysis was detected in 1.8% of patients aged >6 years

[3]. In Godfrey, hemoptysis accounted for only 0.8% of bronchoscopy indications [4]. Previous studies have identified an underlying cause in 75%–90% of pediatric hemoptysis cases, while no specific etiology could be determined in 10%–25% of cases. The most commonly reported causes include infections, bronchiectasis, parenchymal lung diseases, and previously operated congenital heart diseases [4-6]. Infections have consistently been reported as the leading etiologic factor in multiple studies [6-8]. Factitious hemoptysis, as observed in Munchausen syndrome by proxy, involves the deliberate production or simulation of symptoms by patients or caregivers. Factitious causes should be considered in the differential diagnosis in cases of hemoptysis with unclear etiology to avoid unnecessary and potentially harmful interventions [1,9-12].

This study aimed to evaluate the role of clinical and laboratory findings in differentiating hemoptysis from pseudohemoptysis in our tertiary care center and to summarize the characteristics of the diagnostic investigations performed to identify the underlying etiology.

MATERIALS AND METHODS

The data of pediatric patients who presented to our Pediatric Pulmonology outpatient clinic with complaints of oral bleeding between January 2018 and December 2024 were retrospectively obtained from the hospital's digital database and medical record archives. Ethics approval for the study was obtained from the Kartal Koşuyolu Training and Research Hospital Ethics Committee, with decision number 2024/11/842, dated June 4, 2024.

In addition to the patients' demographic data, the color and duration of bleeding, presence of accompanying symptoms, diagnostic methods, etiological causes, and final diagnoses were recorded. The results of investigations such as bronchoscopy and laryngoscopy were also documented if available. The inclusion criterion was pediatric patients who presented to the Pediatric Pulmonology outpatient clinic with oral bleeding complaints. The exclusion criteria were as follows: (1) incomplete medical records, (2) bleeding disorders, and (3) a diagnosis of vasculitis (Figure 1). Hemoptysis is categorized as mild/moderate or massive based on the daily volume of spat blood [1].

Hematemesis is the vomiting of blood originating from the stomach or upper gastrointestinal tract, typically appearing dark red or brown [4-7, 11]. Hematemesis patients were classified as having pseudohemoptysis.

Chest radiographs and thoracic computed tomography (CT) revealed suspicious pathological appearances suggestive of the etiology of hemoptysis, including ground-glass opacities, alveolar consolidation, air bronchograms, nonspecific consolidation, and cysts/cavities.

We re-evaluated and documented flexible bronchoscopy data and video recordings obtained at our center. All flexible bronchoscopy in this study were performed by our pediatric pulmonology physicians in our clinic.

The algorithm begins with history taking and physical examination, differentiating between finding suggestive of gastrointestinal/upper airway sources and those indicating lower respiratory tract origin. In cases suggestive of pseudohemoptysis or hematemesis, upper respiratory tract and gastrointestinal pathologies are evaluated. Chest radiography, thoracic CT, and further laboratory evaluation are recommended for suspected lower airway causes. The algorithm also outlines subsequent steps, including bronchoscopy, lung biopsy, and appropriate management strategies based on recurrence, specific diagnoses (e.g., tuberculosis, bronchiectasis, actinomycosis), or nonspecific findings.

Statistical analysis

An a priori power analysis was conducted in G*Power 3.1 for a chi-square test of contingency tables, assuming a medium effect size (Cohen's w = 0.40), two-sided $\alpha = 0.05$ (95% confidence), power = 0.80, and df = 5. The minimum required total sample size was 81.

Statistical analyses were performed using IBM SPSS Statistics for Windows, Version 22.0 (Armonk, NY: IBM Corp.).

Data are presented as counts and percentages for categorical variables. The Kolmogorov–Smirnov test was used to assess the normality of continuous variables. Continuous variables that did not meet the assumption of normal distribution were expressed as median (minimum–maximum) values, and the Mann–Whitney U test was used to compare the groups. Categorical variables were compared using Pearson's chi-square test (asymptotic significance or exact significance) or Fisher's exact test according to the assumptions. When the omnibus test was significant, Bonferroni-adjusted pairwise comparisons were used to determine the significantly different categories. The categories with different superscript letters were statistically different. A p-value <0.05 was considered statistically significant.

RESULTS

Between January 2018 and December 2024, 7834 patients were evaluated in our pediatric pulmonary outpatient clinic, of whom 94 (1.2%) presented with oral bleeding complaints. Hemoptysis was diagnosed in 0.61% (n = 48) of these cases, whereas pseudohemoptysis was identified in 0.58% (n = 46). The median age of the 94 patients was 159 months (range: 9–243 months), with a male-to-female ratio of 1.09.

Among the patients, 51% (n = 48) was diagnosed with hemoptysis and 49% (n = 46) with pseudohemoptysis. The male-to-female ratio was 1.3 in the hemoptysis group and 0.9 in the pseudohemoptysis group (p=0.414). The median age was 159 months (range:9-243 months) in the hemoptysis group and 140 months (range:10-227 months) in the pseudohemoptysis group (p = 0.443).

Based on the amount of bleeding, massive hemoptysis was observed in only 6.3% (n = 3) of the patients in the hemoptysis

https://doi.org/10.5455/annalsmedres.2025.05.130

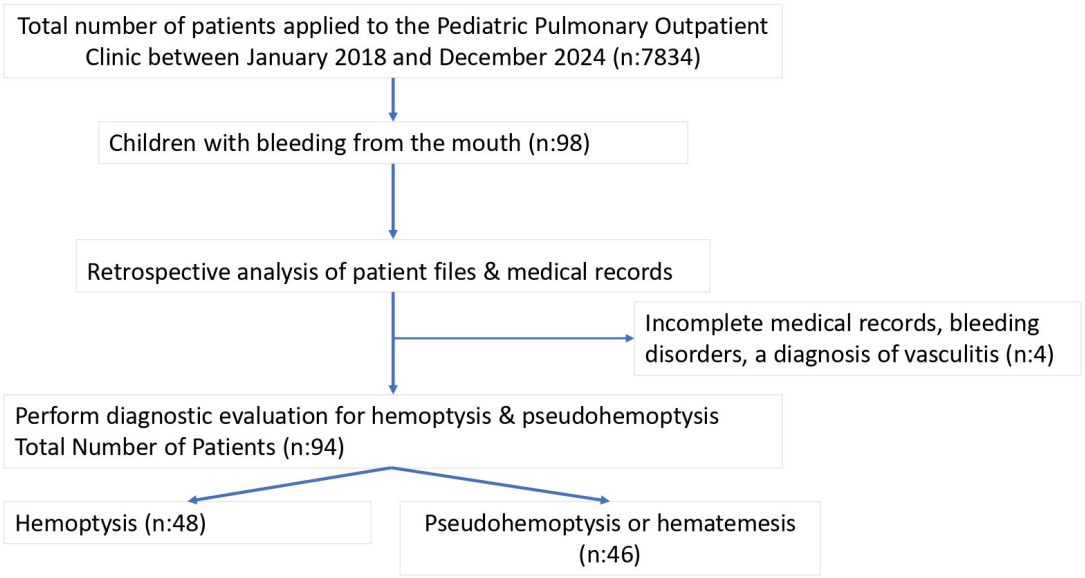

Figure 1. Flow diagram.

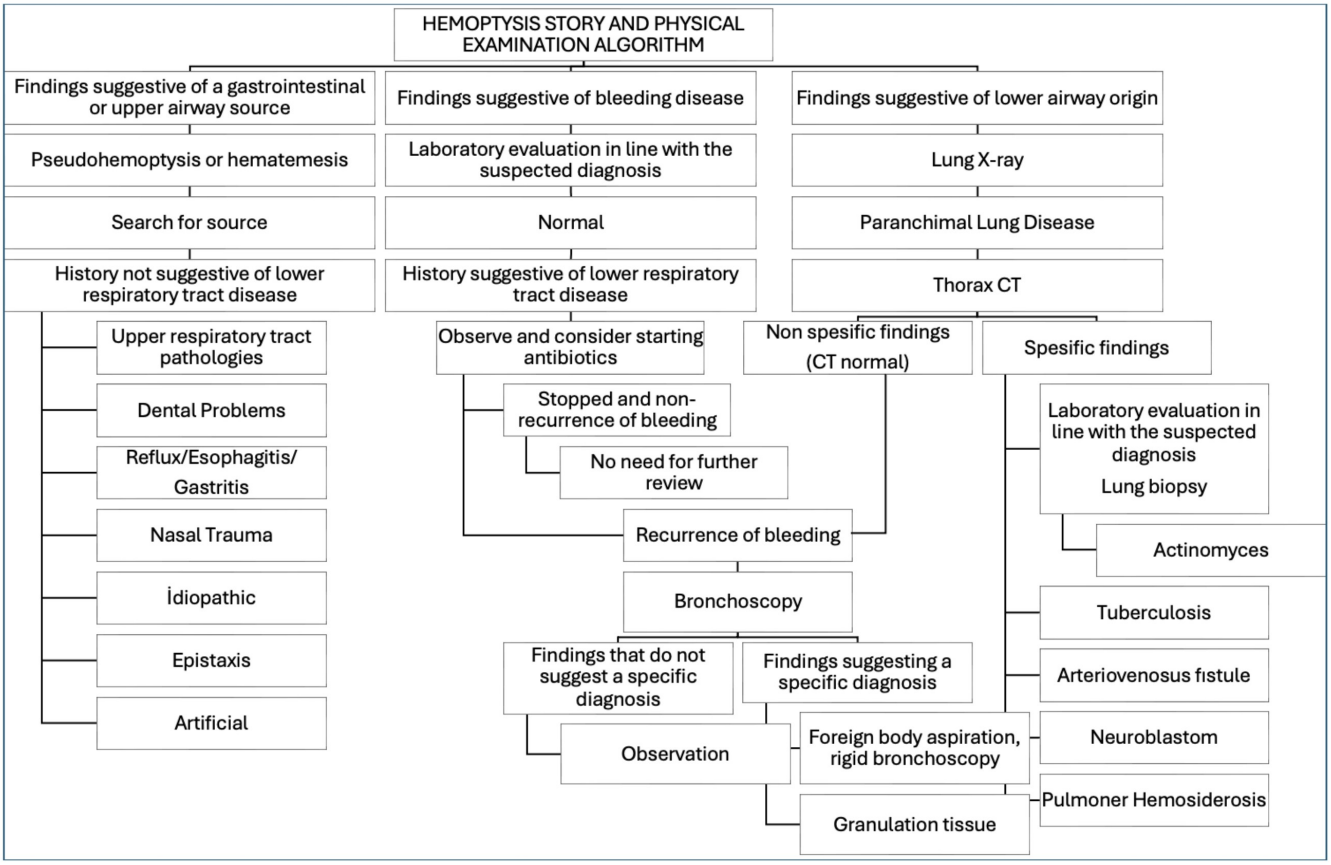

Figure 2. Algorithm for diagnosis in children with hemoptysis was adapted from the literature.

group, whereas the remainder had mild to moderate hemoptysis. All patients in the pseudohemoptysis group exhibited only mild to moderate bleeding (p = 0.082).

Based on bleeding patterns, bleeding accompanied by coughing was observed in 89.6% (n = 43/48) of patients in the hemoptysis group, compared with 30.4% (n = 14/46) in the pseudohemoptysis group, with a statistically significant difference (p<0.001).

In the pseudohemoptysis group, bleeding directly from the mouth was observed in 37% (n = 17/46) and bleeding with

https://doi.org/10.5455/annalsmedres.2025.05.130

Table 1. Comparison of the demographic and clinical characteristics of patients with hemoptysis and pseudohemoptysis.

	Hemoptysis (n=48)	Pseudohemoptysis (n=46)	p
Gender Male, n (%)	27/48 (56.3)	22/46 (47.8)	0.414
Age (months) Median (min-max)	159 (9-243)	140 (10-227)	0.443
	n (%)	n (%)	
Amount of bleeding			
Massive Bleeding	3 (6.3)	0	0.242
Mild/moderate Bleeding	45 (93.8)	46 (100)	0.082
Bleeding pattern			
Cough	43 (89.6)	14 (30.4)	<0.001
Vomiting	6 (12.5)	8 (17.4)	0.506
Epistaxis	2 (4.2)	6 (13)	0.154
Saliva	2 (4.2)	15 (32.6)	<0.001
By direct mouth	5 (10.4)	17 (37)	0.002
Nausea	1 (2.1)	5 (10.9)	0.107
Sputum Examination			
Coagulated appearance	11 (22.9)	7 (15.2)	0.343
Brown	2 (4.2)	7 (14.9)	0.087
From bright red to pink	29 (60.4)	15 (33.6)	0.007
Fresh blood	12 (25)	22 (47.8)	0.008
Accompanying symptoms			
Weight loss	7 (14.6)	7 (15.2)	0.931
Night sweats	9 (18.8)	4 (8.7)	0.233
Fever	6 (12.5)	0	0.027
Purulent sputum	24 (50)	4 (8.7)	<0.001

Pearson's χ^2 test or Fisher's exact test.

Table 2. Comparison of lung X-ray and CT findings of patients with hemoptysis and pseudohemoptysis compared to Balla (1).

	Hemoptysis (n=48) n (%)	Pseudohemoptysis (n=46) n (%)	p
Lung X-ray			<0.001
Suspicious Pathological Finding	21 (56.2)	3 (6.5)	
Normal	27 (43.8)	43 (93.5)	
Thoracic CT			
Lung parenchyma			0.069
Normal	14 (45.1)	16 (76.2)	
Consolidation/Ground Glass Opacity/air broncogram	15 (48.4)	5 (23.8)	
Cavitation	2 (6.5)	0	
Tracheobronchial Tree			0.049
Normal	23 (74.2)[a]	21 (100)[b]	
Intraluminal Content/Soft Tissue	2 (6.5)	0	
Bronchiectasis	6 (19.3)	0	
Pulmonary Artery			0.506
Normal	28 (93.3)	21 (100)	
Filling Defect	2 (6.7)	0	

Pearson's χ^2 test or Fisher's exact test.

saliva in 32.6% (n = 15/46) of patients, which were significantly more frequent than in the hemoptysis group (10.4% [n = 5/48] and 4.2% [n = 2/48]), with statistically significant differences (p=0.002 and p<0.001, respectively).

In sputum examination, a color change from bright red to pink was observed in 60.4% (n = 29/48) of cases in the hemoptysis group and fresh blood was present in 25% (n = 12/48) of cases. In contrast, these rates were 33.6% (n = 15/46) and

https://doi.org/10.5455/annalsmedres.2025.05.130

Table 3. Comparison of bronchoscopy findings.

	Hemoptysis (n=18)	Pseudohemoptysis (n=12)	p
Flexible bronchoscopy findings			<0.001
Normal	7 (38.9%)	12 (100.0%)	
Pathological	11 (61.1%)	0 (0.0%)	
Bleeding focus	2 (11.1)		
Purulent secretion	1 (5.6)		
Mucosal inflammation	2 (11.1)		
Tracheal abrasion	1 (5.6)		
Granulation tissue	3 (16.7)		
Increased vascularity	2 (11.1)		
Dilated mucous gland orifices	1 (5.6)		

Fisher's Exact Test (two-sided).

Table 4. List of etiological factors in patients with hemoptysis and pseudohemoptysis.

Patients (n: 94)	Etiology	n (%)
Hemoptysis (n:48)	Lung Parenchymal Disease	28 (58.3)
	Infections	23 (47.9)
	Bronchitis	10 (21)
	Pneumonia	6 (12.6)
	Bronchiectasis*	4 (8.4)
	Pulmonary Tuberculosis*	1 (2.1)
	Actinomyces	1 (2.1)
	Cist Hydatic	1 (2.1)
	Cystic Fibrosis	1 (2.1)
	Interstitial Lung Diseases	4 (8.4)
	Pulmonary Hypertension	1 (2.1)
	Pulmoner Hemosiderosis	2 (4.2)
	Arteriovenosus Fistule*	1 (2.1)
	Malignancy	1 (2.1)
	Idiopathic	14 (29.2)
	Tracheostomy	4 (8.3)
	Trauma	1 (2.1)
	Foreign Body Aspiration	1 (2.1)
Pseudohemoptysis (n:46)	Adenoid Hypertrophy, Sinusitis	11 (24)
	Idiopathic	10 (21.7)
	Dental Problem	8 (17.3)
	Esophagitis, Reflux	7 (15.2)
	Epistaxis	4 (8.7)
	Artificial	4 (8.7)
	Seasonal Allergic Rhinitis	1 (2.2)
	Trauma	1 (2.2)

*: 1 massive case.

47.8% (n = 22/46) in the pseudohemoptysis group.

The color change from bright red to pink was more frequently observed in the hemoptysis group, whereas the presence of fresh blood was more common in the pseudohemoptysis group (p = 0.007 and p = 0.008, respectively).

Clotted sputum was observed in 22.9% (n = 11/48) of the hemoptysis group and 15.2% (n = 7/46) of the pseudohemoptysis group, whereas brown sputum was noted in 4.2% (n = 2/48) and 14.9% (n = 7/46) of the patients, respectively; however, these differences were not statistically significant (p = 0.343 and p = 0.087, respectively).

Weight loss [14.5% (n = 7/48) us 15.2% (n = 7/46)] and night sweats [18.8% (n = 9/48) us 8.7% (n = 4/46)] were observed at similar rates in both groups (p>0.05). In contrast, fever was more frequently observed in the hemoptysis group (12.5%; n = 6/48), as was purulent sputum at 50% (n = 24/48); these differences were statistically significant (p=0.027 and p<0.001, respectively) (Table 1).

Imaging

Chest radiographs of all patients were obtained. Radiographs were normal in 56.2% (n = 27/48) of the hemoptysis group, compared with 93.5% (n = 43/46) of the pseudohemoptysis group. Suspicious pathological findings on chest radiographs were observed in 43.8% (n = 21/48) of the hemoptysis group, which was significantly higher than the 6.5% (n = 3/46) observed in the pseudohemoptysis group (p<0.001).

Thoracic CT was performed in 52 patients. No statistically significant difference was found in lung parenchymal findings

https://doi.org/10.5455/annalsmedres.2025.05.130

between the two groups (p = 0.069). In the hemoptysis group, 45.1% (n = 14/31) of the patients had normal parenchymal appearance, whereas 76.2% (n = 16/21) in the pseudohemoptysis group. Parenchymal abnormalities, such as consolidation, ground-glass opacities, or air bronchograms, were observed in 48.4% (n = 15/31) of the hemoptysis cases and in 23.8% (n = 5/21) of the pseudohemoptysis cases. Cavitary lesions were identified exclusively in the hemoptysis group (6.5%) and were not detected in patients with pseudohemoptysis.

The tracheobronchial tree showed a statistically significant difference between the groups (p = 0.049). Normal tracheobronchial anatomy was observed in 74.2% (n = 23/31) of patients with hemoptysis and in 100% of patients with pseudohemoptysis (n = 21/21), representing the only category that remained significantly different after Bonferroni-adjusted pairwise comparisons. In the hemoptysis group, intraluminal content or soft-tissue density was detected in 6.5% (n = 2/31) of patients, and bronchiectasis was present in 19.3% (n = 6/31), whereas none of these abnormalities were identified in the pseudohemoptysis group.

Pulmonary artery evaluation revealed normal findings in 93.3% (n = 28/30) of the hemoptysis group and filling defects in 6.7% (n = 2/30). In contrast, all patients in the pseudohemoptysis group (100%, n = 21/21) had normal pulmonary arteries. This difference was not statistically significant (p = 0.506) (Table 2).

Bronchoscopy

A total of 30 patients underwent bronchoscopy. Normal bronchoscopy findings were observed in 38.8% (n = 7/18) of patients in the hemoptysis group, whereas all bronchoscopic evaluations in the pseudohemoptysis group were normal 100% (n = 12/12) (p = 0.005).

Pathological bronchoscopic findings in the hemoptysis group included granulation tissue in 16.7% (n = 3/18), bleeding focus in 11.1% (n = 2/18), mucosal inflammation in 11.1% (n = 2/18), increased vascularity in 11.1% (n = 2/18), tracheal abrasion in 5.6% (n = 1/18), and purulent secretions in 5.6% (n = 1/18). None of these findings were detected in the pseudohemoptysis group (Table 3).

Etiology of bleeding

When the etiological distribution of the cases was examined, the most common cause in the hemoptysis group (n = 48) was pulmonary parenchymal diseases, observed in 58.3% (n = 28/48) of cases. Among the parenchymal diseases, infectious etiologies accounted for 82% (n = 23/28). These infectious causes included bronchitis in 21% (n = 10/48), pneumonia in 12.6% (n = 6/48), bronchiectasis in 8.4% (n = 4/48), and pulmonary tuberculosis, actinomycosis, and hydatid cyst in 2.1% (n = 1/48).

Among non-infectious pulmonary parenchymal etiologies, cystic fibrosis, interstitial lung diseases, pulmonary hypertension, pulmonary hemosiderosis, and arteriovenous fistula were observed in 2.1% (n = 1/48), 8.4% (n = 4/48), 4.2% (n = 2/48), and 2.1% (n = 1/48), respectively. Additionally, malignancy was detected in one patient (2.1%, n = 1/48).

No identifiable cause was found in 29.2% of cases (n = 14/48), and these were classified as idiopathic. Other causes included tracheostomy in 8.3% (n = 4/48), trauma in 2.1% (n = 1/48), and foreign body aspiration in 2.1% (n = 1/48).

In the pseudohemoptysis group (n = 46), the most common etiological cause was adenoidal hypertrophy and sinusitis, observed in 24% (n = 11/46) of patients. This was followed by idiopathic causes in 21.7% (n = 10/46), dental problems in 17.3% (n = 8/46), esophagitis and gastroesophageal reflux in 15.2% (n = 7/46), epistaxis in 8.7% (n = 4/46), artificial bleeding (e.g., from oral mucosa) in 8.7% (n = 4/46), seasonal allergic rhinitis in 2.2% (n = 1/46), and trauma in 2.2% (n = 1/46). No underlying pathology could be identified in 21.7% (n = 10/46) of the patients in the pseudohemoptysis group (Table 4).

The hemoptysis evaluation algorithm presented in Figure 2 was developed to systematically guide the clinical assessment of children presenting with oral bleeding and has been integrated into the current study to support the interpretation of diagnostic findings.

DISCUSSION

This study highlights the diagnostic distinctions between hemoptysis and pseudohemoptysis by comparing the clinical, symptomatic, radiological, and etiological characteristics of patients with these conditions. Among all pediatric patients evaluated, only 1.2% presented with oral bleeding, and only 0.61% was confirmed to have true hemoptysis. Symptoms such as cough, fever, and purulent sputum, along with suspicious pathological findings on chest radiographs, were more frequently observed in the hemoptysis group. While lower respiratory tract infections emerged as the predominant cause in patients with hemoptysis, upper respiratory tract pathologies/infections and factitious hemoptysis were more commonly identified in patients with pseudohemoptysis.

Although hemoptysis is common in adults, it is a rare symptom in children and can present a diagnostic challenge [1,11]. The reported incidence has shown variability due to referrals to different clinics and variations in diagnostic facilities. In our study, the proportion of patients presenting with oral bleeding among all pediatric pulmonology outpatient visits was found to be 1.2%, with approximately half diagnosed with hemoptysis and the other half with pseudohemoptysis. A similar center with a comparable structure reported a rate of 1.8% [6].

Diagnostic and therapeutic strategies differ significantly, and anamnesis and physical examination are crucial in the differential diagnosis [1,6,7,11]. The presence of blood with coughing and the appearance of bright red, frothy blood sug-

https://doi.org/10.5455/annalsmedres.2025.05.130

gest hemoptysis, whereas dark red blood mixed with food particles and associated with vomiting is more indicative of hematemesis. This approach is considered the first-line investigation in many diagnostic algorithms [1,13].

Studies on hemoptysis conducted in the pediatric population typically classify and compare patients based on age groups or the amount of bleeding (mild, moderate, or severe) [2,8]. To the best of our knowledge, no previous study has compared bleeding patterns, sputum characteristics, and accompanying symptoms to differentiate hemoptysis from pseudohemoptysis. The importance of accurately evaluating sputum characteristics and identifying the source of bleeding in the diagnosis of pediatric hemoptysis has been emphasized. In this study, hemoptysis was characterized by bright red blood typically mixed with sputum, whereas pseudohemoptysis was characterized by fresh, unmixed blood [1].

Similar results were found in our study, demonstrating that the presence of bright red or pink blood, along with symptoms such as cough, purulent sputum, and fever, may be indicative of hemoptysis.

However, it is highly likely that a portion of the bleeding initially presumed to be hemoptysis originates from the nose, infected tonsils, or adenoids.

Blood from the nasopharynx can irritate the larynx, inducing coughing and mimicking hemoptysis, a phenomenon classified as pseudohemoptysis [1,14,15]. It should also be noted that aspiration of blood from the gastrointestinal tract can trigger coughing, and swallowed pulmonary blood may be expelled through vomiting. Despite these confounding factors, the prevalence of cough was significantly higher in the hemoptysis group. These findings suggest that visual inspection of sputum and detailed assessment of accompanying symptoms are important tools for differentiating between hemoptysis and pseudohemoptysis. These simple evaluation methods may help prevent unnecessary investigations and invasive procedures in clinical practice.

In cases where a detailed physical examination and medical history of the upper and lower airways are inconclusive, chest radiography followed by thorax computed tomography (CT) scan are among the initial diagnostic tools used to support clinical evaluation [16]. In our study, the rate of chest radiograph use was 100%. Chest radiography serves as a useful objective tool, particularly given the challenges of physical examination and anamnesis in children, although this may appear high.

Although >90% of chest radiographs in the pseudohemoptysis group were normal, 43.8% of the hemoptysis group demonstrated pathological findings, most of which consisted of alveolar infiltrates, consolidations, and ground-glass opacities—radiological indicators of parenchymal bleeding.

When evaluating CT findings of the lung parenchyma, consolidation, air bronchograms, and ground-glass opacities were the most frequently observed abnormalities in patients with hemoptysis. These opacities may be associated with infectious or inflammatory processes. Suspicious pathological findings included alveolar infiltrates, consolidations, bronchiectasis, interstitial opacities, nodules, and cavitary lesions [16].

In their studies, Bhalla and Gaude emphasized that chest radiography plays a critical role in understanding the etiology of hemoptysis; however, the need for advanced imaging is not ruled out by normal radiographic findings [1,16]. Thoracic CT was performed in 52 of 94 patients. Suspicious pathological findings were identified in 55% of the patients in the hemoptysis group, whereas this rate was significantly lower in the patients in the pseudohemoptysis group (24%). Approximately half (48%) of the thoracic computed tomography scans in the hemoptysis group revealed alveolar consolidation or ground-glass opacities, whereas cavitary lesions were observed less frequently. Nonspecific air bronchograms or consolidation were detected in 23% of the thoracic CT scans in the pseudohemoptysis group.

Angiographic thoracic CT is also recommended to rule out pulmonary vascular pathologies [16]. Angiographic thoracic CT was performed in a small subset of patients. Interventional treatment with plug placement was administered to three patients who presented with massive hemoptysis.

The detection of bleeding focus, granulation tissue, and mucosal inflammation in patients with hemoptysis underscores the importance of bronchoscopy as a crucial diagnostic tool [6,11]. The diagnostic yield of bronchoscopy has been reported to range from 40% to 100%, with particularly high sensitivity in cases of bleeding due to bronchiectasis, foreign body aspiration, and pulmonary infections [1,16]. Bronchoscopy was performed in 30 out of 94 patients in our study. In the tracheobronchial tree evaluation, findings such as granulation tissue, intraluminal contents, soft tissue masses, and bleeding foci were more frequently identified bronchoscopically in the hemoptysis group. In contrast, all patients in the pseudohemoptysis group had a normal tracheobronchial system. The predominantly normal bronchoscopic findings in the pseudohemoptysis group support the notion that the source of bleeding in these patients was not pulmonary, but rather originated from the upper respiratory or gastrointestinal tract. Consistent with literature recommendations, our findings underscore the importance of systematically evaluating the lung parenchyma, tracheobronchial tree, and pulmonary arteries when assessing hemoptysis.

Childhood hemoptysis is mild to moderate in volume and tends to be self-limiting in most cases [7]. In both groups, mild to moderate bleeding was more common. However, three of our cases involving massive bleeding episodes were in the hemoptysis group. In one of these cases, endobronchial tuberculosis was diagnosed. The patient was managed solely with anti-TB therapy, and no additional treatment was required despite the presence of massive hemoptysis. A bronchial arteriovenous fistula was identified in the

https://doi.org/10.5455/annalsmedres.2025.05.130

left bronchial artery in the second patient, and bronchial embolization was performed. The third patient, who had previously undergone surgery for Kartagener syndrome and transposition of the great arteries, developed massive hemoptysis and was treated with bronchial artery embolization.

Although the disease groups causing hemoptysis may vary depending on the characteristics of the center and the availability of diagnostic tools, infections are the most commonly reported cause of hemoptysis. In our study, the most frequent causes of hemoptysis were PLDs, with infections being the leading etiology (50%), followed by idiopathic causes (30%) and interstitial lung diseases (8.4%). Similarly, another study conducted in a pediatric pulmonology clinic identified infections as the most common cause (47.4%), followed by neoplasms (22.6%) and autoimmune/immune dysregulation syndromes (19.1%) [12]. In a pediatric pulmonology clinic in our country, respiratory tract infections were identified as the most common cause of hemoptysis in 69 patients (18.8%). The causes of pseudohemoptysis in our study were similar to those reported in the literature and included epistaxis, gingivostomatitis, and factitious origins [3]. In an intensive care study, infection was identified as the underlying cause in half of the 16 children diagnosed with hemoptysis based solely on pulmonary infiltrates seen on chest radiography, followed by bronchiectasis and idiopathic pulmonary hemorrhage [6]. In a study involving 19 pediatric patients, the most common causes of hemoptysis were infections (28.6%) and tracheostomy-related complications (14.3%) [11]. In a general pediatrics clinic, among 40 children with hemoptysis who had no history of trauma, bleeding diathesis, or malignancy, infections (25%) and congenital heart diseases (17.5%) were the most common causes [8]. The mechanism by which infections lead to hemoptysis is associated with inflammation of the bronchial mucosa and disruption of vascular integrity, resulting in bleeding from the bronchial arteries [16,17]. Similarly, bronchitis, pneumonia, and bronchiectasis were identified as the most common infectious causes of hemoptysis in our study. Other types of infections contributing to the etiology of hemoptysis in our cohort included tuberculosis, actinomycosis, and hydatid cyst.

Upper respiratory tract-related causes, such as adenoid hypertrophy, sinusitis, and dental problems, as well as factitious hemoptysis, were found to be more common in patients with pseudohemoptysis [18]. Factitious hemoptysis has been shown to be an important differential diagnosis in cases of unexplained hemoptysis, particularly those with prolonged symptoms and no identifiable underlying cause. This possibility should be considered before proceeding with unnecessary invasive procedures [8]. Cases of factitious hemoptysis associated with Munchausen syndrome may go unnoticed for extended periods in the absence of clinical suspicion and may be linked to child abuse [19]. In our study, factitious causes were found to mimic hemoptysis in four patients, once again emphasizing the critical role of detailed patient history and physical examination. In the first case, a 14-year-old girl was found to have induced pseudohemoptysis by biting the oral mucosa. The second case involved an 8-year-old girl who presented to the outpatient clinic with photos taken solely by her mother, showing what was claimed to be blood. A review of the patient's prior medical history revealed multiple hospital admissions for nasal and rectal bleeding, and the pediatric hematology department had previously diagnosed her with Munchausen by proxy (MBP). In the third case, a 13-year-old girl was hospitalized for hemoptysis. She had drawn blood through a venipuncture site and collected it in a container, presenting it as hemoptysis material.

The fourth case was an 8-year-old boy diagnosed with hypersensitivity pneumonitis and followed up for chronic cough. The mother repeatedly brought the patient to our outpatient clinic, claiming to have seen blood on his pillow at night and presenting photos of the alleged blood. However, no active bleeding was observed during any of the hospitalizations. The mother appeared to derive secondary gain from the situation, and the case was reported to social services.

Despite all laboratory, radiologic, and bronchoscopic evaluations, no source of bleeding could be identified in 14 patients (29.2%), highlighting the diagnostic challenges in the follow-up of pediatric hemoptysis. In our study, idiopathic causes were identified in 29.2% of cases, which is consistent with the previously reported rates of 11%–25% in pediatric cohorts [1-3,5,7,8,11,12].

All patients presenting with complaints of oral bleeding should be evaluated according to a hemoptysis assessment algorithm [1]. This algorithm includes steps designed to identify the source of bleeding and underlying pathology. An algorithmic approach enhances patient safety by preventing unnecessary interventions. The algorithm begins with history taking and physical examination, differentiating between finding suggestive of gastrointestinal/upper airway sources and those indicating lower respiratory tract origin. In cases suggestive of pseudohemoptysis or hematemesis, upper respiratory tract and gastrointestinal pathologies are evaluated. Chest radiography, thoracic CT, and further laboratory evaluation are recommended for suspected lower airway causes. The algorithm also outlines subsequent steps, including bronchoscopy, lung biopsy, and appropriate management strategies based on recurrence, specific diagnoses (e.g., tuberculosis, bronchiectasis, actinomycosis), or nonspecific findings.

CONCLUSION

Approximately half of children with oral bleeding have true hemoptysis. Massive hemoptysis was uncommon in our cohort, absent in pseudohemoptysis, and controlled medically or with bronchial artery embolization. Lower respiratory infections predominated in patients with hemoptysis and upper airway conditions in patients with pseudohemoptysis. Bedside cues (cough/purulent sputum with pink-to-bright-red

https://doi.org/10.5455/annalsmedres.2025.05.130

sputum) and abnormal chest imaging favored a lower-airway source, whereas saliva/epistaxis suggested pseudohemoptysis; bronchoscopy was normal in all pseudohemoptysis cases and abnormal mainly in hemoptysis, supporting the selective use of invasive testing. A pragmatic diagnostic algorithm is also proposed to guide triage and reduce unnecessary procedures.

Acknowledgments: The authors would like to thank Prof. Dr. Saniye Girit, Head of the Department of Pediatric Pulmonology at Istanbul Medeniyet University, for providing the opportunity to conduct this study and for her valuable support and guidance.

Ethics Committee Approval: Ethics approval for the study was obtained from the Kartal Koşuyolu Training and Research Hospital Ethics Committee, with decision number 2024/11/842, dated June 4, 2024.

Informed Consent: The study involved a retrospective review of anonymized data and did not include any identifiable patient information; therefore, written informed consent was not required.

Peer-review: Externally peer-reviewed.

Conflict of Interest: The authors declare that they have no conflicts of interest related to this study.

Author Contributions: Conceptualization: Y.M.Ç; Supervision: Y.M.Ç., S.C.O; Data Curation: Y.M.Ç; Formal Analysis: Y.M.Ç; Investigation: Y.M.Ç; Methodology: Y.M.Ç; Project Administration: Y.M.Ç.; Resources: Y.M.Ç; Software: Y.M.Ç; Validation: Y.M.Ç; Visualization: Y.M.Ç; Writing–Original Draft: Y.M.Ç; Writing–Review and Editing: Y.M.Ç., S.C.O.

Financial Disclosure: This study received no financial support from any funding agency, organization, or sponsor.

Artificial Intelligence Disclosure: We hereby declare that an artificial intelligence–based tool (ChatGPT, OpenAI, GPT-4) was used solely for language editing and linguistic refinement, including improvement of grammar, clarity, and overall readability of the manuscript. The AI tool was not used for study design, data collection, data analysis, interpretation of results, generation of scientific hypotheses, or formulation of conclusions. No original scientific content, clinical interpretation, or academic judgment was generated by the AI system. All AI-assisted text was critically reviewed, edited, and approved by the authors, who retain full responsibility for the accuracy, originality, and scholarly integrity of the manuscript. The use of the AI tool was fully compliant with the journal's ethical guidelines, and no AI system is listed as an author or contributor. We confirm that the manuscript reflects the authors' independent scientific work and judgment.

REFERENCES

1. Gaude GS. Hemoptysis in children. *Indian Pediatr.* 2010;47(3):245-54. doi: 10.1007/s13312-010-0044-z.
2. Coss-Bu JA, Sachdeva RC, Bricker JT, Harrison GM, Jefferson LS. Hemoptysis: a 10-year retrospective study. *Pediatrics.* 1997;100(3):E7. doi: 10.1542/peds.100.3.e7.
3. Şişmanlar Eyüboğlu T, Tana Aslan A. Hemoptysis in Children: Sometimes Petty Sometimes Scary. *Turkish J Pediatr Dis.* 2017;2:112-115. doi: 10.12956/tjpd.2016.257.
4. Godfrey S. Hemoptysis in children. *Pediatr Pulmonol Suppl.* 2004;26:177–179. doi: 10.1002/PPUL.70098.
5. Vijayasekaran D, Gowrishankar NC, Balaji BS, Kalpana S, Nedunchelian K. Etiology of Hemoptysis in Children and Adolescents - Multicentric Retrospective Data (2012-2021) From Chennai. *Indian Pediatr.* 2023;60(4):290-293. PMID: 36633110.
6. Abu-Kishk I, Klin B, Eshel G. Hemoptysis in children: a single institutional experience. *Pediatr Emerg Care.* 2012;28(11):1206-10. doi: 10.1097/PEC.0b013e318271c107.
7. Simon DR, Aronoff SC, Del Vecchio MT. Etiologies of hemoptysis in children: A systematic review of 171 patients. *Pediatr Pulmonol.* 2017;52(2):255-259. doi: 10.1002/ppul.23497.
8. Sim J, Kim H, Lee H, Ahn K, Lee SI. Etiology of hemoptysis in children: a single institutional series of 40 cases. *Allergy Asthma Immunol Res.* 2009;1(1):41-4. doi: 10.4168/aair.2009.1.1.41.
9. Vélez NP, Cabrera OL, Carrasco MT, Albornoz JV, Calle JCO. Lytic Lesion of the sternum due to tuberculosis. *Arch. Bronconeumol.* 2020;56(4):260–261. doi: 10.1016/j.arbr.2019.10.004.
10. Yue P, Zhou K, Hua Y, Fang J, Li Y. Approach to diagnosis of factitious disorder with unexplained hemoptysis: A case report. *Medicine (Baltimore).* 2019;98(6):e14152. doi: 10.1097/MD.0000000000014152.
11. Batra PS, Holinger LD. Etiology and management of pediatric hemoptysis. *Arch Otolaryngol Head Neck Surg.* 2001;127(4):377-82. doi: 10.1001/archotol.127.4.377.
12. Chiel L, Welsh S, Andren K, Mecklosky J, Alexander PMA, Casey A, Fishman MP. Pediatric Hemoptysis without Bronchiectasis or Cardiac Disease: Etiology, Recurrence, and Mortality. *J Pediatr.* 2019;214:66-70. doi: 10.1016/j.jpeds.2019.07.049.
13. Pekcan S. Hemoptysis in Childhood: Causes And Treatment. *Toraks Cerrahisi Bulteni.* 2015;5(4):229–240. doi: 10.5152/tcb.2014.037.
14. Wilmott RW, Deterding R, Li AM, Ratjen F, Sly PD, Zar HJ, et al. Kendig's disorders of the respiratory tract in children. 9th ed. Philadelphia, PA, United States. *Elsevier.* 2019. doi: 10.1016/C2015-0-01292-8.
15. Martin RJ, Kohn A. Pulmonary Hemorrhage, Transient Tachypnea and Neonatal Pneumonia. *Neonatology.* 2012;14:455–9. doi: 10.1007/978-88-470-1405-3_63.
16. Garg A, Bhalla A, Naranje P, Kandasamy D. Pediatric hemoptysis: diagnostic and interventional challenges. *Pediatr Radiol.* 2024;54(11):1769-1784. doi: 10.1007/s00247-024-06002-7.
17. Singh D, Bhalla AS, Veedu PT, Arora A. Imaging evaluation of hemoptysis in children. *World J Clin Pediatr.* 2013;2(4):54-64. doi: 10.5409/wjcp.v2.i4.54.
18. Kefri M, Dyke S, Copeland S, Morgan CV Jr, Mehta JB. Hemoptysis and hematemesis due to a broncholith: granulomatous mediastinitis. *South Med J.* 1996;89(2):243-5. PMID: 8578362.
19. Vlad RM, Dobritoiu R, Turenschi A, Pacurar D. Where Reality and Fantasy Collide-Prolonged Fever to Munchausen Syndrome by Proxy. *Children (Basel).* 2024;11(12):1482. doi: 10.3390/children11121482.

https://doi.org/10.5455/annalsmedres.2025.05.130

Ann Med Res

Current issue list available at Ann Med Res

Annals of Medical Research

journal page: annalsmedres.org

Demographic characteristics of traumatic head injuries in pediatric patients: A single-center neuorsurgery clinic study

Yasin Gokturk[a], Sule Gokturk[a,*], Belgin Oral[a], Faruk Peksoy[a], Sevgi Bozok[a]

[a]University of Health Sciences, Kayseri City Hospital, Department of Neurosurgery, Kayseri, Türkiye
*Corresponding author: suleGOKTURK@outlook.com (Sule Gokturk)

MAIN POINTS

- Pediatric head injuries account for >80% of trauma-related deaths in children.
- Mortality rates are higher in patients with serious injury.
- Various factors, including demographic characteristics and the nature and severity of the injury, can play a significant role in the progression of pediatric head injuries.
- Our study showed that falls were the most frequently identified cause of pediatric head trauma.

Cite this article as: Gokturk Y, Gokturk S, Oral B, Peksoy F, Bozok S. Demographic characteristics of traumatic head injuries in pediatric patients: A single-center neuorsurgery clinic study. *Ann Med Res*. 2026;33(4):172–177. doi: 10.5455/annalsmedres.2025.10.294.

ABSTRACT

Aim: Traumatic brain injury (TBI) significantly contributes to mortality and disability in children aged 0-18 years. TBI is a potentially fatal health emergency, and when severe, children are at high risk of mortality and neurological morbidity. Our goal is to identify the various etiologies of head trauma in pediatric patients and provide examples of preventive measures to prevent further trauma. Our research also highlights the socioeconomic burden of patients with TBI.

Materials and Methods: The institutional electronic health record (HBYS) was queried for all pediatric patients admitted to the Neurosurgery Clinic in Kayseri City Hospital, diagnosed with traumatic head injury by the neurosurgery service, and registered for discharge between January 2021 and June 2025. This study investigated 180 pediatric head trauma cases. Patient nationality (Republic of Turkey or Other) and length of hospital stay (HLOS) were also used as demographic data.

Results: The mean age was 7.2±5.32 (min-max: 0-17) years. Of the 146 children, 146 were Turkish citizens. 15 of the children, 15 (8.3%) underwent cranial surgery, and 69 (38.3%) had a history of intensive care admission. The mean length of hospital stay was 2.73±3.03 (min-max: 1-18) days. The most common type of head trauma in children was linear fractures due to falls from heights and from the same level ($p<0.05$).

Conclusion: Implementing primary prevention strategies, preventing secondary neurological injuries, and collaborating with organized emergency teams can facilitate early intervention in patients with head trauma. Thus, early diagnosis and treatment of high intracranial pressure can reduce the adverse effects of TBI. These preventive measures can reduce morbidity and mortality in children. This study comprehensively examines the etiology and demographic characteristics of pediatric head trauma in a single center in the Central Anatolia Region.

Keywords: Traumatic head injuries, Length of hospital stay, Pediatric outcomes
Received: Oct 07, 2025 **Accepted:** Dec 01, 2025 **Available Online:** Apr 24, 2026

INTRODUCTION

Traumatic head injuries (THIs) represent a major global health issue, contributing substantially to morbidity and mortality across all age groups [1,2]. Among these, pediatric THIs are particularly concerning, as they account for more than 80% of trauma-related deaths [3–5]. Children's anatomical characteristics, including a larger head-to-body ratio compared to adults, make them more susceptible to severe neurological damage. Consequently, the developing brain tissue within the cranial fossa is at heightened risk of significant injury [6] .

Head trauma continues to represent one of the leading sources of socioeconomic burden worldwide from both medical and forensic standpoints. Despite noteworthy advancements achieved over time to curtail its prevalence, it continues to be a significant health concern, particularly among pediatric patients. In the pediatric population, it is the third most prevalent cause of mortality and morbidity [7]. The pattern and severity of head injuries exhibit significant age-dependent variation. Falls are the predominant cause of injury in infants and young children, and even incidents involving similar heights can result in severe cranial trauma [8,9]. High-energy mechanisms, such as vehicle or motorcycle accidents, become the primary cause of head injuries as children mature [10]. Falling from trees is also a possible cause of head trauma in children [11]. Linear skull fractures resulting from

falls constitute the most frequent form of injury in this age group. In contrast, the extent and nature of trauma determine the severity of injury in older children, with severe brain involvement being more prevalent following traffic collisions, motorcycle accidents, or major falls. Therefore, identifying the factors that influence the severity of head trauma and their relationship with critical outcomes, such as intensive care unit (ICU) admission and mortality, is imperative. This is essential for developing targeted approaches to improve clinical management and patient outcomes.

The Glasgow Coma Scale (GCS) is a widely used clinical tool that enables health care professionals to assess the neurological status of individuals who have suffered head trauma [12]. Research indicates that patients with severe head injuries tend to have extended hospitalizations and higher rates of intensive care unit admission [13-15]. Moreover, the mortality rate is markedly higher in patients with severe injuries than in those with mild or moderate head trauma. Several variables—including demographic characteristics, injury mechanism, and degree of severity—significantly influence the prognosis of pediatric head injuries [16]. Notably, a substantial portion of the current knowledge and published studies on trauma and its outcomes originates predominantly from Western countries, particularly North America and Europe.

Head trauma continues to be a major contributor to the global socioeconomic burden from medical and forensic standpoints. Despite advancements in preventive strategies and health care interventions over the years, it remains a prominent cause of mortality and morbidity, particularly among children. Head trauma ranks as the third most frequent cause of death and disability in the pediatric population. The underlying mechanisms and clinical severity of head injuries notably differ across age groups. Falls constitute the predominant cause of head trauma in infants and young children, and falls from relatively low heights may lead to severe cranial injuries in this vulnerable population.

MATERIALS AND METHODS

This study was conducted retrospectively following the approval of the local ethics committee of Kayseri City Hospital District on August 26, 2025, under protocol number 543. All research procedures complied with the ethical principles of the Declaration of Helsinki (1975) and its 1983 revision.

Study design

At Kayseri City Hospital, the institutional electronic health record "HBYS" was queried for all pediatric patients admitted to the Neurosurgery Clinic, the diagnoses of traumatic head injury were evaluated by the neurosurgery clinic, and discharge was documented between January 2021 and June 2025. Data from the past five years were preferred. The retrospective file review was conducted with deidentified data; therefore, institutional informed consent was not required from patients.

Study size

In total, 180 pediatric head trauma cases were analyzed in our study. The age range assessed during the analysis was 0-18 years. The nationality of the patients (Republic of Turkey or Others) was also used as demographic data in the study.

Variables

Injury characteristics included the following: Mechanism of injury (motor vehicle accidents include both drivers and passengers (inside and outside vehicles, motorcycle, bicycle accidents), falls from heights >1 m, falls from the same level ≤1 m, assaults/accidents, and others).

Injury type: Linear skull fracture, depressed skull fracture, brain contusion, epi-subdural hematoma, and traumatic subarachnoid hemorrhage. In children with multiple types of injuries, the worst head injury was considered the type of injury during the analysis. To diagnose head trauma, the patients underwent brain computed tomography (CT) (Figures 1 and 2).

Treatment variables included: Inpatient clinic (ward and intensive care), days spent in the intensive care unit, and total hospital stay. In the analysis, surgical procedures were included if surgical intervention was performed for any reason in patients with head trauma. The primary outcomes were the time of diagnosis and hospitalization.

Inclusion and exclusion criteria: We examined pediatric cases of isolated head trauma between the ages of 0-18. Only patients followed up in the Kayseri City Hospital Neurosurgery Service and Intensive Care were included in the study. Patients who had no pathological findings in their brain tomography scans but were sleepy or had confusion were observed in the emergency department for at least 8 h but were not admitted to the ward.

Statistical analysis

The obtained data were recorded and analyzed using SPSS version 22. The descriptive statistics included frequencies, percentages, mean values, standard deviations, median values, and maximum and minimum (min-max) values. Statistical analysis of categorical data included the Pearson chi-square test, and for values below five, the Fisher exact test. Data were checked for normal distribution using the Kolmogorov-Smirnov test. For quantitative data, the Kruskall-Wallis test (post-hoc Dunn test) was used for more than two independent groups, and statistical significance was set at $p<0.05$.

RESULTS

Of the 180 children included in the study, 49 (27.2%) were female and 131 (72.8%) were male. The mean age was 7.2±5.32 (min-max: 0-17) years. There were 146 Turkish citizens and 34 foreign nationals. The most common trauma mechanism

https://doi.org/10.5455/annalsmedres.2025.10.294

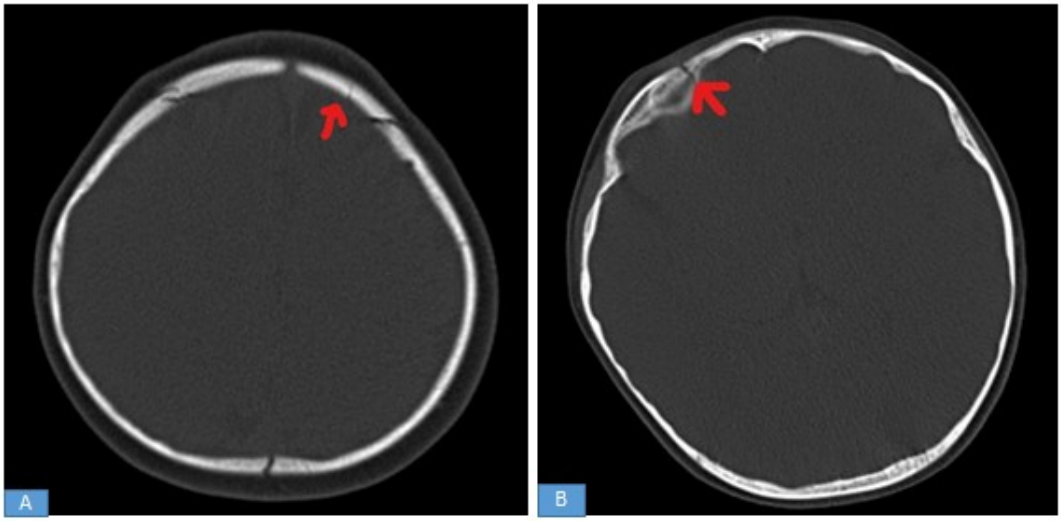

Figure 1. A frontal fracture is observed in the axial section of the brain tomography taken after the fall of a 0-year-old female patient. B: A fracture is observed in the right orbital roof in the axial section of the brain tomography taken after the fall of a 1-year-old male patient.

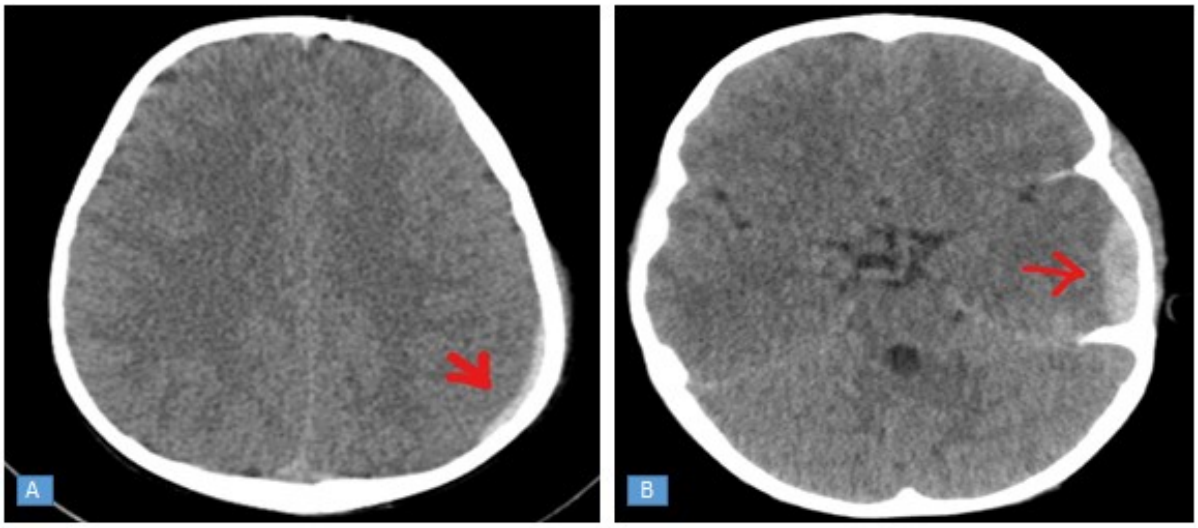

Figure 2. A 3-year-old male patient's post-traumatic brain tomography shows a left parietooccipital subdural hemorrhage in the axial section. B: A left temporal epidural hemorrhage in the axial section is seen in a 5-year-old male patient's post-traumatic brain tomography.

observed in children was falls (n: 95, 52.8%). Surgical intervention was performed in 15 of the children (8.3%), while 69 of them (38.3%) had a history of intensive care admission. Table 1 presents some variables according to the type of trauma.

When some variables were examined according to the type of trauma, no significant association was found with sex and nationality. Children who had traffic accidents had a significantly higher rate of intensive care visits ($p<0.05$). While the most frequently identified trauma type in children involved in motor vehicle accidents is epi-subdural hemorrhages, the most frequently identified trauma type in children falling from heights and the same level is linear fractures ($p<0.05$). Furthermore, the frequency of surgical intervention was significantly higher in children who had traffic accidents (Table 1).

The mean GCS score at the time of hospitalization was 14.48±1.34 (min-max: 8-15). The mean length of hospital stay was 2.73±3.03 (min-max: 1-18) days. Table 2 shows these variables by type of trauma. The median age of children who had traffic accidents was higher, and while GCS scores were significantly lower in children who had traffic accidents, the number of days spent in ICU was significantly higher (Table 2).

Rebleeding in the surgical area is a common postoperative surgical complication. In this case, a second surgical intervention may be necessary, and intensive care follow-up may be prolonged.

DISCUSSION

The key findings of our study include the observation that 131 male patients received follow-up and treatment for trauma, with falls being identified as the most prevalent cause. A considerable proportion of cases required intensive care

https://doi.org/10.5455/annalsmedres.2025.10.294

Table 1. Trauma mechanism and numerical values.

Variables		All Patients		Trauma mechanism						P value
				Motor Vehicle Accidents (n:38)		Falls from Heights of >1 m (n:95)		Falls from the Same Level ≤1 m (n:47)		
		n	%	n	%	n	%	n	%	
Gender	Female	49	27.2	9	23.7	30	31.6	10	21.3	0.370*
	Male	131	72.8	29	76.3	65	68.4	37	78.7	
Nationality	The Republic of Turkey	146	81.1	32	84.2	74	77.9	40	85.1	0.504*
	Others	34	18.9	6	15.8	21	22.1	7	14.9	
Follow up	Inpatient service	111	61.7	15	39.5	59	62.1	37	78.7	0.001*
	Neurosurgery ICU	69	38.3	23	60.5	36	37.9	10	21.3	
Trauma mechanism	Epidural-subdural hemorrhage	30	16.7	12	31.6	15	15.8	3	6.4	<0.001**
	Linear fracture	99	55.0	8	21.1	61	64.2	30	63.8	
	Contusion	15	8.3	5	13.2	7	7.4	3	6.4	
	Cranial bone compression fracture (CBF)	24	13.3	9	23.7	5	5.3	10	21.3	
	Subarachnoid hemorrhage	12	6.7	4	10.5	7	7.4	1	2.1	
Surgery history	Yes	15	8.3	8	21.1	5	5.3	2	4.3	0.012**
	No	165	91.7	30	78.9	90	94.7	45	95.7	

*Pearson chi-square test, ** Fisher's exact test.

Table 2. Distribution of age, GCS score, and length of hospital stay according to the trauma mechanism.

Variables	Trauma mechanism						P value
	Motor Vehicle Accidents (n:38)		Falls from Heights of >1 m (n:95)		Falls from the Same Level ≤1 m (n:47)		
	Meant±SD	Median	Meant±SD	Median	Meant±SD	Median	
Age	10.65±4.46	11[a]	6.94±4.98	5[b]	4.91±5.31	3[c]	<0.001
Glasgow Coma Score	14.05±1.55	15[a]	14.62±1.08	15[b]	14.57±1.58	15[b]	0.001
Neurosurgery ICU days	4.21±3.88	3[a]	2.52±2.99	1[b]	1.97±1.71	1[b]	<0.001

*Kruskall-Wallis test (Dunn's test a,b,c; the difference is significant between groups that do not have the same letter on the same line).

management; specifically, 69 patients, accounting for 38.3% of the total cohort, were admitted to the neurosurgical intensive care unit. Notably, 23 of these admissions were due to motor vehicle accidents—a remarkably high figure within the pediatric patient population.

In our literature review, Tardif et al. conducted a retrospective, multicenter cohort study of 11,199 adult patients with a diagnosis of TBI who were registered with the Canadian trauma system between 2007 and 2012 [17]. Patients with TBI reported longer than expected hospital stays and days spent in intensive care (56% and 119%, respectively) than all other diagnoses. This study demonstrated the importance of considering patients with TBI as a distinct population when making resource allocation or quality improvement plans. In our study, the mean length of ICU stay for pediatric head trauma patients was found to be 4.21 ± 3.88 days. In our country, according to 2024 data values, the social security cost of a 24-hour (one-day) intensive care unit (ICU) stay and treatment is approximately 10,000 ₺ (300 $) according to 2024 data values.

Ninety-nine patients were hospitalized with a diagnosis of linear fracture, and their hospital observation period was often 24 h (one day). Filardi et al. reviewed skull X-rays of patients aged 2 years who were treated for mild TBI in tertiary hospital emergency departments between 2014 and 2017 [18]. For a TBI to be considered mild, it must result from low-energy mechanical trauma, meaning a fall from the patient's own height or from less than sixty inches away, and the patient's GCS level must be above "13." Patients with linear skull fractures and a normal computed tomography (CT) scan were observed in the emergency department for a maximum of 24 h. Furthermore, all patients with a confirmed fracture diagnosis were clinically followed up in outpatient neurosurgery consultations one month later.

When evaluating the imaging methods in THIs, the role of plain craniographs in detecting injuries in minor head traumas is limited, and more than half of cranial fractures are not detected on plain craniographs. Most children with minor head trauma present either asymptomatic or with minimal symptoms to the emergency department. Because neurolog-

https://doi.org/10.5455/annalsmedres.2025.10.294

ical examinations are particularly challenging in children under 2 years of age, cranial computed tomography is the best imaging modality of choice. Consequently, a high frequency of cranial CT scans is performed in this age group [19].

Patients at high risk for traumatic brain injury, including those presenting within 24 hours of acute head trauma, those younger than 17 years of age, those with a GCS score of 13-15, those presenting with transient loss of consciousness, amnesia, disorientation, more than one vomiting, and irritability (aged 2 years and younger), were identified as high-risk. Patients with a GCS score <15 two hours after the trauma, suspicion of an open or depressed skull fracture, worsening headache, and restlessness during examination are considered high-risk. Patients with evidence of a skull base fracture, a potentially dangerous trauma mechanism, or a large, soft scalp hematoma were identified as intermediate risk [19]. Early brain computed tomography (CT) imaging may be crucial in patients with intermediate- and high-risk

The most frequently identified pediatric head trauma in our study (n: 95, 52.8%) was falls, and linear fractures were the most common type of TBI. The patients were kept under 24-hour observation and were also called for follow-up at the neurosurgery clinic 1 month later. In addition to the 24-hour inpatient observation period, outpatient clinic visit fees also increase the economic cost.

Hospital length of stay (HLOS) following traumatic brain injury (TBI) is a key indicator of injury severity, associated economic burden, and accessibility of acute post-traumatic care services. In a study conducted by Yue et al. data from 1,638 adult patients diagnosed with acute TBI between August 2019 and April 2022 were analyzed within a single-center cohort in the United States [20]. The mean hospital stay was 7.6 days (SD: 13.3 days) and the median length of stay was 3.0 days (IQR: 2-8 days). In our study, the mean hospital stay was 2.73±3.03 days (min-max: 1-18). These variables differed according to trauma type. Motor vehicle accidents were the most common in the intensive care unit (38.3), while patients who fell from the same level were admitted to the inpatient clinic (78.7).

Many patients with TBI undergo a lengthy rehabilitation period after severe head trauma. In the United States, more than 275,000 individuals with traumatic brain injury are hospitalized annually, with 60% of these being monitored in intensive care units [21,22]. Large multicenter studies have shown that the median HLOS for patients with TBI requiring acute care is 7–13 days [22,17], whereas the median HLOS for severely injured patients is 23 days [17]. In general, patients of the same age and sex with TBI have significantly longer hospital stays than individuals with different diagnoses.

Yue et al. estimated a higher mortality rate in patients with longer hospital stays (22% vs. 8%). This can be explained by the degree of TBI, other accompanying organ system injuries, and the debilitated condition of the patient [20]. This conclusion is inescapable, considering that 72% of patients underwent craniotomy/craniectomy and 33.3% underwent surgical procedures due to multiple traumas. In our study, 8 of the 15 patients who underwent surgical procedures had been in motor vehicle accidents, and the mean GCS score was 14.05, which was lower than that for other causes of trauma. This suggests a more severe TBI.

Limitations

Our study has some limitations. Our data were extracted retrospectively from the institutional "HBYS" system, and the level of detail inherent in HBYS-based studies is limited by incomplete data entry and data entry errors. Our target population consisted of patients with pediatric head trauma. Of these patients, only those who were followed and treated at a single center and only at the Neurosurgery Clinic were included in the study. Our study awaits validation in future large, multicenter retrospective and prospective studies.

CONCLUSION

We present a series of 180 children who were followed and treated for pediatric head trauma. All cases were followed and treated by the Neurosurgery Clinic according to the criteria of our center. Educating families are crucial to prevent future pediatric falls and to help the Social Security Institution alleviate the financial burden. We believe that our descriptive data will serve as a valuable example for readers.

Ethics Committee Approval: This study was approved by the Ethics Committee of the Kayseri City Hospital (approval number: 543; date: August 26, 2025) and in accordance with the principles stated in the 1975 Helsinki Declaration, revised in 1983.

Informed Consent: The retrospective file review was conducted with deidentified data; therefore, institutional informed consent was not required from patients.

Peer-review: Externally peer-reviewed.

Conflict of Interest: There is no conflict of interest.

Author Contributions: Conception: Y.G, S.G; Design: Y.G, S.G; Supervision: Y.G, S.G; Data Collection and/or Processing: Y.G, S.G, F.P, S.B; Statistical Analysis: B.O, Writing: Y.G, S.G.

Financial Disclosure: No financial support was obtained for this study.

Artificial Intelligence Disclosure: In our research and main text, no AI support was used in data collection and analysis. Only for English language editing was support obtained from the AI programs "Perplexity Sonar GPT-5.2 and Chat-GPT-5.2". The authors assure that there is absolutely no artificial intelligence contribution to the scientific data. All authors acknowledge that AI program support was used for English language editing.

https://doi.org/10.5455/annalsmedres.2025.10.294

REFERENCES

1. Alqudah Z, Nehme Z, Alrawashdeh A, Williams B, Oteir A, Smith K. Paediatric traumatic out-of-hospital cardiac arrest: A systematic review and meta-analysis. *Resuscitation*. 2020;149:65–73. doi: 10.1016/j.resuscitation.2020.01.037.
2. Wyen H, Jakob H, Wutzler S, Lefering R, Laurer HL, et al. Prehospital and Early Clinical Care of Infants, Children, and Teenagers Compared to an Adult Cohort: Analysis of 2961 Children Compared to 21,435 Adult Patients from the Trauma Registry of DGU in a 15-Year Period. *Eur J Trauma Emerg Surg*. 2010;36(4):300–7. doi: 10.1007/s00068-010-1124-4.
3. Aoki M, Abe T, Saitoh D, Oshima K. Epidemiology. Patterns of treatment and mortality of patients with pediatric trauma in Japan. *Sci Rep*. 2019;9(1):917. doi: 10.1038/s41598-018-37579-3.
4. Bayreuther J, Maconochie I. The evidenced-based care behind the early management of head injured children. *Trauma*. 2008;10(2):85–92. doi: 10.1177/1460408608088770.
5. Pennington N. Head injuries in children. *J Sch Nurs*. 2010;26(1):26–32. doi: 10.1177/1059840509341881.
6. Bayreuther J, Wagener S, Woodford M, Edwards A, Lecky F, et al. Pediatric trauma: Injury pattern and mortality in the United Kingdom. *Arch Dis Child Educ Pract Ed*. 2009;94(2):37–41. doi: 10.1136/adc.2007.132787.
7. Şahin S, Doğan Ş, Aksoy K. Çocukluk çağı kafa travmaları. *Uludağ Üniversitesi Tip Fakültesi Dergisi*. 2000;28(2):45-51.
8. Falk AC, Klang B, Paavonen EJ, von Wendt L. Current incidence and management of children with traumatic head injuries: The Stockholm experience. *Dev Neurorehabil*. 2007;10(1):49–55. doi: 10.1080/13638490600864066.
9. Hyder AA, Sugerman D, Ameratunga S, Callaghan JA. Falls among children in the developing world: a gap in child health burden estimations? *Acta Paediatr*. 2007;96(10):1394–8. doi: 10.1111/j.1651-2227.2007.00419.x.
10. Araki T, Yokota H, Morita A. Pediatric Traumatic Brain Injury: Characteristic Features, Diagnosis, and Management. *Neurol Med Chir (Tokyo)*. 2017;57(2):82–93. doi: 10.2176/nmc.ra.2016-0191.
11. Taçyıldız A E, Çekmen B, Uzun A, Çiftçi TC, Uzuncu, HB, et al. A retrospective analysis of spinal and cranial injury patterns caused by a fall from a tree in the Karabük province. *Neurosurgery*. 2022;30:101628. doi: 10.1016/j.inat.2022.101628.
12. Zuercher M, Ummenhofer W, Baltussen A, Walder B. The use of Glasgow Coma Scale in injury assessment: a critical review. *Brain Inj*. 2009;23(5):371–84. doi: 10.1080/02699050902926267.
13. Stevenson M, Segui-Gomez M, Lescohier I, Di Scala C, McDonald-Smith G. An overview of the injury severity score and the new injury severity score. *Inj Prev*. 2001;7(1):10–3. doi: 10.1136/ip.7.1.10.
14. Alghnam S, Towhari JA, Al Babtain I, Al Nahdi M, Aldebasi MH, et al. The associations between injury mechanism and extended hospital stay among pediatric patients: findings from a trauma Center in Saudi Arabia. *BMC Pediatr*. 2019;19(1):177. doi: 10.1186/s12887-019-1559-7.
15. Huang YT, Huang YH, Hsieh CH, Li CJ, Chiu IM. Comparison of Injury Severity Score, Glasgow Coma Scale, and Revised Trauma Score in Predicting the Mortality and Prolonged ICU Stay of Traumatic Young Children: A Cross-sectional Retrospective Study. *Emerg Med Int*. 2019;2019:5453624. doi: 10.1155/2019/5453624.
16. Vlaam GK-d, Mulder HD, Dijkstra SK, Burgerhof JGM, Kneyber MCJ. Characteristics and outcomes of critically ill children with moderate-to-severe traumatic brain injury. *Intensive Care Med–Pediatr Neonatal*. 2024;2(1):e00033-6. doi: 10.1007/s44253-024-00033-6.
17. Tardif PA, Moore L, Boutin A, Dufresne P, Omar M, et al. Hospital length of stay following admission for traumatic brain injury in a Canadian integrated trauma system: a retrospective multicenter cohort study. *Injury*. 2017;48(1):94-100. doi: 10.1016/j.injury.2016.10.042.
18. Filardi AM, Serrano FM, Salvado RL, Canuto DV, Domingo JA, Jurado Portero JC. Linear skull fracture in infants after mild traumatic brain injury: Influence of computed tomography in management. *Radiologia (Engl Ed)*. 2020;62(6):487-492. doi: 10.1016/j.rx.2020.04.005.
19. Durak F. Indications for brain computed tomography in patients with pediatric head trauma. 21. Mersin Pediatri Günleri Bildiri Kitabı. *Mersin Univ Saglık Bilim Derg*. 2022;15(Özel Sayı-1): 67-72.
20. Yue JK, Krishnan N, Chyall L, Haddad AF, Vega P, et al. Predictors of Extreme Hospital Length of Stay after Traumatic Brain Injury. *World Neurosurg*. 2022;167:e998-e1005. doi: 10.1016/j.wneu.2022.08.122.
21. Faul M, Coronado V. The epidemiology of traumatic brain injury. *Handb Clin Neurol*. 2015;127:3-13. doi: 10.1016/B978-0-444-52892-6.00001-5.
22. Levant S, Chari K, DeFrances C. National Hospital Care Survey Demonstration Projects: Traumatic Brain Injury. *Natl Health Stat Report*. 2016;97: 1-16. PMID: 27483022.

https://doi.org/10.5455/annalsmedres.2025.10.294

Ann Med Res

Current issue list available at Ann Med Res

Annals of Medical Research

journal page: annalsmedres.org

Belinostat in relapsed/refractory peripheral T-cell lymphoma: A real-world multicenter experience

Sureyya Yigit Kaya[a,*], Gulsah Akyol[b], Esra Yildizhan[c], Serhat Celik[d], Huseyin Saffet Bekoz[a], Senem Maral[a], Omur Gokmen Sevindik[e], Leylagul Kaynar[a]

[a]Istanbul Medipol University, Faculty of Medicine, Department of Hematology, Istanbul, Türkiye
[b]Erciyes University, Faculty of Medicine, Department of Hematology, Kayseri, Türkiye
[c]Kayseri City Hospital, Clinic of of Hematology, Kayseri, Türkiye
[d]Ankara Yıldırım Beyazıt University, Yenimahalle Training and Research Hospital, Department of Hematology, Ankara, Türkiye
[e]Demiroglu Bilim University, Faculty of Medicine, Department of Hematology, Istanbul, Türkiye
*Corresponding author: sureyyayigitkaya@hotmail.com (Sureyya Yigit Kaya)

MAIN POINTS

- Belinostat demonstrated clinical benefit in a subset of heavily pretreated R/R PTCL patients, with two achieving CR.
- Treatment was well tolerated with no dose reductions or discontinuations due to adverse events.
- This multicenter real-world analysis provides valuable evidence supporting the role of belinostat as a salvage option in advanced R/R PTCL.

Cite this article as: Yigit Kaya S, Akyol G, Yildizhan E, Celik S, Bekoz HS, Maral S, Sevindik OG, Kaynar L. Belinostat in relapsed/refractory peripheral T-cell lymphoma: A real-world multicenter experience. *Ann Med Res*. 2026;33(4):178–184. doi: 10.5455/annalsmedres.2025.07.193.

ABSTRACT

Aim: Peripheral T-cell lymphoma (PTCL) is a rare and aggressive subtype of non-Hodgkin lymphoma with limited treatment options, particularly in relapsed/refractory (R/R) cases. Belinostat, a pan-histone deacetylase inhibitor, has emerged as a potential therapeutic agent in this setting.

Materials and Methods: This retrospective study analyzed nine patients with relapsed/refractory PTCL treated with belinostat across three centers between 2018 and 2025. Clinical data and treatment outcomes were collected, and responses were evaluated using the Lugano criteria. Overall survival and progression-free survival were calculated with the Kaplan–Meier method.

Results: Of the nine R/R PTCL patients treated with belinostat, two (22.2%) achieved complete remission (CR), one (11.1%) experienced stable disease, four (44.4%) developed progressive disease and two (22.2%) died from lymphoma progression before the second cycle could be administered. Notably, one patient maintained a prolonged CR through 14 belinostat cycles, while another continued to use belinostat as a bridge to allogeneic stem cell transplantation and as maintenance after allogeneic transplantation. Belinostat was generally well tolerated, and no treatment discontinuations or dose reductions were required due to adverse events.

Conclusion: Although these real-world findings suggest that belinostat may provide meaningful clinical benefit in a subset of heavily pretreated R/R PTCL patients, the high rate of early progression emphasizes the need for improved patient selection and prospective validation in larger studies.

Keywords: Peripheral T-cell lymphoma, Relapsed/refractory, Histone deacetylase inhibitors, Belinostat

Received: Jul 16, 2025 **Accepted:** Dec 08, 2025 **Available Online:** Apr 24, 2026

INTRODUCTION

Peripheral T-cell lymphoma (PTCL) is a type of non-Hodgkin lymphoma that arises from post-thymic T cells and is marked by significant heterogeneity. Clinically, PTCLs often exhibit an aggressive clinical course and are associated with poor outcomes [1,2]. According to the 5th edition of the classification of World Health Organization of hematolymphoid tumors, PTCL is categorized within mature T- and NK-cell neoplasms and encompasses several subtypes, each displaying distinct and complex clinicopathological features. Common subtypes of PTCL include not otherwise specified (PTCL-NOS), nodal T follicular helper (TFH) cell lymphoma-angioimmunoblastic T-cell lymphoma (AITL) and anaplastic large cell lymphoma (ALCL) [2]. Despite ongoing research, PTCL therapy remains challenging due to the limited number of available treatment options and their modest efficacy. In recent years, histone deacetylase (HDAC) inhibitors have emerged as novel epigenetic therapeutic agents for both newly diagnosed and relapsed/refractory (R/R) PTCL cases. Their complex mechanisms of action

include inducing cell cycle arrest and apoptosis, promoting cellular differentiation, inhibiting angiogenesis, and modulating cytokine signaling [3,4]. By targeting key pathways underlying the molecular complexity of PTCL, HDAC inhibitors offer a comprehensive approach to suppressing tumor growth and progression [5]. Belinostat is a hydroxamic acid–derived pan-HDAC inhibitor that broadly inhibits all zinc-dependent HDAC enzymes, exhibiting high affinity for class I, II, and IV HDACs [6,7]. In recent years, studies have been conducted to evaluate the safety and therapeutic outcomes of HDAC inhibitor monotherapy or its combination with conventional regimens in patients with untreated or R/R PTCL [7–9]. However, real-world data the use of these agents remain limited. In this study we present data from nine R/R PTCL patients who received belinostat treatment at different centers. These real-world data may provide valuable insights into the patient population receiving advanced-line therapies, which remains underrepresented in clinical trials.

MATERIALS AND METHODS

Study design and patient selection

This retrospective, multicenter study included nine patients with R/R PTCL. Eligible patients had a histologically confirmed diagnosis of PTCL and received belinostat therapy between 2018 and 2025 at one of the participating centers. Patients with incomplete clinical data or missing follow-up information were excluded from the analysis. Demographic data, prior therapies, bone marrow transplantation history, disease progression status and belinostat outcomes were systematically recorded using a standardized data collection form.

This study was conducted in accordance with the Declaration of Helsinki and Good Clinical Practice guidelines. Ethical approval was obtained from Istanbul Medipol University Ethics Committee (Date: 22-05-2025, Number: 580).

Response evaluation

Radiologic assessments were conducted at each participating center using computed tomography (CT), magnetic resonance imaging (MRI), or positron emission tomography–computed tomography (PET) scans, as clinically indicated. Treatment response was evaluated according to the Lugano criteria. Patients underwent PET-CT scanning to assess response after two belinostat cycles and the results were classified as complete remission (CR), partial remission (PR), stable disease (SD) or progressive disease (PD). Adverse events were graded based on the Common Terminology Criteria for Adverse Events (CTCAE) version 5.0.

Statistical analysis

All calculations were performed using descriptive statistics. Continuous variables are presented as medians (range), while categorical variables are expressed as counts (n) and percentages (%). No further comparative analyses were performed due to the limited sample size. Overall survival (OS) was defined as the time from the date of first belinostat administration to the date of death from any cause. Patients who remained alive at the time of data cutoff were censored at their last known date alive. Progression-free survival (PFS) was defined as the time from first belinostat administration to the date of either documented disease progression or death from any cause, whichever occurred first. Patients without PD or death by the data cutoff were censored at the date of their last tumor assessment. In addition, if a patient initiated a subsequent anticancer therapy prior to experiencing PD or death, they were censored at the date of their final tumor evaluation. OS and PFS were estimated using the Kaplan–Meier method. Statistical analysis was performed using Statistical Package of Social Science (SPSS Inc., Chicago, IL), version 22.0 for Windows.

RESULTS

A total of nine patients with R/R PTCL were included in this study. The median age at the time of belinostat initia-

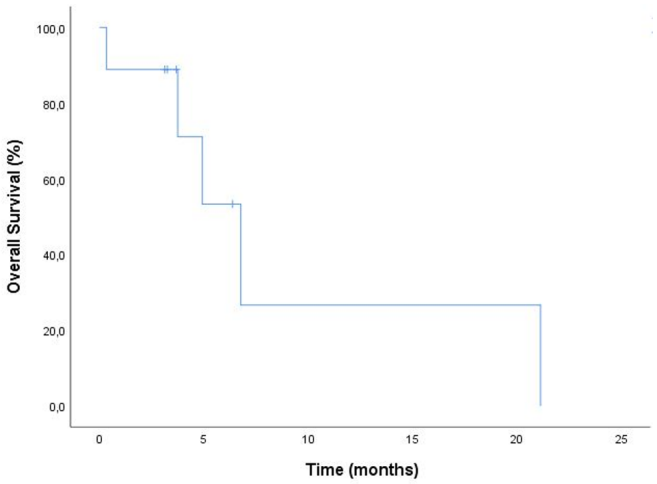

Figure 1. The median OS was 6.8 months (95% CI, 3.9 to 9.6).

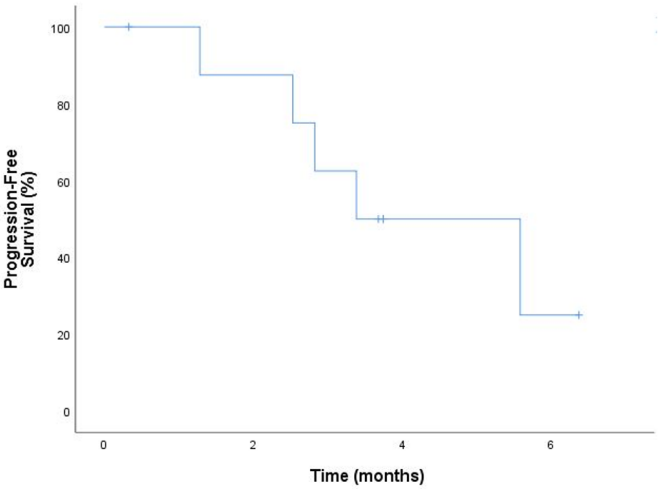

Figure 2. The median PFS was 3.4 months (95% CI, 0.8 to 5.6).

https://doi.org/10.5455/annalsmedres.2025.07.193

Table 1. Patient demographics, previous treatments, and clinical outcomes.

Patient	Age/ Sex	Stage	PTCL Subgroup	ECOG	Comorbidity	Previous Treatments (response)	Clinical Outcomes and Complications
1	65/F	4 (bone involvement)	PTCL, NOS	1	HTN, DM	3xCHOP (SD) 2xICE + RT (PR) 2xBelinostat (PD) 2xGEMOX (PD) 1xPralatrexate (Ongoing treatment)	No AE, Alive
2	52/F	4 (bone and skin involvement)	ALCL, ALK-	1	No comorbidity	6xBV-CHP (CR), BEAM-ASCT (CR) External beam radiation therapy + MTX + 6-MP (CR) 2xBV-ICE (CR) 3xBelinostat + RT (CR) Allo-SCT (CR) + Maintenance Belinostat	No AE, Alive
3	70/M	3	PTCL, NOS	1	HTN	4xCHOEP (PD) 2xBV-Bendamustine (PD) 1xBelinostat (NE)	No AE, Exitus because of lymphoma progression
4	78/M	4 (bone and skin involvement)	ALCL, ALK-	1	CHD	6xCHOP (SD) 6xBV-Bendamustine (SD) 2xGEMOX (PD) 2xBelinostat (PD) RT	No AE, Exitus because of lymphoma progression
5	56/F	3	PTCL, NOS	1	No comorbidity	5xCHOP (CR) 1xICE (PD) 1xGEMOX (PD) 2xBelinostat (PD) 1xPralatrexate (Ongoing treatment) + IT chemotherapy (ARA-C + Methotrexate + Hydrocortisone)	No AE, Alive
6	62/M	4 (gastric involvement)	PTCL, NOS	1	No comorbidity	6xCHOP (CR), BEAM-ASCT (CR) 6xBV-GDP (CR) Allo-SCT (PD) 4xBelinostat (SD) 2xRomidepsin (PD)	No AE, Exitus because of lymphoma progression
7	59/M	3 (splenic involvement)	Nodal TFH cell lymphoma, follicular type	1	DM	6xCHOP (CR) 2xDHAP (SD) 14xBelinostat (CR)	No AE, Alive
8	71/F	4 (lung and pleural involvement)	PTCL, NOS	2	CHD, AF, Depression	Interferon (2 years) +RT (CR) 4x CHOP (PD) 1xBelinostat (NE)	No AE, Exitus because of lymphoma progression
9	78/F	3	AITL	2	HTN, DM	6xCHOP (CR) 8x Gemsitabine + Vinorelbine (CR) 2xBelinostat (PD) 11xLenalidomid (PD)	No AE, Exitus because of lymphoma progression

Abbreviations: M, male; F, female; ALCL, anaplastic large cell lymphoma; TFH, T-follicular helper; PTCL-NOS, peripheral T-cell lymphoma, not otherwise specified; AITL, angioimmunoblastic T-cell lymphoma; ECOG, Eastern Cooperative Oncology Group; HTN, hypertension; DM, diabetes mellitus; CHD, coronary heart disease; AF, atrial fibrillation; AE, adverse event; CR, complete response; PR, partial response; SD, stable disease; PD, progressive disease; NE, not evaluable; CHOP, cyclophosphamide, doxorubicin, vincristine, prednisolone; BV-CHP, brentuximab vedotin, cyclophosphamide, doxorubicin, prednisolone; ICE, ifosfamide, carboplatin, etoposide; BEAM, carmustine, etoposide, cytarabine, melphalan; RT, radiotherapy; DHAP, dexamethasone, cytarabine, cisplatin; BV-GDP, brentuximab vedotin, gemcitabine, dexamethasone, cisplatin; GEMOX, gemcitabine, oxaliplatin; CHOEP, cyclophosphamide, doxorubicin, etoposide, vincristine, prednisolone; allo-SCT, allogeneic stem cell transplantation; ASCT, autologous stem cell transplantation.

tion was 65 years (range, 52 - 78). Four patients were male and five were female. PTCL subtypes consisted of five PTCL-NOS, two ALCL, one nodal TFH cell lymphoma follicular-type and one AITL. At the time of diagnosis, five patients were stage IV and four were stage III. According to the International Prognostic Index score, 2 patients had a score of 1, 4 had a score of 2, 2 had a score of 3, and 1 had a score of 4. Two patients had B symptoms at the time of diagnosis (Patient

https://doi.org/10.5455/annalsmedres.2025.07.193

5, 8) and an Eastern Cooperative Oncology Group (ECOG) performance status of 1, except for two patients (both ECOG 2). EBV positivity was not detected in any of the patients by in situ hybridization. Patient demographics, clinical characteristics, treatment courses, and responses are summarized in Table 1.

One patient (Patient 7) had splenic involvement. Five patients (Patients 1, 2, 4, 6, 8) had extranodal diseases in one or more lung, pleura, bone, skin or gastric sites at diagnosis. None of the patients had bone marrow involvement.

All patients had received multiple prior therapies (median three lines; range: 3-4 lines) before belinostat, including CHOP (cyclophosphamide, doxorubicin, vincristine, prednisolone)-based chemotherapy, gemcitabine-based combinations (e.g., GEMOX [gemcitabine, oxaliplatin] and BV-GDP [brentuximab vedotin, gemcitabine, dexamethasone, cisplatin]), bendamustine-based regimens, or high-dose chemotherapy with stem cell transplantation. Despite these intensive approaches, patients were considered either relapsed or refractory at the time of belinostat initiation.

Of the nine patients, two (Patients 2, 6) underwent autologous stem cell transplantation (ASCT). Two additional patients (Patients 1, 5) achieved successful stem cell mobilization but were ultimately unable to proceed with ASCT due to disease progression or inadequate response. The remaining patients were deemed ineligible for transplantation. Among the two patients who had undergone ASCT, disease relapse required allogeneic stem cell transplantation (allo-SCT). In one case (Patient 2), belinostat served as bridging therapy prior to allo-SCT, whereas in the other (Patient 6) it was administered post-allo-SCT following relapse.

Belinostat treatment and response

Belinostat was administered off-label in accordance with national regulations, as a monotherapy at a dose of 1000 mg/m^2 once daily on days 1–5 of a 21-day cycle. Of the nine R/R PTCL patients treated with belinostat, two (22.2%) achieved CR, one (11.1%) had SD, four (44.4%) developed PD and two (22.2%) died from lymphoma progression before a second cycle could be administered. The number of belinostat cycles ranged from 1 to 14 across the cohort. All patients were followed for a median of 37 months (range, 8-74 months). Response evaluations were performed using the Lugano criteria, primarily with PET-CT imaging after two cycles or earlier if clinically indicated. Among the nine patients, two achieved CR, one had SD, four showed PD, and two were not evaluable.

Complete remission

Two patients achieved CR (22.2%). One patient (Patient 2, ALCL, ALK-negative) achieved a complete response in all bone, skin, and nodal lesions following two cycles of belinostat. However, a new extramedullary lesion emerged in the right 7th costa. Radiotherapy was initiated for this lesion, and the third cycle of belinostat was administered concurrently. The patient achieved a complete response by the end of all treatment courses. Subsequently, she underwent allogeneic stem cell transplantation and remained alive and disease-free at the last follow-up. She is currently in the seventh month post-transplant and continues to receive belinostat as maintenance therapy. Another patient (Patient 7, nodal TFH lymphoma follicular type) experienced a prolonged CR after 14 cycles of belinostat and is also alive without progression.

Stable disease

One patient (Patient 6, PTCL-NOS; 11.1%) reached SD after four cycles. However, subsequent therapy with romidepsin was unsuccessful and the patient ultimately succumbed to disease progression.

Progressive disease

Four patients (Patients 1, 4, 5, 9; 44.4%) showed PD at the time of reassessment (after two cycles) or shortly thereafter. Two of these individuals (Patients 4, 9) died due to rapid disease progression, while the other two continued further lines of therapies (GEMOX and/or pralatrexate) with varying outcomes; both remain alive at data cutoff. Notably, response assessments conducted after two cycles of belinostat therapy revealed disease progression in extranodal sites that were not initially involved at the initiation of treatment. Specifically, Patient 1 exhibited bone marrow involvement, Patient 4 developed cutaneous involvement and Patient 5 demonstrated cerebrospinal fluid involvement.

Not evaluable

Two patients (Patients 3, 8; 22.2%) could not be formally evaluated for response, as both received only one cycle of belinostat and died from lymphoma progression before a follow-up assessment could be completed.

Survival and safety

The median OS was 6.8 months (95% CI, 3.9 to 9.6; Figure 1). At last follow-up, 4 (Patients 1, 2, 5, 7) of the 9 patients (44%) were alive, and 2 of these continued belinostat therapy. Five patients (Patients 3, 4, 6, 8, 9) died from PTCL progression. The median PFS was 3.4 months (95% CI, 0.8 to 5.6; Figure 2). The six-month PFS rate, defined as the proportion of patients surviving without progression, was 25%. No patient experienced grade 3-4 adverse events related to belinostat, and there were no treatment discontinuations or dose reductions due to toxicity. All patients tolerated belinostat without requiring hospitalization for toxicity management.

DISCUSSION

PTCL poses a major therapeutic challenge due to its limited treatment options and poor responses to conventional chemotherapy, particularly in the R/R setting [10–12].

https://doi.org/10.5455/annalsmedres.2025.07.193

HDACs have recently gained attention as novel epigenetic targets in PTCL, as dysregulated acetylation and deacetylation processes can drive genomic instability and aberrant gene expression in this disease [5]. While salvage chemotherapy and ASCT remain standard approaches for R/R PTCL, their limited effectiveness highlights the continuous need for novel therapeutic approaches. First-line treatment for PTCL typically involves combination chemotherapy, most frequently the CHOP regimen or a CHOP-like protocol [13].

Promising findings were reported from a Phase I, single-arm trial evaluating belinostat combined with CHOP (Bel-CHOP) in newly diagnosed PTCL, yielding a 71% complete response rate and an 86% overall response rate (ORR) [8]. Although patients did not undergo consolidation with ASCT, the regimen was well tolerated, suggesting that earlier incorporation of HDAC inhibitors may confer clinical benefit for selected patient populations [8]. In the R/R setting, outcomes remain dismal; a retrospective analysis reported median PFS and OS of only 3.1 months and 5.5 months, respectively [12]. Against this setting, belinostat has shown promise, with the pivotal phase II BELIEF study leading to its accelerated FDA approval for R/R PTCL [7]. In that landmark trial, 120 evaluable patients achieved an ORR of 26% (CR, 11%), with a median duration of response of 13.6 months [7]. A later multicenter phase II study also confirmed the activity of belinostat in PTCL and cutaneous T-cell lymphoma (CTCL) but with somewhat lower response rates and shorter durations of response [14]. Overall, these observations suggest that belinostat may have clinical utility with an acceptable tolerability profile characterized mainly by grade 3–4 cytopenias.

While initial clinical trials have provided preliminary insights into efficacy of belinostat and safety, real-world data remain limited. The experience in the small, published Turkish cohort of 10 patients with R/R PTCL reported by Akdeniz et al. [15] reported a 50% objective response rate, with only one case of grade 3 neutropenia. More recently, the large-scale BELBRA study, conducted across 90 Brazilian lymphoma centers, examined belinostat in R/R PTCL and presented interim findings for 97 patients: an ORR of 45%, SD in 10%, and disease progression in 45% [9]. Notably, belinostat was generally well tolerated over an average of five treatment cycles, underscoring its potential as a salvage therapy for patients who have failed prior treatments [9].

Our own retrospective analysis included nine patients with R/R PTCL treated at three institutions, covering a spectrum of histopathological subtypes. All had advanced disease (Stage III–IV) and significant comorbidities. which limited their eligibility for transplantation. Despite these challenges, belinostat was administered as a third- to fifth-line treatment. According to national regulations, belinostat has not been approved as an early-line therapy and can only be used off-label in patients who have failed multiple prior treatments. Therefore, in our cohort, belinostat was administered in later lines of therapy. This reflects restrictions imposed by national health insurance coverage rather than physician preference. None of the patients experienced notable adverse events. Two patients (22.2%) achieved CR, including one who proceeded to allo-SCT and remains disease-free, and another who has sustained remission for 14 months on ongoing belinostat monotherapy. Four patients (44.4%) experienced disease progression by or soon after their second cycle, necessitating other salvage therapies; two subsequently died. An additional two patients received only a single cycle of belinostat and died from progression before response assessment. One patient achieved SD after four cycles but later succumbed to progression despite switching to another HDAC inhibitor. The median OS was 6.8 months and the median PFS was 3.4 months. The six-month PFS rate, defined as the proportion of patients surviving without progression, was 25%.

Another observation that was notable in our cases was the emergence of new extranodal involvement in four patients during belinostat treatment, despite positive responses in pre-existing nodal and extranodal lesions. We found no data on this topic in the literature. In general, these results reflect the aggressive nature of PTCL in an elderly and comorbid population and are consistent with previous literature indicating that belinostat may provide durable remission in a subgroup of patients but that early relapse is observed in many patients. There are primary or acquired resistance mechanisms to HDAC inhibitors. These mechanisms have been characterised in lymphoma models and may contribute to early progression. Resistance mechanisms include: reactivation of survival pathways such as PI3K/AKT and NF-κB, inadequate reprogramming due to epigenetic plasticity, increased anti-apoptotic signal transduction, and drug efflux via P-glycoprotein (ABCB1) [16,17]. Various combination strategies are being investigated to overcome resistance. In particular, the combination of HDAC inhibitors with hypomethylating agents (e.g., azacitidine + romidepsin) has been shown to achieve high response rates in TFH phenotypes in clinical trials and real-world data [18,19].

Impressively, none of our patients experienced serious adverse events or required therapy discontinuation due to toxicity, consistent with the safety profile observed in previous studies [7,9]. This finding is encouraging, although the small cohort size and retrospective data collection prevent definitive conclusions regarding tolerability.

Going forward, further research is needed to optimase the use of belinostat in PTCL. Exploring combination therapies -such as frontline Bel-CHOP or pairing belinostat with immunotherapies or other targeted agents- may offer improved effectiveness. Prospective multicenter or registry-based studies with larger sample sizes are essential to clarify belinostat's long-term safety, durability of response, and its most appropriate place in the treatment plan for both newly diagnosed and R/R PTCL.

https://doi.org/10.5455/annalsmedres.2025.07.193

Limitations

Our findings should be interpreted with caution for several reasons. First and foremost the small sample size which limits statistical power and the capability to generalize the results. Second, the retrospective nature of our data gathering may introduce selection bias, given that each patient's treatment was at the discretion of their physician in everyday clinical practice. Third differences in follow-up intervals between the three centers, and two patients died before formal response evaluation, could potentially result in some outcomes being underestimated or missed. Lastly, the heterogeneity of PTCL subtypes and prior therapies, and the advanced stage of disease in most patients, may complicate direct comparison with clinical trial populations.

CONCLUSION

In summary, the findings from our study underscore potential of belinostat inducing durable responses in a subset of heavily pretreated R/R PTCL patients. However, the small sample size and retrospective design emphasize the need for larger prospective trials to validate efficacy and optimize patient selection.

Ethics Committee Approval: Ethical approval was obtained from Istanbul Medipol University Ethics Committee (Date: 22-05-2025, Number: 580).

Informed Consent: Informed consent was not obtained due to the retrospective design of the study.

Peer-review: Externally peer-reviewed.

Conflict of Interest: The authors declare that they have no conflict of interest.

Author Contributions: Materials and Data collection: G.A., E.Y., H.S.B., Ö.G.S.; Concept: S.Y.K.; Design: S.Y.K., L.K.; Data Collection or Processing: G.A., E.Y., S.M.; Analysis or Interpretation: S.Ç., S.Y.K., S.M.; Literature Search: L.K., S.Y.K.; Writing: S.Y.K., L.K.

Financial Disclosure: There is nothing to disclose.

Artificial Intelligence Disclosure: The authors declare that an artificial intelligence–based tool (ChatGPT 5.2) was used solely for language editing and improving the clarity and readability of the manuscript. The AI tool did not contribute to the study design, data analysis, interpretation of results, or scientific conclusions. All content was critically reviewed and approved by the authors, who take full responsibility for the manuscript.

REFERENCES

1. Piccaluga PP, Khattab SS. A Comparison of the Fifth World Health Organization and the International Consensus Classifications of Mature T-Cell Lymphomas. *Int J Mol Sci.* 2023;24(18):14170. doi: 10.3390/ijms241814170.
2. Alaggio R, Amador C, Anagnostopoulos I, Attygalle AD, Araujo IB de O, Berti E, et al. The 5th edition of the World Health Organization Classification of Haematolymphoid Tumours: Lymphoid Neoplasms. *Leukemia.* 2022;36(7):1720–48. doi: 10.1038/s41375-022-01620-2.
3. Lindemann RK, Gabrielli B, Johnstone RW. Histone-deacetylase inhibitors for the treatment of cancer. *Cell Cycle.* 2004;3(6):779–88. PMID: 15153801.
4. Ma X, Ezzeldin HH, Diasio RB. Histone Deacetylase Inhibitors: Current Status and Overview of Recent Clinical Trials. *Drugs.* 2009;69(14):1911-34. doi: 10.2165/11315680-000000000-00000.
5. Irimia R, Piccaluga PP. Histone Deacetylase Inhibitors for Peripheral T-Cell Lymphomas. *Cancers (Basel).* 2024;16(19):3359. doi: 10.3390/cancers16193359.
6. Poole RM. Belinostat: First global approval. *Drugs.* 2014;74(13):1543–54. doi: 10.1007/s40265-014-0275-8.
7. O'Connor OA, Horwitz S, Masszi T, Van Hoof A, Brown P, Doorduijn J, et al. Belinostat in patients with relapsed or refractory peripheral T-cell lymphoma: Results of the pivotal phase II BELIEF (CLN-19) study. *J Clin Oncol.* 2015;33(23):2492–9. doi: 10.1200/JCO.2014.59.2782.
8. Johnston PB, Cashen AF, Nikolinakos PG, Beaven AW, Barta SK, Bhat G, et al. Belinostat in combination with standard cyclophosphamide, doxorubicin, vincristine and prednisone as first-line treatment for patients with newly diagnosed peripheral T-cell lymphoma. *Exp Hematol Oncol.* 2021;10(1):15. doi: 10.1186/s40164-021-00203-8.
9. De Moura RP, Abdo ANR, Chiattone C, Canutti V, Fischer T, O'Connor OA. First Interim Results of the Real-Life Study Evaluating the Efficacy and Safety of Belinostat in Patients with R/R PTCL in Brazil (BELBRA). *Blood.* 2024;144(Supplement 1):7749. doi: 10.1182/blood-2024-199240.
10. Escalón MP, Liu NS, Yang Y, Hess M, Walker PL, Smith TL, et al. Prognostic factors and treatment of patients with T-cell non-Hodgkin lymphoma: The M. D. Anderson Cancer Center experience. *Cancer.* 2005;103(10):2091–8. doi: 10.1002/cncr.20999.
11. AbouYabis AN, Shenoy PJ, Sinha R, Flowers CR, Lechowicz MJ. A Systematic Review and Meta-Analysis of Front-line Anthracycline-Based Chemotherapy Regimens for Peripheral T-Cell Lymphoma. *ISRN Hematol.* 2011;2011:623924. doi: 10.5402/2011/623924.
12. Mak V, Hamm J, Chhanabhai M, Shenkier T, Klasa R, Sehn LH, et al. Survival of Patients With Peripheral T-Cell Lymphoma After First Relapse or Progression: Spectrum of Disease and Rare Long-Term Survivors. *J Clin Oncol.* 2013;31(16):1970–6. doi: 10.1200/JCO.2012.44.7524.
13. Ngu HS, Savage KJ. Past, present and future therapeutic approaches in nodal peripheral T-cell lymphomas. *Haematologica.* 2023;108(12):3211–3226. doi: 10.3324/haematol.2021.280275.
14. Foss F, Advani R, Duvic M, Hymes KB, Intragumtornchai T, Lekhakula A, et al. A Phase II trial of Belinostat (PXD101) in patients with relapsed or refractory peripheral or cutaneous T-cell lymphoma. *Br J Haematol.* 2015;168(6):811–9. doi: 10.1111/bjh.13222.
15. Akdeniz A, Keklik Karadag F, Atalay F, Miskioglu M, Deveci B, Aytan P, Saydam G Outcome of Belinostat in Patients with Peripheral T Cell Lymphoma, Multicenter Real-Life Data, Turkey. *Osmangazi Journal of Medicine.* 2022;44(4):454-459. doi: 10.20515/otd.1038937.
16. Kiesslich T, Mayr C, Bekric D, Neureiter D. New insights into possible HDAC inhibitor resistance in DLBCL - Comment on "defining cellular responses to HDAC-selective inhibitors reveals that efficient targeting of HDAC3 is required to elicit cytotoxicity and overcome naïve resistance to pan-HDACi in diffuse large B cell lymphoma" by Havas et al. *Transl Oncol.* 2024;44:101820. doi: 10.1016/j.tranon.2023.101820.
17. Robey RW, Chakraborty AR, Basseville A, Luchenko V, Bahr J, Zhan Z, et al. Histone deacetylase inhibitors: Emerging mechanisms of resistance. *Mol Pharm.* 2011;8(6):2021-31. doi: 10.1021/mp200329f.
18. Falchi L, Ma H, Klein S, Lue JK, Montanari F, Marchi E, et al. Combined oral 5-azacytidine and romidepsin are highly effective in patients with PTCL: a multicenter phase 2 study. *Blood.* 2021;137(16):2161-2170. doi: 10.1182/blood.2020009004.

https://doi.org/10.5455/annalsmedres.2025.07.193

19. Kalac M, Jain S, Tam CS, Xiao Z, Montanari F, Kanakry J, et al. Real-world experience of combined treatment with azacitidine and romidepsin in patients with peripheral T-cell lymphoma. *Blood Adv.* 2023;7(14):3760-3763. doi: 10.1182/bloodadvances.2022009445.

https://doi.org/10.5455/annalsmedres.2025.07.193

Ann Med Res

Current issue list available at Ann Med Res

Annals of Medical Research

journal page: annalsmedres.org

Analyses of human papillomavirus genotypes in cervical cancer patients using real-time PCR

Halil Ozturk[a], Seyhun Sucu[b], Ibrahim Taskum[b,*], Zehra Bozdag[c], Tekin Karsligil[d], Ozcan Balat[e]

[a]Private Medline Hospital, Clinic of Obstetrics and Gynecology, Adana, Türkiye
[b]Gaziantep City Hospital, Clinic of Obstetrics and Gynecology, Gaziantep, Türkiye
[c]İnönü University, Faculty of Medicine, Department of Pathology, Malatya, Türkiye
[d]Gaziantep University, Faculty of Medicine, Department of Medical Microbiology, Gaziantep, Türkiye
[e]Gaziantep University, Faculty of Medicine, Department of Obstetrics and Gynecology, Gaziantep, Türkiye
*Corresponding author: ibrahimtaskum@gmail.com (Ibrahim Taskum)

MAIN POINTS

- HPV 16, 18, and 45 were identified as the most frequent genotypes in cervical cancer cases in Gaziantep.
- The relatively high prevalence of HPV 45 appears to be a distinctive regional feature compared with national and international reports.
- Regional HPV genotyping provides valuable epidemiological data for tailoring vaccination strategies and clinical management.
- The nonavalent HPV vaccine, covering the most prevalent types found in this study, should be considered the most effective option for preventing cervical cancer in this population.

Cite this article as: Ozturk H, Sucu S, Taskum I, Bozdag Z, Karsligil T, Balat O. Analyses of human papillomavirus genotypes in cervical cancer patients using real-time PCR. *Ann Med Res*. 2026;33(4):185–191. doi: 10.5455/annalsmedres.2025.09.258.

ABSTRACT

Aim: The aim of this study was to identify the most prevalent Human Papillomavirus (HPV) genotypes associated with cervical cancer in Gaziantep and to determine the most appropriate HPV vaccine for individuals who have not yet been infected.

Materials and Methods: This retrospective cross-sectional study included 74 patients diagnosed with cervical cancer at Gaziantep University Faculty of Medicine between December 2005 and June 2019. Formalin-fixed paraffin-embedded tissue samples were retrieved from the pathology archives. HPV DNA was extracted and genotyping of 14 high-risk HPV types was carried out by real-time PCR.

Results: All patients were histopathologically diagnosed with squamous cell carcinoma. Single HPV type infection was detected in six patients (8.2%) (HPV 16 in five, HPV 56 in one), whereas multiple infections were observed in 68 patients (91.8%). Among these, HPV 16 was identified in 100% of cases, HPV 45 in 82%, HPV 18 in 45%, HPV 56 in 19%, and HPV 33 in 16%. Overall, HPV 16, 45, and 18 genotypes emerged as the most frequent types contributing to cervical cancer in this region.

Conclusion: Given the genotypes identified in this study, the nonavalent HPV vaccine (9-valent; HPV types 6, 11, 16, 18, 31, 33, 45, 52, and 58) appears to be the most suitable option for our population. However, due to its limited availability in Turkey, the quadrivalent HPV vaccine (4-valent; HPV types 6, 11, 16, and 18), which may provide partial cross-protection against HPV 45, could serve as a reasonable alternative.

Keywords: Human papillomavirus, HPV vaccine, Cervical cancer, Genotype, Real-time PCR
Received: Sep 08, 2025 **Accepted:** Dec 08, 2025 **Available Online:** Apr 24, 2026

INTRODUCTION

Cervical cancer is the fourth most frequently diagnosed malignancy and the fourth leading cause of cancer-related mortality among women worldwide, with an estimated 604,000 new cases and 342,000 deaths reported in 2020. The disease remains a significant global health burden, particularly in sub-Saharan Africa, Melanesia, South America, and South-Eastern Asia, where it ranks as either the most common or the most fatal malignancy among women. Conversely, incidence and mortality rates are 7–10 times lower in high-income regions, such as North America and Western Asia. These geographic disparities primarily reflect inequities in access to screening and vaccination programs, as the vast majority of deaths occur in countries with limited resources and inadequate preventive strategies [1].

According to 2015 statistics from the Turkish Ministry of Health, cervical cancer is the tenth most prevalent malignancy

among women in Turkey, with an incidence rate of 4.5 per 100,000 individuals. The disease is often preceded by precursor lesions, most notably cervical intraepithelial neoplasia (CIN). Established risk factors include the early initiation of sexual activity, multiple sexual partners, sexually transmitted infections (STIs), and multiparity [2].

The strength of the association between persistent Human Papillomavirus (HPV) infection and cofactors such as smoking and oral contraceptive use remains a subject of ongoing debate; however, inconsistent findings across studies suggest these factors may significantly contribute to cervical carcinogenesis [3,4]. Notably, numerous studies indicate a more robust correlation between smoking and cervical squamous cell carcinoma (SCC) [5,6]. Cervical cancer is infrequently diagnosed in nulliparous or virginal women. Furthermore, male circumcision has been shown to reduce the risk of HPV acquisition and reinfection while increasing HPV clearance in the glans, thereby indirectly reducing the risk of cervical cancer in women [7]. Additionally, in utero exposure to diethylstilbestrol (DES) is associated with an elevated risk of clear-cell adenocarcinoma of the cervix and vagina; while this risk is most pronounced at younger ages, recent evidence indicates it may persist into midlife and older age [8].

HPV, primarily transmitted through sexual contact, is recognized as the primary etiological agent in the development of cervical cancer [9]. High-risk types, specifically HPV-16 and HPV-18, are responsible for over 70% of cases, though other oncogenic genotypes—including HPV-31, 33, 35, 39, 45, 51, 52, 56, and 58—also play a substantial role [10]. HPV infection occurs most frequently in young women aged 18–30 years. Although approximately 90% of these infections clear spontaneously within 12–36 months, persistent infections can progress to invasive cervical cancer later in life [11].

The objective of this study was to investigate the distribution of HPV genotypes among patients with cervical cancer in Gaziantep, Turkey. By doing so, we aimed to determine the most suitable vaccine formulations for HPV-negative individuals and to highlight the critical role of genotyping in supporting early detection and clinical management for HPV-positive, unvaccinated women.

MATERIALS AND METHODS

Patient selection

Between December 1, 2005, and June 1, 2019, a total of 90 patients who histopathologically diagnosed with HPV-related cervical cancer were retrospectively identified from the electronic database of the Pathology Department. Among these, 74 patients with adequate formalin-fixed paraffin-embedded (FFPE) tissue blocks and sufficient DNA quality were included in this retrospective cross-sectional study. Cases with tissue insufficiency or poor DNA quality were excluded. The study was approved by institutional review board in terms of scientific and ethical conduct. The study was conducted in accordance with the ethical principles of the Declaration of Helsinki and was approved by the Gaziantep University Clinical Research Ethics Committee (approval date: October 2, 2019; approval number: 2019/376).

Tissue processing and DNA isolation

Formalin fixed paraffin embedded (FFPE) cervicale cancer tissues were prepared for analysis. Five slices, each 10 μm thick, were excised from each block and deposited into sterile tubes using the laboratory's usual protocol. Deparaffinization was performed with xylene and graded ethanol via standard centrifugation procedures. Subsequent to drying, the tissue was incubated at 56 °C for 2 hours in a solution comprising ATL lysis buffer and Proteinase K. A 700 μL aliquot of the resultant lysate was then subjected to automated nucleic acid extraction using the QIAsymphony DSP Virus/Pathogen Midi Kit (QIAGEN, Hilden, Germany) on the QIAsymphony SP system. Each sample was extracted a single time, according to the manufacturer's instructions. The purity of DNA and its amplification capability were evaluated using the internal control reactions included in the commercial kit. A total of 60 μL of DNA eluate was collected from each specimen.

HPV DNA analysis and genotyping

HPV DNA detection was conducted utilizing real-time PCR on the QIAGEN Rotor-Gene system. The thermal cycling protocol commenced with an initial denaturation step at 95 °C for 15 minutes, succeeded by a pre-amplification phase consisting of 5 cycles (95 °C for 5 seconds, 60 °C for 20 seconds, and 72 °C for 15 seconds). Subsequently, 40 amplification cycles were conducted at 95 °C for 5 seconds, 60 °C for 30 seconds, and 72 °C for 15 seconds. Genotyping was performed utilizing a commercial kit (NLM Diagnostici, Italy) specifically developed for the detection of 14 oncogenic HPV types. Four PCR reactions were conducted for each patient, utilizing primer sets that targeted HPV types 16, 18, 31, 33, 35, 39, 45, 51, 52, 56, 58, 59, 66, and 68. Each run included positive and negative controls to ensure the assay's reliability. All reactions were performed on a microplate-based real-time PCR platform to ensure precise amplification and detection.

Evaluation of results

Amplification curves obtained from the PCR software were evaluated using the threshold value recommended by the manufacturer (threshold = 0.03). Representative examples of raw fluorescence data from the detection channels are presented in Figure 1.

Statistical analysis

Data were analyzed using SPSS version 22.0 (IBM Corp., Armonk, NY, USA). Descriptive statistics are reported as frequencies (n) and percentages (%). Given the descriptive nature of this study, no comparative statistical tests were performed. The prevalence of each HPV genotype was expressed as a percentage of the total number of cases. To account for

https://doi.org/10.5455/annalsmedres.2025.09.258

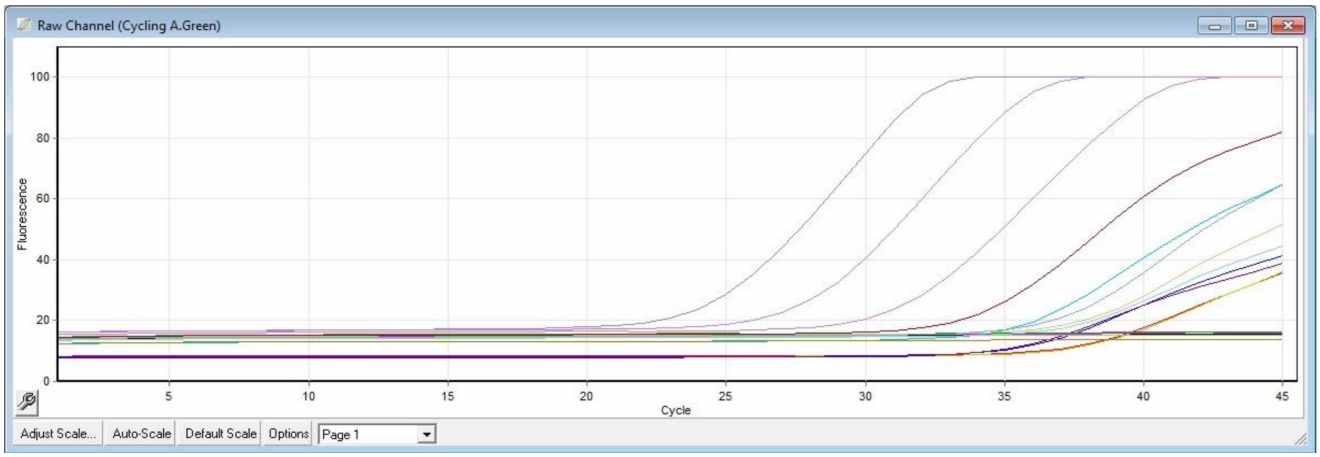

Figure 1. Raw amplification curves from the real-time PCR analysis. (Fluorescence signal curves obtained from the PCR software were evaluated according to the threshold value of 0.03. Different channels represent the HPV genotypes analyzed).

the relatively small sample size, 95% confidence intervals (CIs) were calculated using the Clopper–Pearson exact binomial method. The resulting data are summarized in the accompanying tables.

RESULTS

Seventy-four patients with pathologically confirmed cervical cancer were included in the analysis. Real-time PCR detected HPV DNA in all samples, resulting in a total positivity rate of 100%. The distribution of HPV genotypes and their 95% confidence intervals are presented in Table 1. Infections involving a single HPV type were relatively uncommon ($n = 6$, 8.2%), whereas the vast majority of patients ($n = 68$, 91.8%) harbored multiple HPV types (Table 2).

The mean age of the patients was 52.6 ± 11.8 years, with a range of 29–78. The distribution of HPV genotypes was described across three age groups (≤40, 41–50, and >50 years). HPV 16 was the most common genotype identified in all groups, followed by HPV 45 and HPV 18. Overall, the pattern of genotype distribution appeared similar across all age categories (Table 3).

The temporal distribution of cervical cancer cases based on biopsy identification years (2005–2019) is summarized in Table 4. The number of cases varied slightly from year to year, ranging between two and eight cases annually, with no clear upward or downward trend observed throughout the 14-year study period. HPV 16 remained the predominant genotype across all years, followed by HPV 45 and HPV 18, without any apparent temporal shift in genotype distribution.

The most frequently observed co-infections were HPV 16/45 and HPV 16/18/45, each of which was detected in 13 patients (17.6%). Additional combinations that appeared with notable frequency included HPV 16/33/45 (4.1%), HPV 16/39/45 (5.4%), and HPV 16/56 (5.4%). Across all patterns, HPV 16 was consistently the dominant genotype and was present in nearly every combination.

Table 1. Variation of HPV genotypes in our study.

HPV Genotype	n (%) [95% CI]
HPV 16	5 (6.8) [2.2--15.2]
HPV 16/45	13 (17.6) [9.8--28.5]
HPV 16/18/45	13 (17.6) [9.8--28.5]
HPV 56	1 (1.4) [0.0--7.3]
HPV 16/31/45	2 (2.7) [0.3--9.4]
HPV 16/18/39/45	2 (2.7) [0.3--9.4]
HPV 16/18/33/45/56	1 (1.4) [0.0--7.3]
HPV 16/45/66	2 (2.7) [0.3--9.4]
HPV 16/18/45/56/66	1 (1.4) [0.0--7.3]
HPV 16/45/56	2 (2.7%) [0.3--9.4]
HPV 16/39/45	4 (5.4) [1.5--13.2]
HPV 16/58	1 (1.4) [0.0--7.3]
HPV 16/18/45/59	1 (1.4) [0.0--7.3]
HPV 16/33/52	1 (1.4) [0.0--7.3]
HPV 16/18/33/39/45	1 (1.4) [0.0--7.3]
HPV 16/18/33/45	2 (2.7) [0.3--9.4]
HPV 16/56	4 (5.4) [1.5--13.2]
HPV 16/45/59	1 (1.4) [0.0--7.3]
HPV 16/68	1 (1.4) [0.0--7.3]
HPV 16/18/45/51	2 (2.7) [0.3--9.4]
HPV 16/33/39/45	1 (1.4) [0.0--7.3]
HPV 16/33/45	3 (4.1) [0.9--11.5]
HPV 16/18/31/45	2 (2.7) [0.3--9.4]
HPV 16/18	1 (1.4) [0.0--7.3]
HPV 16/18/45/56	2 (2.7) [0.3--9.4]
HPV 16/18/33/35/56	1 (1.4) [0.0--7.3]
HPV 16/31/56/68	1 (1.4) [0.0--7.3]
HPV 16/39	1 (1.4) [0.0--7.3]
HPV 16/18/31	1 (1.4) [0.0--7.3]
HPV 16/18/33/35/45/52/68	1 (1.4) [0.0--7.3]

Values are presented as number (percentage) with 95% confidence intervals (Clopper–Pearson exact method). The table summarizes the distribution of HPV genotypes detected in 74 cervical cancer cases.

DISCUSSION

In this study, the most common HPV genotypes among cervical cancer cases in a tertiary hospital in Gaziantep were identified as genotypes 16, 18, and 45. The predominance of HPV 16 and 18 is consistent with both national and international reports, while the relatively high prevalence of HPV 45 indi-

https://doi.org/10.5455/annalsmedres.2025.09.258

Table 2. Descriptive statistical data of the patients infected with a single or multiple HPV types.

Infection type	N	%
Single HPV type	6	8.2
Multiple HPV types	68	91.8
Total	74	100

Table 3. Distribution of HPV genotypes according to age groups.

HPV Genotype	≤40 years (%)	41–50 years (%)	>50 years (%)
HPV 16	28.6	32.1	31.8
HPV 18	28.6	17.0	13.0
HPV 31	0.0	0.0	3.9
HPV 33	0.0	5.7	5.2
HPV 35	0.0	3.8	0.0
HPV 39	0.0	5.7	3.9
HPV 45	28.6	24.5	26.6
HPV 51	0.0	0.0	1.3
HPV 52	0.0	1.9	0.6
HPV 56	14.3	5.7	5.2
HPV 58	0.0	0.0	0.6
HPV 59	0.0	1.9	0.6
HPV 66	0.0	0.0	1.9
HPV 68	0.0	1.9	1.3

Values represent the percentage of patients in each age group positive for the indicated genotype. Multiple infections were possible. Median age: 52 years, IQR: 44–60.

Table 4. Annual distribution of cervical cancer cases (2005--2019).

Year	Number of cases (n)
2005	3
2006	4
2007	6
2008	5
2009	7
2010	6
2011	5
2012	8
2013	6
2014	5
2015	4
2016	4
2017	5
2018	4
2019	2

cates a high prevalence in the region. These findings highlight the regional variation in HPV genotype distribution and emphasize the importance of incorporating local epidemiological data into cervical cancer prevention and vaccination strategies.

The highest frequency of HPV infection occurs in sexually active young women, particularly those aged 25–29 years, after which the prevalence tends to stabilise or slightly decline [12]. Recent Turkish data also support the high prevalence of HPV infection even among women with normal cytology. In a study by Görür et al. [13], high-risk HPV genotypes were detected in 43% of 270 women aged 19–69 years using multiplex polymerase chain reaction (PCR).

The infection rate was significantly higher in patients with abnormal cytology (77%) compared to those with normal cytology (37%). Consistent with this age-related pattern, a multicenter Turkish study involving only women with normal cytology reported the highest HPV prevalence in the 25–29 age group, with HPV 16 and HPV 45 identified as the most frequent genotypes [14]. These findings underscore the fact that a substantial proportion of women may harbor high-risk HPV types despite having normal cytologic results, emphasizing the critical value of molecular HPV testing in cervical cancer screening and risk assessment. Consequently, detailed HPV genotyping is essential for mapping regional epidemiological patterns and tailoring preventive strategies. Genotyping further serves to refine regional data, guide national vaccination programs, and direct clinical follow-up for infected individuals. Accordingly, this research aims to determine the distribution of HPV subtypes most commonly associated with cervical cancer in Gaziantep and its surrounding regions. Based on these findings, we intend to identify the optimal vaccine formulations for preventive use in HPV-negative individuals aged 11–12 years, while highlighting the necessity of early detection and effective treatment for previously infected, unvaccinated patients.

Several investigations conducted across Turkey have documented varying HPV prevalence rates, which are largely influenced by the specific study populations and diagnostic techniques employed. Güney et al. (1997) used PCR and DNA in situ hybridization (DISH) to detect HPV DNA in 9.5% of pregnant women and 45% of women presenting with condyloma or dysplasia [15]. In a large screening cohort of 22,488 tests, abnormal cytology and HPV positivity were detected in 7.5% and 7.4% of cases, respectively. Among the HPV-positive samples, non-16/18 genotypes were most frequent (62.2%), followed by HPV 16 (22.9%) and HPV 18 (7.3%), while multiple-type infections occurred in 7.7% of cases. In this cohort, HPV testing demonstrated higher sensitivity but lower specificity than cytology in detecting high-grade cervical lesions (CIN2–CIN3) [16]. Similarly, Özçelik et al. found a prevalence of 6.1% among 230 participants [17]. In another study, HPV DNA was detected in 40.4% (150/371) of cervical samples; among these positive cases, cytological abnormalities were present in 12.9%, while 25.3% showed no cytological changes. The most common genotype was HPV 16 (45.3%), followed by HPV 56 (17.3%), HPV 18 (12.0%), and HPV 51 (12.0%) [18].

Onan et al. reported HPV DNA detection rates of 4.2% in CIN I, 14.8% in CIN II, and 45% in CIN III [19]. In a screening series of 1,353 women, İnal et al. identified HPV DNA in 1.5% of cytologically normal individuals, whereas all patients with abnormal cytology tested positive [20]. Ergünay et al. found HPV DNA in 80% of 35 cytologically abnormal cases, with high-risk genotypes present in 78.6% of those samples [21]. Yıldız et al. observed that p16 expression was positive

https://doi.org/10.5455/annalsmedres.2025.09.258

in all high-grade squamous intraepithelial lesion (HSIL) cases and 80% of low-grade squamous intraepithelial lesion (LSIL) cases, with an overall HPV DNA positivity rate of 48.6% [22]. Furthermore, Işıklı et al. reported LSIL or HSIL in 11.7% of women undergoing colposcopy following Pap smear screening [23], while Özgül et al. demonstrated p16INK4a positivity in all HSIL and cervical cancer cases, compared to 46.2% in LSIL cases [24]. Similarly, Müderris et al. reported that HPV 16 was the most common genotype in both cytologically normal and abnormal cases. They also noted that the frequencies of ASC-US and HSIL were significantly higher in women infected with HPV 16 than in those infected with other genotypes, further supporting the strong association between specific high-risk HPV types and cytological abnormalities in the Turkish population [25].

In Samsun Province, Taşkın et al. reported a high-risk HPV positivity rate of 9.17% among 5,406 women, with HPV 16 and HPV 18 accounting for 28.62% and 9.67% of infections, respectively; other high-risk types constituted 78.83% of cases. HPV 16 positivity peaked in women aged 30–39 years, while HPV 18 and other high-risk types were more frequent in the 40–49 age group. Notably, the highest prevalence was observed during the summer months, particularly in June 2021 [26]. Recent region-specific studies further demonstrate marked geographical variability in HPV distribution. In Mersin province, Yaman et al. reported a high-risk HPV prevalence of 12.6% among 12,641 women screened between 2019 and 2022, with significantly higher rates among those with abnormal cytology and HPV 16 as the dominant genotype [27]. A hospital-based study from Ankara involving 4,267 women reported an overall HPV positivity rate of 14.2%, with HPV 16 and HPV 18 detected in 2.4% and 0.7% of samples, respectively, and pooled high-risk HPV types identified in 8.8% [28]. Similarly, an Istanbul-based analysis of 2,285 cervical samples found a high-risk HPV positivity rate of 36.3%. The highest prevalence was seen in women aged 17–34 years, with HPV 16 (30.9%), HPV 39 (14.6%), and HPV 51 (14.2%) as the most frequent genotypes; multiple high-risk infections were observed in 40.7% of the positive cases [29].

In a multicenter hospital-based analysis across Turkey, Dursun et al. assessed a cohort of 6,388 women from 12 gynecologic oncology centers, reporting an overall HPV positivity rate of 25%. HPV DNA positivity was significantly higher among women with abnormal cytology compared to those with normal findings (52% vs. 27%, $p < 0.05$). The most frequently detected genotypes included HPV 16 (32%), HPV 6 (17%), HPV 11 (9%), HPV 18 (8%), HPV 31 (6%), HPV 51 (5%), and HPV 33 (3%). This indicates that while HPV 16 remains the predominant genotype, a considerable proportion of infections are attributable to non-16/18 types [30]. Finally, Usubütün et al. identified HPV DNA in 93.5% of 248 cervical cancer specimens, with HPV 16 being the most prevalent, followed by HPV 18 and HPV 45; together, HPV 16 and 18 comprised 75.4% of all invasive cases [31]. Avcı et al. documented HPV DNA in 61% of 77 women undergoing colposcopy, noting that all HSIL cases tested positive [32]. These findings, alongside large-scale clinical trials like the PATRICIA study, demonstrate that HPV vaccines may confer partial cross-protection against non-vaccine oncogenic types such as HPV 31, 33, and 45 [33].

Limitations and Strengths

This study has certain limitations. Due to its retrospective design, individual risk factors for HPV infection, including sexual history, HIV status, sociodemographic characteristics, and vaccination history, could not be assessed. Additionally, the analysis relied exclusively on paraffin-embedded tissue samples, precluding the determination of viable virus presence. The limited sample size and the study's confinement to a single institution restrict the generalizability of the results. A further limitation is that only the high-risk HPV types present in the commercial kit were evaluated; low-risk and less prevalent types were excluded from assessment. Furthermore, real-time PCR did not facilitate the evaluation of viral load or the integration of viral genomes. The lack of a control group hindered direct comparison, as the primary emphasis of the study was on the distribution of HPV genotypes in cervical cancer patients.

Notwithstanding these limitations, the research had significant merits. Genotyping was performed by real-time PCR on archival paraffin-embedded tissue specimens from patients with histologically confirmed cervical cancer who were treated at a tertiary referral facility in southeastern Turkey. These data provide significant epidemiological insight into the regional distribution of HPV types. This information may guide public health efforts, especially in customizing immunization campaigns to meet regional requirements.

CONCLUSION

In summary, HPV genotypes 16, 18, and 45 were found to be the predominant types associated with cervical cancer in our region. The findings emphasize the importance of continuous surveillance of genotype distribution to better tailor regional prevention and vaccination strategies. Expanding access to the nonavalent vaccine and strengthening screening programs may significantly reduce the burden of HPV-related cervical cancer in the future.

Ethics Committee Approval: This study was approved by the Gaziantep University Clinical Research Ethics Committee with decision no: 2019/376 on October 2, 2019.

Informed Consent: We did not need an informed consent for the data we obtained were from the archived specimens of the patients.

Peer-review: Externally peer-reviewed.

https://doi.org/10.5455/annalsmedres.2025.09.258

Conflict of Interest: The authors declare no conflict of interest for this article.

Author Contributions: Concept: HÖ; Methodology: HÖ, SS, ZB, ÖB; Data Collection: ZB, TK; Data Analysis: İT, TK; Writing: HÖ, İT, ÖB; Review & Editing: ÖB.

Financial Disclosure: This study was supported by the Scientific Research Projects Coordination Unit of Gaziantep University (Project No: TF.UT.19.57).

Data Availability Statement: All data obtained or analyzed during this study are included in this published article. Further information is available from the corresponding author upon reasonable request.

Artificial Intelligence Disclosure: The authors declare that an artificial intelligence–based tool (ChatGPT, OpenAI) was used solely for language editing and improving the clarity of the manuscript. The AI tool did not contribute to the study design, data analysis, data interpretation, or scientific conclusions. All data, analyses, and interpretations were generated entirely by the authors. All content was critically reviewed and approved by the authors, who take full responsibility for the manuscript.

REFERENCES

1. Sung H, Ferlay J, Siegel RL, Laversanne M, Soerjomataram I, et al. Global cancer statistics 2020: GLOBOCAN estimates of incidence and mortality worldwide for 36 cancers in 185 countries. *CA Cancer J Clin*. 2021;71(3):209–249. doi: 10.3322/caac.21660.
2. Bowden SJ, Doulgeraki T, Bouras E, Markozannes G, Athanasiou A, et al. Risk factors for human papillomavirus infection, cervical intraepithelial neoplasia and cervical cancer: an umbrella review and follow-up Mendelian randomisation studies. *BMC Med*. 2023;21(1):274. doi: 10.1186/s12916-023-02965-w.
3. Drill VA. Oral contraceptives: relations to mammary cancer, benign breast lesions, and cervical cancer. *Annu Rev Pharmacol*. 1975;15:367–385. doi: 10.1146/annurev.pa.15.040175.002055.
4. Melamed MR, Flehinger BJ. Early incidence rates of precancerous cervical lesions in women using contraceptives. *Gynecol Oncol*. 1973;1(4):290–298. doi: 10.1016/0090-8258(73)90021-8.
5. Nagelhout G, Ebisch RM, van der Hel O, Meerkerk GJ, Magnée T, et al. Is smoking an independent risk factor for developing cervical intra-epithelial neoplasia and cervical cancer? A systematic review and meta-analysis. *Expert Rev Anticancer Ther*. 2021;21(7):781–794. doi: 10.1080/14737140.2021.1888719.
6. Malevolti MC, Lugo A, Scala M, Gallus S, Gorini G, et al. Dose-risk relationships between cigarette smoking and cervical cancer: a systematic review and meta-analysis. *Eur J Cancer Prev*. 2023;32(2):171–183. doi: 10.1097/CEJ.0000000000000773.
7. Smith JS, Backes DM, Hudgens MG, Mei W, Chakraborty H, et al. Male circumcision reduces penile HPV incidence and persistence: a randomized controlled trial in Kenya. *Cancer Epidemiol Biomarkers Prev*. 2021;30(6):1139–1148. doi: 10.1158/1055-9965.EPI-20-1272.
8. White MC, Weir HK, Soman AV, Peipins LA, Thompson TD. Risk of clear-cell adenocarcinoma of the vagina and cervix among US women with potential exposure to diethylstilbestrol in utero. *Cancer Causes Control*. 2022;33(8):1121–1124. doi: 10.1007/s10552-022-01598-3.
9. Hu Z, Ma D. The precision prevention and therapy of HPV-related cervical cancer: new concepts and clinical implications. *Cancer Med*. 2018;7(10):5217–5236. doi: 10.1002/cam4.1501.
10. Bosch FX, Lorincz A, Muñoz N, Meijer CJ, Shah KV. The causal relation between human papillomavirus and cervical cancer. *J Clin Pathol*. 2002;55(4):244–265. doi: 10.1136/jcp.55.4.244.
11. Okunade KS. Human papillomavirus and cervical cancer. *J Obstet Gynaecol*. 2020;40(5):602–608. doi: 10.1080/01443615.2019.1634030.
12. Bruni L, Albero G, Rowley J, Alemany L, Arbyn M, et al. Global and regional estimates of genital human papillomavirus prevalence among men: a systematic review and meta-analysis. *Lancet Glob Health*. 2023;11(9):e1345–e1362. doi: 10.1016/S2214-109X(23)00305-4.
13. Gorur L, Dolanbay M, Ozturk F, Canoz O, Donmez-Altuntas H. High-risk human papillomavirus in Turkish patients with clinically suspicious cervical lesions analyzed by multiplex-PCR. *Indian J Med Res*. 2022;156(6):786–791. doi: 10.4103/ijmr.IJMR_2335_20.
14. Demir ET, Ceyhan M, Simsek M, et al. The prevalence of different HPV types in Turkish women with a normal Pap smear. *J Med Virol*. 2012;84(8):1242–1247. doi: 10.1002/jmv.23333.
15. Guney AI, Ince U, Kullu S, Pekin S, Cirakoglu B. Detection and typing of human papillomavirus in cervical specimens of Turkish women. *Eur J Gynaecol Oncol*. 1997;18(6):546–550. PMID: 9443034.
16. Lu Z, Knapp M, Downs S, Ali RA, Morgan TK, et al. Retrospective analysis of human papillomavirus genotyping and cytology (Pap smears) in cervical cancer screening: an institutional experience in the state of Oregon, USA. *Diagnostics (Basel)*. 2025;15(4):419. doi: 10.3390/diagnostics15040419.
17. Ozcelik B, Serin IS, Gokahmetoglu S, Basbug M, Erez R. Human papillomavirus frequency of women at low risk of developing cervical cancer: a preliminary study from a Turkish university hospital. *Eur J Gynaecol Oncol*. 2003;24(2):157–159. PMID: 12701968.
18. Nalca Erdin B, Cetin Duran A, Ogut S, Koyuncuoglu M. Evaluation of HPV-DNA prevalence and genotype distribution and cytological examination results in cervical samples. *Flora*. 2024;29(3):342–349. doi: 10.5578/flora.2024031115.
19. Onan MA, Taskiran C, Bozdayi G, et al. Assessment of human papilloma viral load of archival cervical intraepithelial neoplasia by real-time polymerase chain reaction in a Turkish population. *Eur J Gynaecol Oncol*. 2005;26(6):632–635. PMID: 16398225.
20. Inal MM, Kose S, Yildirim Y, Ozdemir Y, Töz E, et al. The relationship between human papillomavirus infection and cervical intraepithelial neoplasia in Turkish women. *Int J Gynecol Cancer*. 2007;17(6):1266–1270. doi: 10.1111/j.1525-1438.2007.00944.x.
21. Ergunay K, Misirlioglu M, Pinar F, Tuncer ZS, Tuncer S, Ustacelebi S. Human papilloma virus DNA in cervical samples with cytological abnormalities and typing of the virus. *Mikrobiyol Bul*. 2007;41(2):219–226. PMID: 17682708.
22. Yildiz IZ, Usubutun A, Firat P, Ayhan A, Kucukali T. Efficiency of immunohistochemical p16 expression and HPV typing in cervical squamous intraepithelial lesion grading and review of the p16 literature. *Pathol Res Pract*. 2007;203(6):445–449. doi: 10.1016/j.prp.2007.03.010.
23. Isikli B, Ozalp S, Oner U, Kalyoncu C, Yalcin OT, Kucuk N, et al. PAP smear screening among married women living in Osmangazi University ALPU training area. *Asian Pac J Cancer Prev*. 2007;8(1):60-2. PMID: 17477773.
24. Ozgul N, Cil AP, Bozdayi G, Usubutun A, Bulbul D, et al. Staining characteristics of p16INK4a: is there a correlation with lesion grade or high-risk human papilloma virus positivity? *J Obstet Gynaecol Res*. 2008;34(5):865–871. doi: 10.1111/j.1447-0756.2008.00795.x.
25. Muderris T, Afsar I, Yildiz A, Varer CA. HPV genotype distribution among women with normal and abnormal cervical cytology in Turkey. *Rev Esp Quimioter*. 2019;32(6):516–524. PMID: 31642640.
26. Taskin MH, Nursal AF, Oruc MA, Kariptas E. Genotype distribution and prevalence of high-risk human papillomavirus infection among women in Samsun Province of Turkey. *Asian Pac J Cancer Prev*. 2022;23(7):2477–2482. doi: 10.31557/APJCP.2022.23.7.2477.
27. Yaman M, Ozcan HEA, Bakir A. High-risk human papilloma virus genotype distribution and correlation with cervical cytomorphological data in Turkish and immigrant women in Mersin Province. *New Microbiol*. 2024;47(1):88–97. PMID: 38700888.
28. Altay-Kocak A, Kazanci F, Dogu-Tok C, Onan A, Erdem O, et al. The prevalence and distribution of human papillomavirus in 4267 Turkish women with or without cervical lesions: a hospital-based study. *J Med Virol*. 2022;94(10):5026–5032. doi: 10.1002/jmv.27921.

29. Alacam S, Bakir A. Human papillomavirus prevalence and genotype distribution in cervical swab samples in Istanbul, Turkey. *J Infect Dev Ctries.* 2021;15(8):1190–1196. doi: 10.3855/jidc.14663.
30. Dursun P, Ayhan A, Mutlu L, Çağlar M, Haberal A, et al. HPV types in Turkey: multicenter hospital-based evaluation of 6388 patients in Turkish gynecologic oncology group centers. *Turk Patoloji Derg.* 2013;29(3):210–216. doi: 10.5146/tjpath.2013.01188.
31. Usubutun A, Alemany L, Kucukali T, Ayhan A, Yüce K, et al. Human papillomavirus types in invasive cervical cancer specimens from Turkey. *Int J Gynecol Pathol.* 2009;28(6):541–548. doi: 10.1097/PGP.0b013e3181aaba0d.
32. Avci G, Bozdayi G, Taskiran C, Ozkan S, Onan M. Cesitli servikal patolojiye sahip kadinlarda HPV prevalansi ve filogenetik analizi. *J Turk Soc Obstet Gynecol.* 2013;10(3):151-9. doi: 10.5505/tjod.2013.03779.
33. Wheeler CM, Castellsagué X, Garland SM, Szarewski A, Paavonen J, et al. Cross-protective efficacy of HPV-16/18 AS04-adjuvanted vaccine against cervical infection and precancer caused by non-vaccine oncogenic HPV types: 4-year end-of-study analysis of the randomised, double-blind PATRICIA trial. *Lancet Oncol.* 2012;13(1):100–110. doi: 10.1016/S1470-2045(11)70287-X.

https://doi.org/10.5455/annalsmedres.2025.09.258